INFORMATION TO USERS

This material was produced from a microfilm copy of the original document. While the most advanced technological means to photograph and reproduce this document have been used, the quality is heavily dependent upon the quality of the original submitted.

The following explanation of techniques is provided to help you understand markings or patterns which may appear on this reproduction.

1. The sign or "target" for pages apparently lacking from the document photographed is "Missing Page(s)". If it was possible to obtain the missing page(s) or section, they are spliced into the film along with adjacent pages. This may have necessitated cutting thru an image and duplicating adjacent pages to insure you complete continuity.

2. When an image on the film is obliterated with a large round black mark, it is an indication that the photographer suspected that the copy may have moved during exposure and thus cause a blurred image. You will find a good image of the page in the adjacent frame.

3. When a map, drawing or chart, etc., was part of the material being photographed the photographer followed a definite method in "sectioning" the material. It is customary to begin photoing at the upper left hand corner of a large sheet and to continue photoing from left to right in equal sections with a small overlap. If necessary, sectioning is continued again – beginning below the first row and continuing on until complete.

4. The majority of users indicate that the textual content is of greatest value, however, a somewhat higher quality reproduction could be made from "photographs" if essential to the understanding of the dissertation. Silver prints of "photographs" may be ordered at additional charge by writing the Order Department, giving the catalog number, title, author and specific pages you wish reproduced.

5. PLEASE NOTE: Some pages may have indistinct print. Filmed as received.

University Microfilms International
300 North Zeeb Road
Ann Arbor, Michigan 48106 USA
St. John's Road, Tyler's Green
High Wycombe, Bucks, England HP10 8HR

ELECTRICAL AND ELECTROCHEMICAL INVESTIGATIONS OF POLYMER MEMBRANE ION-SELECTIVE ELECTRODES

by

Gary David Carmack

A Dissertation Submitted to the Faculty of the

DEPARTMENT OF CHEMISTRY

In Partial Fulfillment of the Requirements
For the Degree of

DOCTOR OF PHILOSOPHY

In the Graduate College

THE UNIVERSITY OF ARIZONA

1 9 7 7

THE UNIVERSITY OF ARIZONA

GRADUATE COLLEGE

I hereby recommend that this dissertation prepared under my direction by Gary David Carmack

entitled Electrical and Electrochemical Investigations of Polymer Membrane Ion-Selective Electrodes

be accepted as fulfilling the dissertation requirement for the degree of Doctor of Philosophy

Henry Freiser — Dissertation Director

7 Apr 77 — Date

As members of the Final Examination Committee, we certify that we have read this dissertation and agree that it may be presented for final defense.

M B Denton	3-23-77
Paul R Huley MD	3-23-77
Gary S Wilson	3-24-77
Richard S Johnson	3-24-77

Final approval and acceptance of this dissertation is contingent on the candidate's adequate performance and defense thereof at the final oral examination.

STATEMENT BY AUTHOR

This dissertation has been submitted in partial fulfillment of requirements for an advanced degree at The University of Arizona and is deposited in the University Library to be made available to borrowers under rules of the Library.

Brief quotations from this dissertation are allowable without special permission, provided that accurate acknowledgment of source is made. Requests for permission for extended quotation from or reproduction of this manuscript in whole or in part may be granted by the head of the major department or the Dean of the Graduate College when in his judgment the proposed use of the material is in the interests of scholarship. In all other instances, however, permission must be obtained from the author.

SIGNED: Gary D. Carnoske

ACKNOWLEDGMENTS

The author wishes to express his gratitude to Dr. Henry Freiser, who directed this research, for his assistance in both the experimental work and in the preparation of this dissertation.

The author also wishes to thank Dr. Archie Deutschman for his help with the high pressure experiments.

Special thanks are extended to Mary Therese Goff for her valuable assistance in the preparation of this dissertation.

The financial support of the Office of Naval Research is gratefully acknowledged.

TABLE OF CONTENTS

TABLE OF CONTENTS--Continued

LIST OF TABLES

LIST OF TABLES--Continued

LIST OF ILLUSTRATIONS

LIST OF ILLUSTRATIONS--Continued

LIST OF ILLUSTRATIONS--Continued

ABSTRACT

This study deals with investigations in two major areas, that of the electrical charge conductivity in polymer films impregnated with chelates or ion-association complexes (quaternary ammonium salts), and the electrochemical behavior of coated-wire ion-selective electrodes.

The observation that solutions of ion-association complexes dissolved in a polymeric matrix exhibited a very high temperature coefficient of resistance led to the systematic study of the experimental parameters that play important roles in this semiconductor-like behavior. Electrothermal analyses showed that the electrical conductivity of these polymer mixtures are reminiscent of that observed with organic semiconductor materials in which electrons are the charge carriers. However, the polymer films had about 10^9-fold higher conductivity than organic semiconductors of comparable activation energy of conduction values. Furthermore, studies of the electrical conductivity measured as a function of time, voltage, and dielectric constant indicated that the conduction mechanism was ionic.

The pressure dependence of conductivity of the filled polymer films was also studied. The activation volumes obtained from such studies ranged from 30-93 cm^3/mole, demonstrating the involvement of particles of far greater size than electrons or protons. These studies also led to the conclusion that both ions in the ion-pair are charge carriers. The electrical conductivity of Dowex-1 in the Cl^-, Br^-, I^-,

and NO_3^- forms was determined at pressures ranging up to 2000 atmospheres. Activation volumes for the conduction process closely match the crystallographic volumes of the anions.

Resolution of the individual contributions to the activation energy of conduction, i.e., the energy for mobility and the dissociation energy for charge creation, was attempted by the use of isodielectric plasticizers and polymer-free systems. These experiments suggested that the energy for mobility and the dissociation energy are roughly equal.

The electrical studies were extended to include electrothermal and high pressure measurements of polymeric mixtures incorporating the macrotetrolide valinomycin. Electrical conductivity in this system was similarly ionic, but the mechanism appeared more complex, showing a greater degree of dependency on the nature of the polymeric matrix. Additionally, conduction parameters for some selected chelates are reported.

A number of findings in the conductivity studies have direct bearing on the mechanism of the behavior of ion-selective electrodes. Mobility terms, useful in electrode selectivity studies, can be calculated from the conduction data. Further, a brief study of the effect of conductor type on electrode response suggested that an ionic diffusion mechanism was responsible for charge-coupling in the coated-wire ion-selective electrodes.

CHAPTER 1

INTRODUCTION

The description polymer membrane ion-selective electrodes refers to a sub-class of membrane electrodes which consists of a thin section of electrically conducting material that regulates the diffusion of charged species through it, thereby giving rise to an electrode potential.

In 1906, the first membrane ion-selective electrode, the hydrogen-responsive glass electrode, was developed by Cremer (1) and extensively characterized by Haber and Klemensiewicz (2). Tendeloo (3) reported, in 1936, an attempt to fabricate a non-glass membrane electrode by utilizing calcium fluorite dispersed in a paraffin matrix. Potentiometric electrodes incorporating polymeric matrices were reported as early as the 1950's by Wyllie and Patnode (4), and Parsons (5). Overall, however, these early polymeric membrane electrodes displayed poor selectivity and erratic response.

The development of successful polymer membrane electrodes was realized through studies by Pungor (6-8) using silicone rubber, and later by Shatkay (9) who used a poly(vinyl chloride) matrix. During the past decade, a number of highly selective and sensitive polymer membrane ion-selective electrodes have been introduced (10-14).

A number of detailed reviews are available (15-19) which thoroughly cover the history and development of the entire spectrum of membrane ion-selective electrodes.

Initially, ion-selective electrodes were classified on the basis of their physical form (20, 21) or according to the nature of the electroactive material used in the membrane (22, 23). However, classifications based on electrode fabrication are no longer valid because many of the active materials can be incorporated into a variety of configurations. Hence, the classification scheme of: (i) solid-state, (ii) heterogeneous, and (iii) liquid membrane ion-selective electrodes, has given way to: (i) glasses, (ii) insoluble inorganic salts, and (iii) organic materials including chelating agents (24).

The early introduction of the glass electrode relative to other types of ion-selective electrodes has made it the most widely used and studied. The conventional glass membrane is made from a mixture of alkali metal oxides and alumina (25) but is often modified by the addition of other elements (26-29). The incorporation of these elements into the glass melts modifies or enhances certain properties and can lead to selectivity for non-protonic cations.

Inorganic insoluble salt-based electrodes have been fabricated from a variety of electroactive materials and into a number of useful forms. The best characterized of these is the single crystal fluoride sensitive electrode (5, 30-32) consisting of lanthanum fluoride doped with europium. Insoluble metal sulfides or silver halides may also be used as electrodes by directly layering them upon a conductive substrate, e.g., hydrophobized graphite, the "selectrode" (33, 34). Additionally, they can be sintered to produce the so-called "ceramic" electrode (20, 35). Heterogeneous forms of this group of electrodes can be prepared by

impregnating an inert matrix material with the insoluble inorganic salts. Pungor and others (36-38) have reported the preparation of this type of electrode using a silicone rubber matrix; Hirata and Date (39) used an epoxy resin matrix; a number of other polymers have also been employed (22, 38, 40).

Organic materials and chelating agents used in membrane electrodes have in common their ability to bind ions selectively and reversibly at either charged counterion sites or at neutral sites associated with macrocyclic molecules. Simplest representative compounds of this class are the long chain tetraalkylammonium salts (41-43). Organic chelating or sequestering agents such as the substituted phenanthroline ligands (44, 45) or the important group of neutral carrier substances, the macrotetrolide ligands (46, 47), serve as useful electrode membranes.

The earliest developments in transforming the liquid membrane electrode design into a solid-state (more correctly referred to as an immobilized liquid membrane) fabrication were reported by Shatkay (9). In this electrode, the electroactive materials were dispersed in a poly(vinyl chloride) matrix. Hirata and Date (39) prepared a copper (II) electrode by incorporating cuprous sulfide into a silicone rubber or epoxy resin to which direct electrical contact was made with a metallic conductor. In this manner, the usual internal reference electrode design was eliminated. The coated-wire ion-selective electrode (10, 11), developed shortly thereafter, combined both of these features by directly coating a platinum conductor with a poly(vinyl chloride) film containing the electroactive material. The coated-wire design has been recently

extended to include graphite (48) and carbon paste conductors (49). In reality, the extended designs are modifications of the Ruzicka selectrode (34, 50, 51).

Interestingly, the initial attempts at eliminating the internal reference electrode were made more than four decades ago when Kolthoff and Sanders (52) coated a platinum wire with silver halides. Glass electrodes which utilized an internal solid conductor had also been constructed at this time (53, 54). More recently, Niedrach (in 55) and Covington (24) have reported all solid-state glass electrodes using similar constructions.

A requisite for any ion-selective electrode, whether of coated-wire design or not, is the ability of the electroactive material to conduct electricity (24). The conduction process may proceed by a variety of mechanisms: ionic (including protonic), electronic, or defect diffusion.

The glass electrode due to its early introduction has been the subject of a number of mechanistic studies (28, 29). Its operation has generally been accepted to involve, amongst other parameters, ionic conduction of interstitial cations through the interior of the glass (56, 57). Although the correlation between the glass resistance and performance is unclear, unquestionably a minimum conductance value is necessary.

Electrical conduction through silver halide, crystalline membranes most likely is due to a Frenkel, defect mechanism (58, 59). Silver ion acts as the charge carrier by moving from one lattice vacancy

to the next. Such membranes owe their great selectivity to the fact that only ions of the appropriate size and charge will possess sufficient lattice mobility. For heterogeneous membrane electrodes, therefore, the correct ratio of inert binder to electroactive material must be selected to ensure particle contact (60). In many cases, doping the crystalline material or the inert matrix with ionic conductors will impart sufficient electrical conduction to achieve proper electrode function where none was observed previously (61).

Although electrical conduction in liquid (or immobilized liquids) phase electrodes is essential (24), the conduction process has not been characterized. Reports from this study (62) have shown that ionic conduction exists in these membranes. Thomas (63) has confirmed this observation via radiotracer studies of the diffusion of calcium ions through a poly(vinyl chloride) membrane.

Transport properties of the important class of neutral carrier electrodes, in particular the valinomycin-based electrode for potassium, have been studied (64, 65) in an attempt to elucidate the potential response mechanism. The valinomycin-polymer membrane electrodes are somewhat unique in that their response depends critically on matrix composition (66, 67). Furthermore, they often fail to function at temperatures below ca. 25°.

Sharp (in 68, 69) recently introduced a series of ion-selective electrodes based on salts of the organic semiconductor 7,7,8,8,-tetracyanoquinodimethane. It is tempting to state, as was done, that the radical-ion salts are electronic semiconductors as is the parent

compound (70), yet there exists no substantiating evidence for this proposal. Indeed, an ionic mechanism may well be involved in the conduction process.

The coated-wire design and its extensions present something of a mystery to classical electrochemical theory. Apparently functioning without any internal reference electrode, they have been termed "blocked interfaces" (22) through which conduction proceeds by some unknown mechanism. As pointed out by Covington (24), it is at least certain that a change in the conduction mechanism, from ionic to electronic, must take place somewhere in the vicinity of the internal conductor.

A number of experimental approaches have been utilized to attempt an understanding of the membrane conduction mechanism. Electrolysis experiments were used by Haugaard (71) to study glass electrodes and by Durst and Ross (72) for their study of the lanthanum fluoride electrode. Wikby and Johansson (73, 74) used a more refined constant current pulse technique to further investigate glass membrane electrodes. Electrical impedance studies have also been conducted by Brand and Rechnitz (75) of glasses and homogeneous silver halides and by Buck (22) of blocked interface systems. Both of these studies involved the use of low voltage, ca. 10 mV peak-to-peak, a.c. potentials to measure capacitive reactance parameters and Faradaic current. Unfortunately, the absence of any apparent Faradaic current in these studies has often been interpreted to indicate that there is no ionic conduction (instead a capacitive coupling mechanism is proposed). These interpretations are in direct

contradiction to proven cases of ionic mobility in the silver halide membranes (59).

Although the experimental techniques described above would be useful for a study of the electrical conductivity in polymer membrane ion-selective electrodes, even more suitable approaches are known in the field of organic semiconductors for the study of similar materials. These experimental techniques have been extensively reviewed (76-79).

In this dissertation, the investigation of the electrical conductivity in polymeric membranes is reported. In Section 3.1, polymer membranes containing quaternary ammonium salts were studied by electrothermal, electrolytic, dielectric, and high pressure techniques. This study was extended to ion-exchange resins in Section 3.2, where a model characterizing the conduction process was proposed. Membranes prepared from valinomycin and other chelating systems were further explored in subsequent sections. Finally, in Section 3.5, the applicability of the conductivity results to describing ion-selective electrode behavior was demonstrated. Throughout these studies, membrane compositions identical to those used in polymer membrane electrodes were selected.

CHAPTER 2

EXPERIMENTAL

2.1 Materials

ACS Reagent Grade chemicals were used except as noted. Aliquat 336S (tricaprylymethylammonium chloride) was obtained from General Mills Chemicals, Inc. and was used as received. The quaternary ammonium salt can be represented as $(R_3NCH_3)^+$, Cl^-, where R is described by the manufacturer as a mixture of C_8 and C_{10} normal alkyl groups. Other tetraalklyammonium halides were from Eastman Kodak.

Valinomycin (Sigma Chemical Co.) and Calcium Di-n-decyl Phosphate (Specialty Organics, Inc.) were used as received.

Poly(vinyl chloride), chromatographic grade; poly(styrene), molecular weight 30,000; poly(ethylene), medium molecular weight; and poly(methacrylate), medium molecular weight, were obtained from Polysciences, Inc. Nylon 66 was from DuPont. Epoxy resin and curing agent (diethylene triamine) were of the ordinary household type (Wilhold).

Dibutyl phthalate, dipentyl phthalate, dioctylphthalate, bis(2-ethylhexyl) phthalate, bix(2-ethylhexyl) adipate, dibutyl sebacate, and trioctyl phosphate were used as plasticizers (described in greater detail in appropriate sections) and were of Eastman reagent grade.

2.2 Sample Preparation

2.2.1 Preparation of Electroactive Materials

A 15-ml sample of Aliquat 336S was shaken with approximately six 10-ml aliquots of the appropriate sodium salt to effect the anion exchange. Many of the salts, notably the ClO_4^- ion-pair, are solid at room temperature and 2-ml of decanol was added to the solution. Shaking time on a wrist-action shaker was approximately 10 min for each aliquot. After each shaking, the aqueous phase was tested for the presence of exchanged chloride with an acidified $AgNO_3$ solution. The absence of Cl^- indicated complete exchange. The organic phase was washed twice with water and centrifuged overnight, giving a clear, straw-colored solution.

Similarly, valinomycin was loaded with potassium by shaking a 10-ml chloroform solution containing 10^{-3} M valinomycin with three 10-ml portions of a 1 M potassium chloride solution. The solution was washed with water and evaporated to dryness.

2.2.2 Polymer Mixtures

Specimens of unplasticized polymers were dissolved in minimal amounts of appropriate solvent: poly(ethylene) in formic acid, poly(styrene) in chloroform, Nylon 66 in benzene, poly(methyl methacrylate) in methyl acetate, and poly(vinyl chloride) in tetrahydrofuran. Epoxy resin was mixed with an equal weight of curing agent.

Samples were prepared for conductivity measurements by mixing the electroactive material with plasticizer or other desired agents and casting the mixture into two general shapes.

Early measurements using quaternary ammonium salt-polymer mixtures were performed on samples which were cast as small beads ca. 2.5 mm in diameter, in which were embedded two fine (No. 30) platinum or copper wire electrodes spaced ca. 0.15 mm apart.

Subsequent samples were case into disks by allowing approximately 1 ml of the sample solution to evaporate slowly in a 16-mm (i.d.) glass ring. Larger diameter samples for dielectric measurements were prepared by using a 20-fold greater quantity of the membrane materials and casting the mixture in a 70-mm glass ring.

The prepared samples were dried in vacuo for 12-24 h and then placed in a dry argon atmosphere for storage.

For an identical polymer composition, both sample geometries produced similar electrical characteristics but the thin disks were more reproducible in form and, hence, volume resistivity.

These procedures produced samples with compositions similar to those used as polymer membrane ion-selective electrodes.

2.3 Electrical Conductivity Measurements

2.3.1 Sample Electrodes

Metal foil electrodes (copper or aluminum) were attached during the casting procedure for some of the membranes; others were securely clamped between thin, circular aluminum electrodes prior to measurement. In either case, ohmic contacts result. Since guard-ring electrodes proved unnecessary, surface conductivity was considered to be insignificant for the sample geometries and conditions utilized for conductivity

measurements. The specifications of ASTM procedure #257-61 (80) with regard to sample and electrode geometry were observed throughout this study.

2.3.2 Conductivity Cell

A sample holder was constructed for a 3-cm square block of Teflon to which 0.5-cm wide, spring-steel "arms" were attached. Samples were placed in the holder which was suspended by spring-steel wires inside a jacketed, cylindrical (5.5 x 12 cm i.d.) glass vessel. Feed-through electrical conductors were glass sealed into the top of the vessel permitting application of vacuum to the cell.

The entire sample-free assembly had a leakage resistance of more than 10^{15} ohms. Externally heated water, circulated through the outer jacket, was used to control the sample cell temperature. Water heating is preferable to electrically heated tape because finer temperature control is possible and spurious coupling of the a.c. heating voltage is eliminated. Additional electric shielding was provided by surrounding the entire assembly with grounded copper foil.

Sample temperature was measured by placing a Yellow Springs Instrument Co. thermistor composite (#44018) in close proximity to the sample. Identical suspension and feed-through construction was used as described previously. The complete thermistor assembly, termed a "thermilinear thermistor network" (YSI #44201), consists of precise, matched resistors and thermistors in a circuit (see Figure 2.1) which produces an output voltage linear with respect to temperature. An

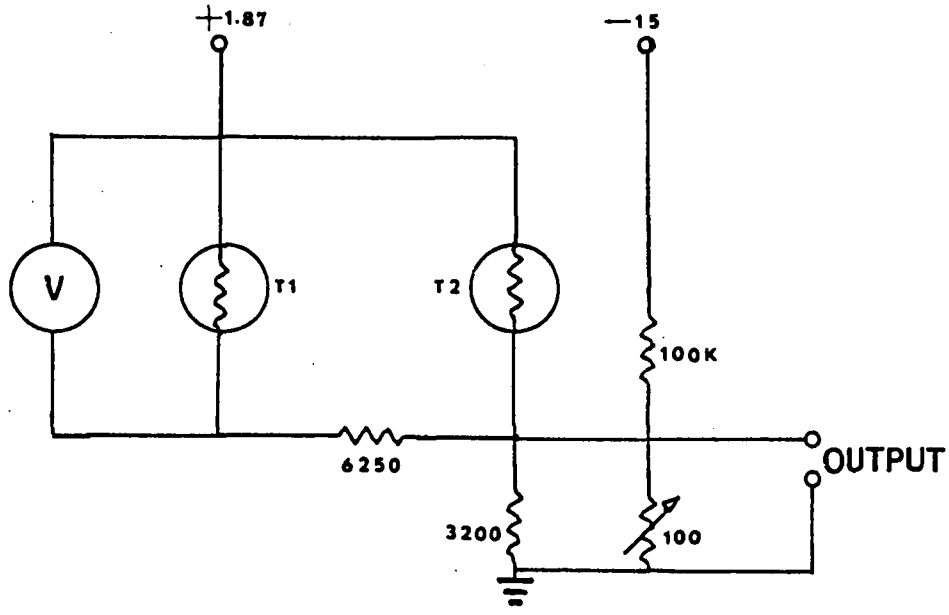

Figure 2.1 Thermistor Network.

equation which describes the behavior of the device is E_{out} = (+ 0.0053483 E_{in})T + 0.13493 E_{in}. An E_{in} = 1.870 V was selected to give an E_{out} = 10.00 mV/°C. The voltage output, displayed on an Orion Model 701 digital pH meter in the expanded mV mode, was found to be accurate to ± 0.1 °C and linear to the same degree. Time constant for response was ca. 1 s.

2.3.3 Instrumentation

Voltage was applied to the sample membranes using power supplies selected according to the range of interest: 0-10 V, Heath EU-80A; 100-300 V, Philbrick R 100B; and 100-1500 V, Kepco ABC.

Direct current measurements were made using a Keithley Model 616 digital electrometer whose analog output was connected to a Keithley Model 160 digital voltmeter. A schematic of the experimental conductivity measuring circuit is shown in Figure 2.2.

Calibration of the complete assembly using known resistors demonstrated that currents as small as 10^{-14} A could be accurately (within 8%) determined. Typical accuracy for measurements made in the usual range 10^{-9}-10^{-13} A was ± 5%.

2.3.4 Minicomputer Interface

The system used for automated control of the conductivity measurements consisted of a Data General Nova 2/10 (16K words) minicomputer equipped with a Xebec Systems, Inc., XFD-100 flexible disk system furnished with two disk drive units. A Model 33 Teletype and Infoton Vistar display terminal were used as I/O devices.

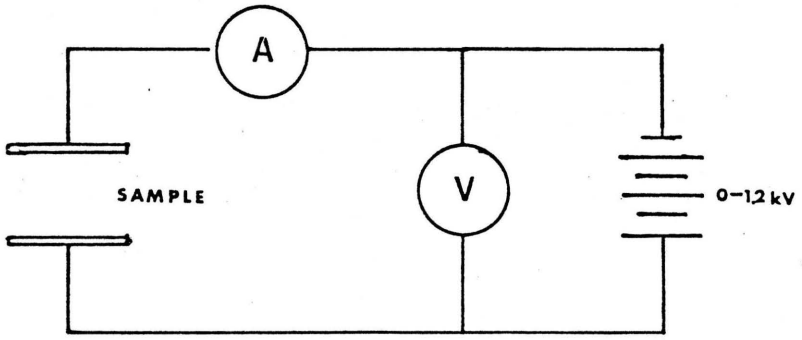

Figure 2.2 Conductivity Measuring Circuit.

Xebec Systems Disk Operating System (XDOS) (81), a general purpose (Nova 2) operating system, was used for controlling and performing the normal tasks required for program development and maintenance such as source editing, assembling, and compiling. In addition, it was used as an interface for transferring files of data between the control programs and the I/O devices available through XDOS.

A Nova 2 general purpose interface was constructed and control software was written which allows acquisition of BCD output from the current and temperature measuring devices.

Hardware. TTL-compatible integrated circuit components were wire-wrap connected using a MDB Systems GP interface board. A schematic of the circuit is shown in Figure 2.3. BCD outputs from the Orion DVM and Keithley DMM (representing temperature and current readings, respectively) were digitally inverted and gated by open-collector NAND gates. Individual meters were selected by outputting the appropriate strobe signal ($\overline{DIA}$ or $\overline{DIB}$) with a device select code of 21 which acts both to place a hold on the desired meter and strobe the output into the MDB input registers. Both strobe lines are ANDed, permitting either to transfer the BCD information into the Nova input buffers. Hardware timing is accomplished via a programmable, real-time clock; the circuit is shown in Figure 2.4. A 1 MHz oscillator signal is transformed into a square wave by a Schmitt-trigger input NAND and divided by a series of divide-by-ten counters. The desired count rate (from 10μs-100s) is selected using a 74151 multiplexer and switched to the COUNT-DOWN input of a preset 74193 UP/DOWN counter which in turn gives a 1-15 multiple of

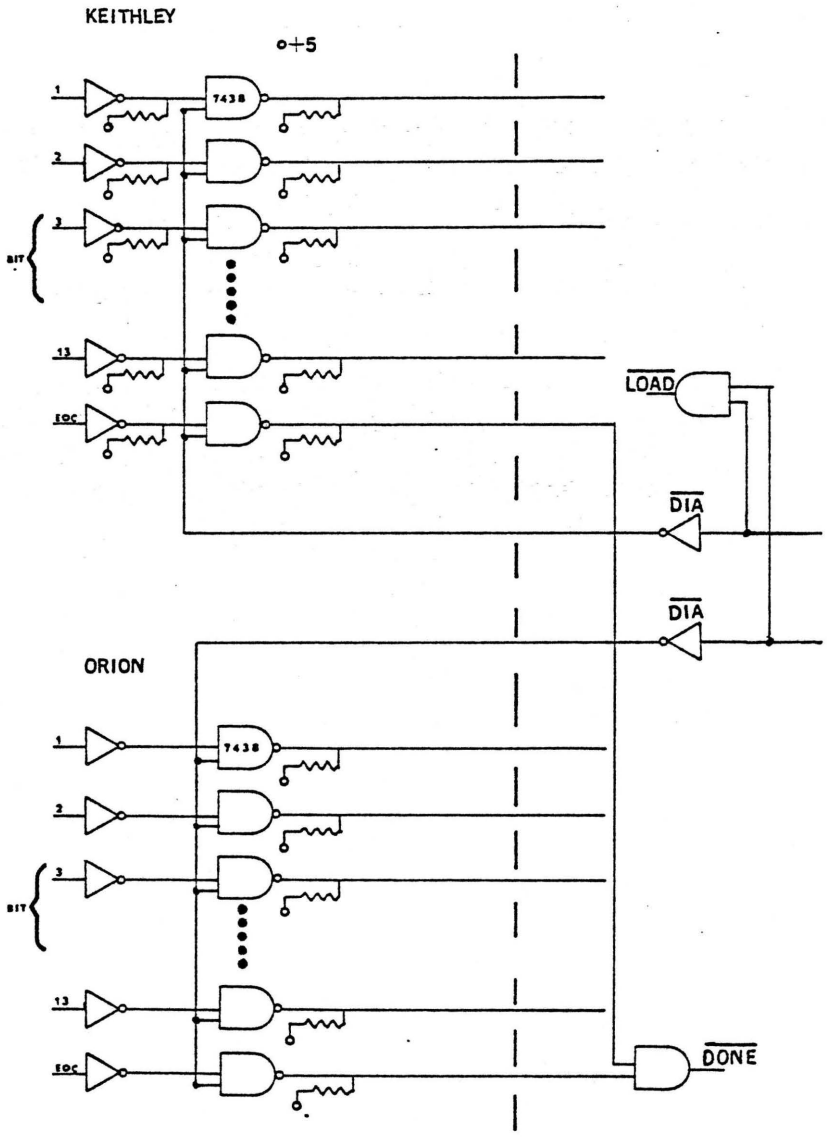

Figure 2.3 Computer Interface.

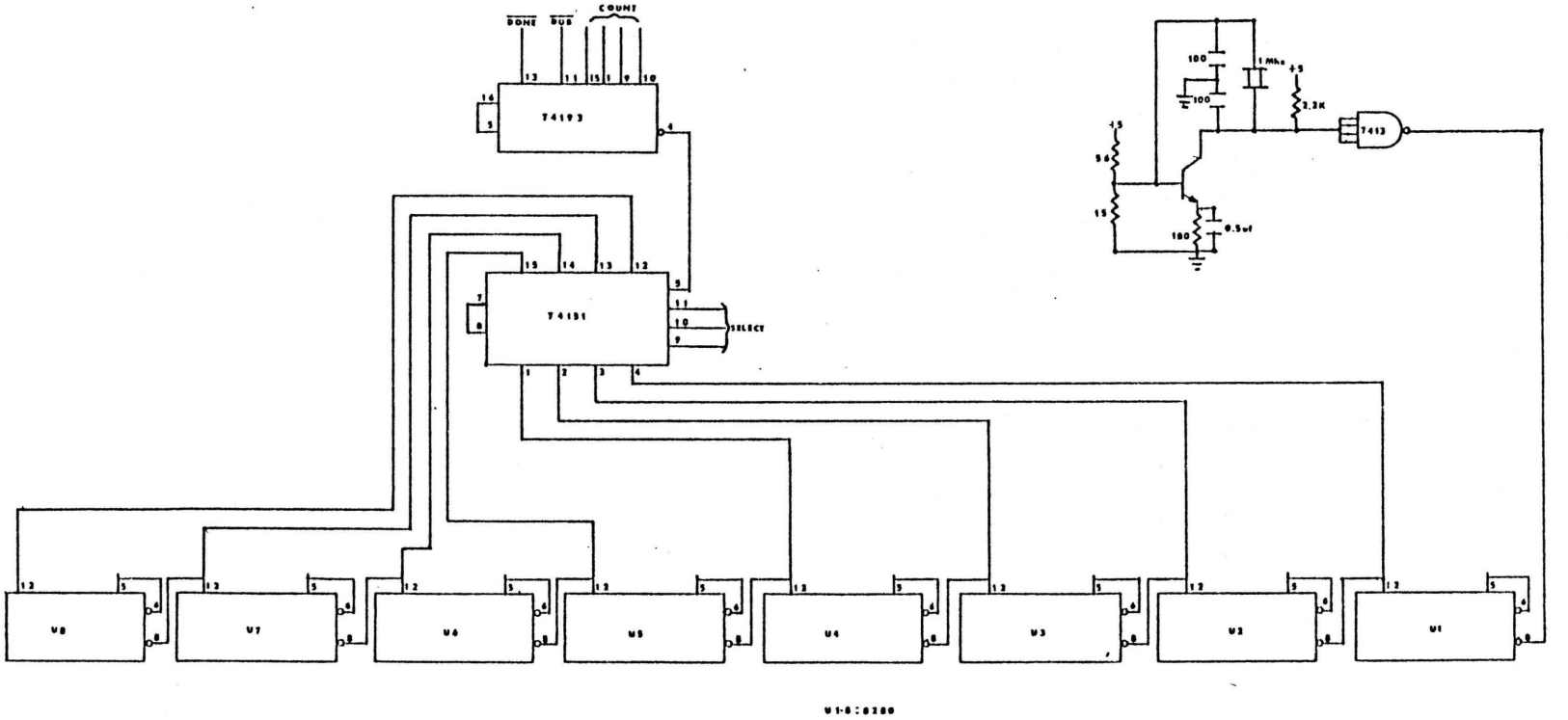

Figure 2.4 Real-Time Clock.

the original count rate. Accuracy of the programmable clock is better than ± 0.01% over the entire count range (10μs-1500s).

Software. Documented computer programs used in this study are listed in Appendix A. Programs were written in Data General's FORTRAN IV (82), modified for XDOS compatibility.

Primary control and data processing tasks were handled by a main FORTRAN program. A least-squares (LSQ), a teletype plotting routine (PLOT), and a disk writing routine (DISKST) were included as FORTRAN subroutines.

Assembly language programs were used to access the hardware interface allowing acquisition of BCD data from the digital multimeters. Algorithms were included in these programs for BCD to binary conversion (.BCDB) and generation of timing functions (TIME). Assembly language drivers were also written to control the various peripheral devices (buret, real-time clock, and voltage relay). All of the assembly language routines incorporated the appropriate software interfacing (83) to permit them to be callable as FORTRAN subroutines.

2.3.5 Electrothermal Analysis (ETA) Procedure

Electrothermal analyses, i.e., conductivity vs. temperature, of the sample membranes were made using the electrical circuit shown in Figure 2.2. Potential was applied to a sample and the current passing through it was measured with the electrometer in the FAST current mode. In this mode, the Model 616 operates as a feedback picoammeter in which the current flows through the feedback resistor of the voltage amplifier.

The use of the feedback mode increased the speed of the response at low current levels and reduced the noise level.

Samples were placed in the sample holder, inserted into the water-jacketed conductivity cell, and the system evacuated to a pressure of approximately 1 torr. The sample was heated by circulating heated water from the external bath through the outside jacket. Current and temperature measurements were made at regular time intervals. Inasmuch as the thermistor network was in thermal contact with the sample holder, it was unnecessary to maintain a constant temperature in order to establish thermal equilibrium. Nevertheless, a relatively slow heating rate of ca. 2°/min was selected.

Earlier experiments with samples incorporating the embedded wire electrodes were performed with the samples enclosed in argon-filled capillary tubes thermostated in an insulated water bath. Approximately 5 min were necessary for thermal equilibrium to be established at each new temperature for this configuration.

Upon application of a voltage across the samples, the current was observed to decrease asymptotically toward a limiting value. Instead of using an extrapolated, zero-time current, the value after 10.0s was used. This procedure gave results that were reproducible to better than 3%.

The sequence of operations performed in an automated, computer-controlled ETA experiment is shown in flow-chart form in Figure 2.6. Included in this figure are some of the assembly language interface control commands (and their respective function); greater documentation is provided with the appropriate programs listed in the Appendix.

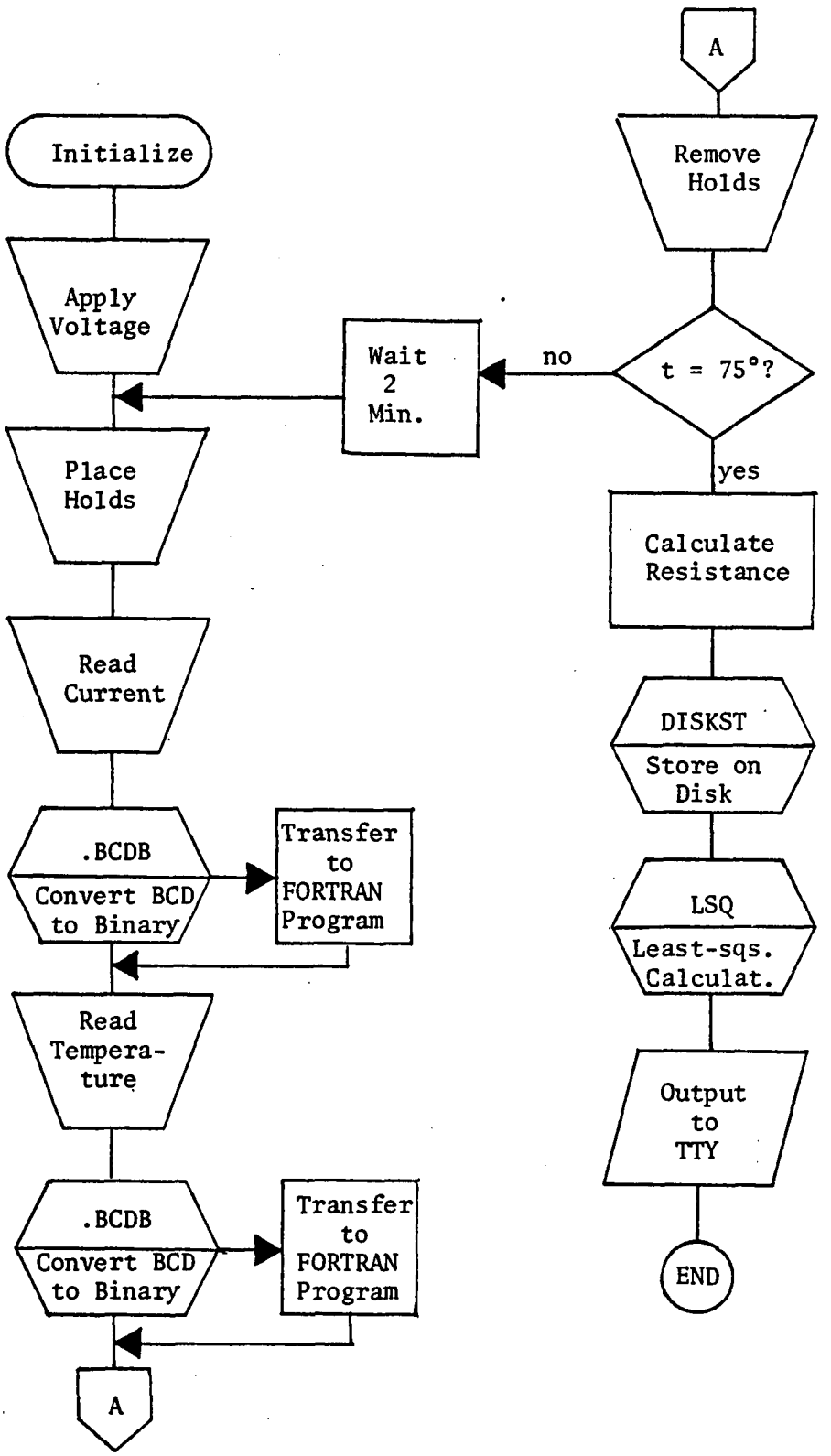

Figure 2.5 Flowchart of Computer-Controlled Electrothermal Analysis Procedure.

2.4 Differential Scanning Calorimetry

2.4.1 Apparatus

A Perkin-Elmer Model DSC-1B differential scanning calorimeter with a Leeds and Northrup Model W potentiometric recorder was used for all transition temperature determinations. A low temperature sample cell was constructed by jacketing the sample holder cover with a rubber cover. Dried nitrogen gas, at a flow rate of 15 ml/min, was used as the purge gas.

2.4.2 Procedure

Approximately 40 mg of the polymeric sample, sealed in a volatile sample pan, was placed into the low-temperature cell. Dry ice was added to the jacket and the cell thermostat set for an initial temperature of ca. -10°. Differential temperature scans versus an empty sample pan were made using a heating rage of 5°/min. Sensitivity of the detection system was set for 1 calorie/s.

2.4.3 Annealing Procedure

The detection of low energy transitions associated with second-order phase changes in polymeric materials generally is very difficult due to insufficient instrumental sensitivity. By over-filling the aluminum sample pans and carefully optimizing all instrumental parameters, transitions on the order of 0.03 cal/s were detectable. However, desired DSC results were not usually obtained until the annealing procedure of Barral and Johnson (84) was adapted. By annealing the polymer samples at temperatures greater than the Tg (glass transition

temperature), or temperatures of expected transitions, useful DSC profiles were obtained where distinct Tg's were not observable earlier.

2.5 Thermal Discharge Current Measurements

The experimental procedure for investigating thermally stimulated discharge (TSD) currents involved measurement of currents flowing between short-circuited electrodes adjacent to opposite surfaces of a sample while being subjected to a linear thermal program.

The equipment and apparatus described for electrothermal measurements (Section 2.3.5) are employed for TSD measurements except that no potential is applied while determining discharge current.

A convenient procedure for measuring TSD current was to cool the sample assembly after the completion of an electrothermal analysis run, and to then repeat the thermal program while measuring the short-circuited current with the electrometer. Occasionally, other experimental protocals were followed such as polarizing the sample with a high potential for several minutes at elevated temperature prior to examining the TDS current (a procedure termed "poling").

2.6 Current-Time Measurements

The current versus time relationship alluded to previously was determined experimentally using the electrothermal analysis apparatus and equipment. Current was determined isothermally at 25°. A flow chart of the automated procedure is shown in Figure 2.6; applied potentials between 0.1 and 10 V were studied.

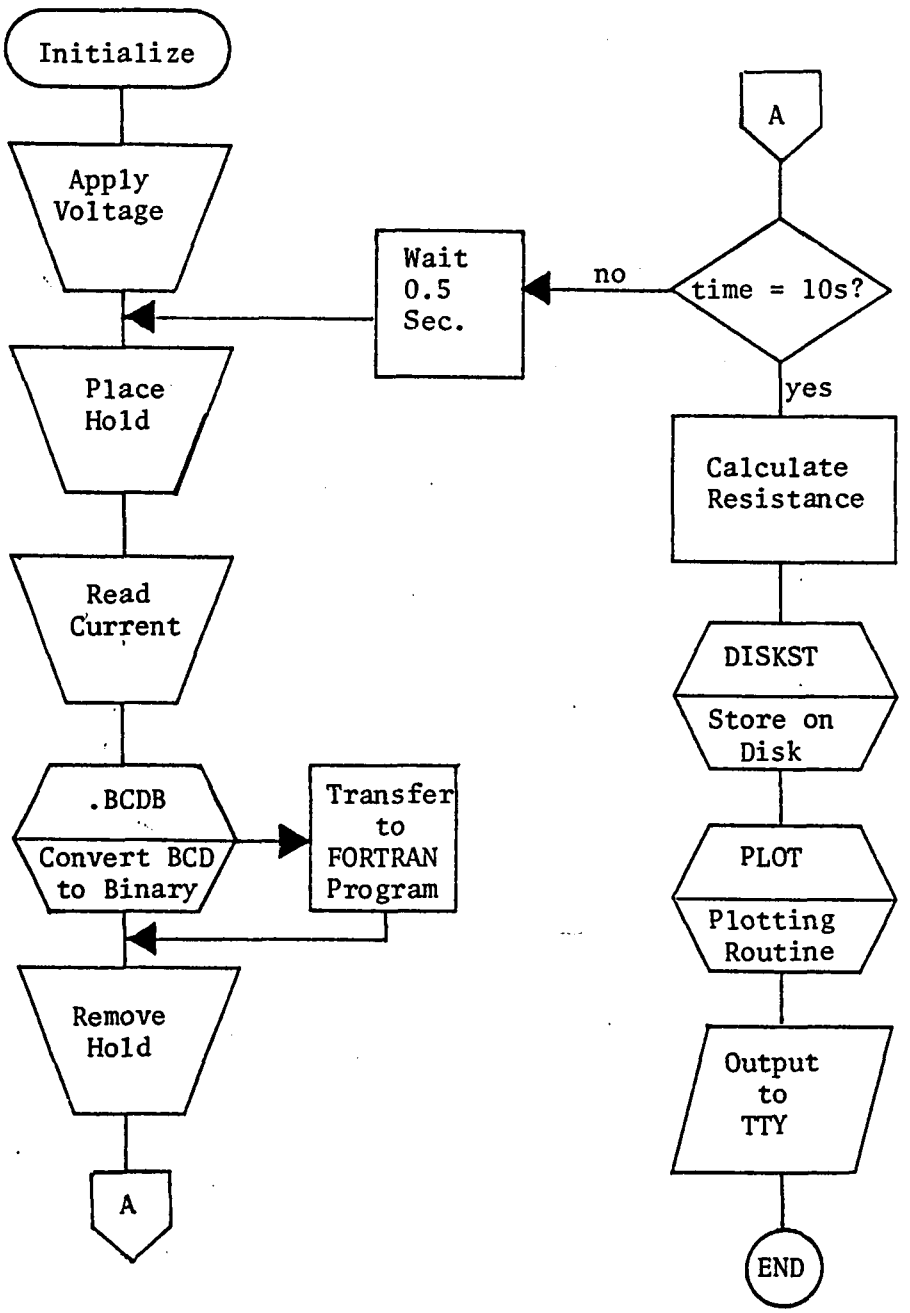

Figure 2.6 Flowchart of Computer-Controlled Current-Time Procedure.

The electrothermal Nova interface was flexible enough to be converted to a current vs. time interface by simply retaining the current measuring channel and generating computer timing (either by software loops or through the programmable real-time clock). Current is automatically sampled at 0.5 s intervals for as long as desired (usually 10 s).

2.7 Current-Voltage Measurements

The measurement system described in Section 2.5 was used isothermally at 25°. Voltage was determined by inserting the digital multimeter in parallel with the remainder of the electrical circuit. Ohm's law behavior was tested by measuring the current arising from applied potentials between 0.1 and 500 V which corresponds to field strengths between 0.3 and 1.5 kV/cm. Procedurally, 10-second current values were measured (see Section 2.3.5) and the sample electrodes short-circuited for at least 1 minute between voltage applications. Inasmuch as a small amount of residual sample polarization remained even after prolonged discharging, voltage was always applied in steps from low to high values.

2.8 Determination of the Effect of Solvent Vapor

Organic solvent vapors had been observed to increase the apparent electrical conductivity of poly(vinyl chloride) samples. To further quantitate this effect, the change of conductivity upon exposure to acetone, chloroform, and toluene (ACS Reagent Grade; Matheson, Coleman, and Bell, Inc.) vapors was studied.

2.8.1 Equipment

Two 125-ml and one 250-ml gas washing bottles with stopcocks on inlet and outlets were series-connected to a vacuum pump. A bead-type sample was suspended inside the middle bottle. Electrical conductivity was measured using the equipment and electrical circuit described previously (Section 2.3.3). Temperature was maintained at 25° by immersing the gas washing bottles in a thermostated water bath.

2.8.2 Procedure

A few milliliters of the desired organic solvent were placed into the outermost 250-ml washing bottle (the one farthest from the vacuum pump). The air inside the bottle was saturated with organic vapor by permitting the sealed bottle to equilibrate for 1 h with the water bath. The evacuated, sample-containing (middle) bottle was quickly filled with the saturated vapor by opening the stopcock between it and the solvent-containing bottle. Successive dilutions of this saturated atmosphere were made in an identical fashion using the third bottle with the inlet of the sample-containing bottle opened to the air. Conductivity measurements were usually made after 3-5 min of vapor contact, although the effect of longer contact times was also investigated.

Vapor-saturated air data were converted to vapor pressure values by using the empirical form of the Antoine equation (85):

$$\log P = A - B/(C + T) \qquad (2.1)$$

where P is the vapor pressure of the organic solvent in mm of mercury and T is the Centigrade temperature; the remainder of the terms are constants for each solvent.

2.9 Electrolysis Measurements

The electrolysis study was performed in accordance with the Tubandt (in 86) as modified by Mizzoni (87).

2.9.1 Preparation of Samples

Aliquat 336S/epoxy mixtures (1:1 by weight) were cast into thin, circular disks similar to those used for the electrothermal analysis experiments (Section 2.3.5). After curing, two experimental sample-electrode arrangements were tested. In Method I, the samples were simply "sandwiched" between copper-foil electrodes. In the other arrangement, Method II, a sample was tightly clamped between two other samples (of approximately one-half the thickness) which had copper electrodes attached to them.

2.9.2 Apparatus and Procedures

Electrical current was determined using the system described for the current-time measurements (Section 2.6).

The applied voltage was initially adjusted to produce currents between 10^{-3} and 10^{-5} A in the samples (at room temperature) for 14-28 h. Total charge that had passed through a sample was determined either by recording the current as a function of time, or by measuring it with the electrometer in the coulombmeter position.

The weight change of the samples after electrolysis was measured to $\pm$ 0.05 mg with a Mettler balance.

2.10 Current-Dielectric Constant Measurements

2.10.1 Equipment

Dielectric properties of the membranes were measured with a General Radio Model 1620-A Capacitance Measuring Assembly. The Model 1620-A is actually an assemblage of discrete units: a Model 1310-B Oscillator, a Model 1232-A Tuned Amplifier and Null Detector, and a Model 1615 Capacitance Bridge. Measurements were made using a 2 V P-P, 1 kHz oscillator signal.

A Balsbaugh Laboratories Model LD-3 dielectric cell, equilibrated at 25° was used in the three-terminal configuration for all dielectric determinations. In this arrangement, the liquid cell had one guarded and one unguarded electrode. The unguarded electrode is movable by a micrometer adjustment so the inter-electrode spacing is known and can be reproduced. The guarded and unguarded electrodes are connected by coaxial cables to the "low" and "high" terminals of the capacitance bridge, respectively. Such a system permits highly accurate (88) measurements because of the well-defined area of the active electrode and the elimination of corrections for fringe fields at the electrode edges. Both parameters are potential sources of error in the commonly used two-terminal configuration.

2.10.2 Sample Preparation

Because of the large size (6.3 cm diameter) of the dielectric cell electrodes, speciments much larger than the usual 16 mm ones were necessary to produce a useful change in cell capacitance upon insertion.

Therefore, larger diameter samples were prepared by using a 20-fold larger quantity of the membrane materials and casting the mixture in an inverted 70 mm bell jar. After evaporation of solvent, samples were removed and trimmed to 6.0 cm.

2.10.3 Two-Fluid Procedure

Initially, dielectric constant was determined by the air gap method of ASTM D-1673-61 (89). However, the two-fluid method suggested by Johnson and Chomicz (90) was more applicable for the thin specimens (thickness less than 0.08 cm) used in this study. Dielectric constant was calculated from the following expression:

$$\varepsilon' = \frac{1}{C_0}\left[C_1 + \frac{\Delta C_1 C_4 (C_2 - C_1)}{\Delta C_1 C_4 - \Delta C_2 C_3}\right] \qquad (2.2)$$

where C is the cell capacitance under conditions described by the subscript 0, for vacuum; 1, air filled, 2, filled with second fluid; 3, filled with sample plus air; 4, filled with sample plus second fluid; and $\Delta C_1 = (C_3 - C_4)$, $\Delta C_2 = (C_4 - C_2)$.

2.11 High Pressure Conductivity Measurements

2.11.1 High Pressure Apparatus

A high pressure system was constructed at the University of Arizona High Pressure Laboratory and is shown diagrammatically in Figure 2.7. A miniature sample holder was fabricated by machining a block of Teflon to a 2.5 x 7.6 cm cylinder to which recessed spring steel

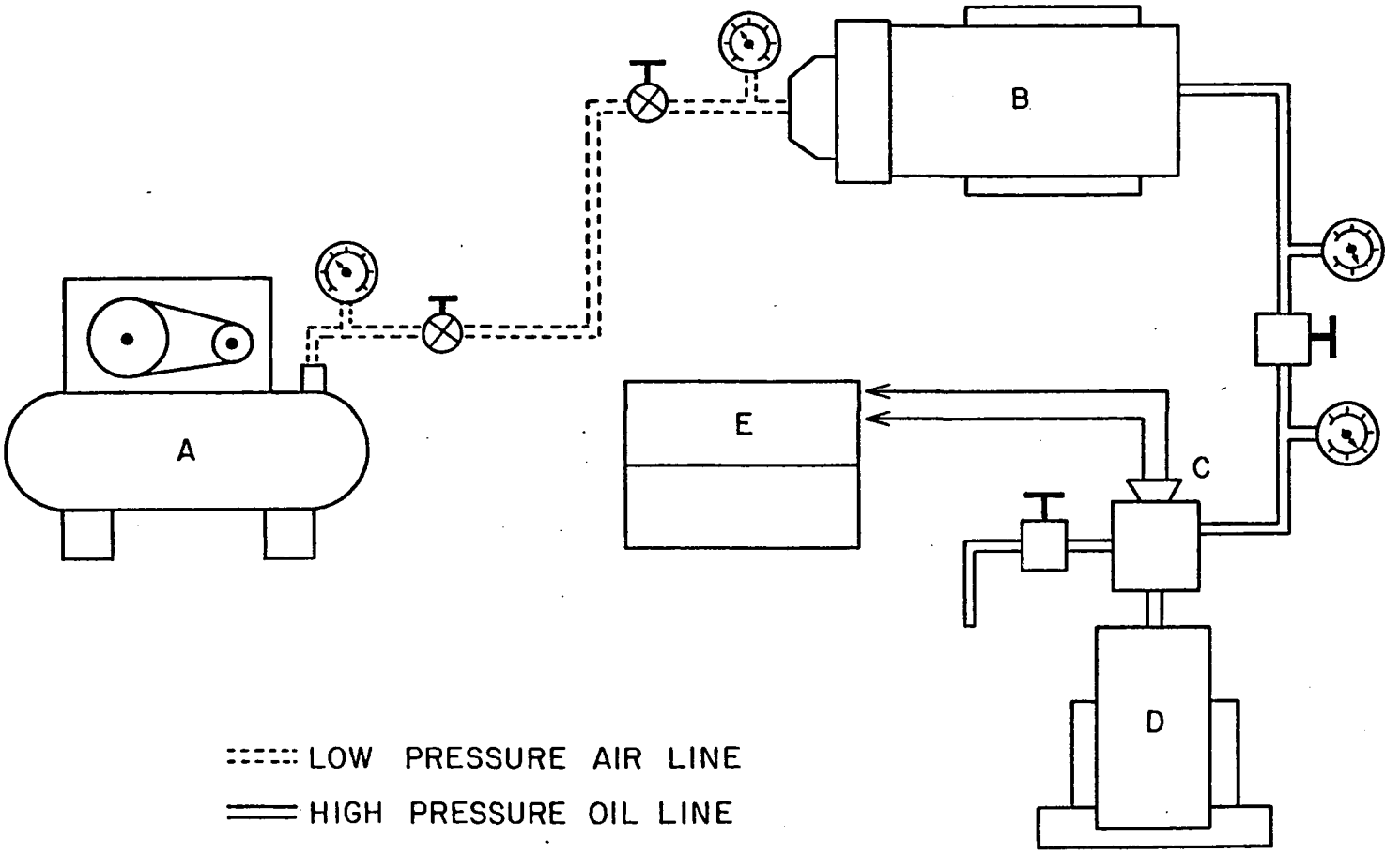

Figure 2.7 Schematic of High Pressure Conductivity Measuring Apparatus. -- (A) Air compresser; (B) pump, Haskel Model DXHW-602; (C) phenolic feed-through insulator; (D) high pressure cell; (E) conductivity measuring assembly.

electrode clamps were attached. Tests of this assembly showed that it had a leakage resistance of 10^{12} ohms.

Electrical contact to the sample holder was made by attaching one electrode arm to the body of the high pressure vessel and the other to a Teflon-covered No. 8 spring steel wire which was threaded through the high pressure oil line. The wire was brought out of the pressure vessel through a specially fabricated phenolic insulator which was carefully torqued into the T-head block.

2.11.2 Procedure

The system was operated by filling the pump with Baker AR grade mineral oil and applying 0-4 kg/cm^2 oil pressure to the low side of the pump and regulating the high side oil pressure. A maximum pressure of 3000 atm could be produced by the pumping system, but most measurements were made with an oil pressure below 2200 atm to avoid the possibility of premature failure of the insulating fittings.

The large size of the pressure vessel precluded effective thermostating in a liquid bath; it also served to keep the temperature rise small. It was found possible to maintain essentially constant temperature ($\pm$ 1°C) by simply waiting 15 minutes before measurement.

Current leakage through the assembled system was determined to be sufficiently low to permit a sample resistance of up to 10^9 Ω to be measured accurately. Furthermore, the activation energy and bulk resistance of the samples were unchanged upon immersion in the mineral oil.

The electrical conduction through the polymer membrane samples decreased progressively when there were subjected to increasing pressure (1 to 2000 atm). As mentioned above, a constant temperature was maintained for each conductivity-pressure measurement in view of the high temperature sensitivity of the samples. The fact that a possible error due to heating of the polymer mixture would be evidenced as a positive coefficient of conductivity is reassuring in light of the results obtained. After completion of a measurement cycle, with the pressure returned to 1 atm, the sample resistance was usually within 10% of that measured initially.

2.12 Ion-Exchange Resins

2.12.1 Sample Preparation

Approximately 10 g of Dowex-1X8 (Dow Chemical) anionic exchange resin, present as the chloride form was converted to the desired anionic form by vigorously shaking it with three successive 30-ml portions of the appropriate 1 M sodium salt. Complete exchange was judged by the absence of Cl^- (tested with acidic $AgNO_3$) in the aqueous phase following the final shaking. Resins were then thoroughly washed with distilled, deionized water and partially dried by lightly pressing them between sheets of filter paper.

A few grams of the resin, in a KBr-type die, were pressed to a force of 8500 kg/cm^2 (8260 atm), producing a "jelly-like" product easily suspended in water. Some degradation of the resin may occur under compression in the form of disruption of cross-linkages. Films of the

resins were prepared by coating glass slides with aqueous resin mixtures and allowing the water to evaporate. Circular samples (15 mm x 1 mm) were cut from the air-dried master films then vacuum-dried at room temperature for 48 hours.

Using this technique, it has been possible to prepare the Cl^-, Br^-, I^-, and NO_3^- anionic forms of the resin from which uniform, pliable films could be cast.

2.12.2 Conductivity Measurements

Electrical conductivity measurements were performed using the previously described high pressure system (Section 2.11) and electrical conductivity instrumentation (Section 2.3.2).

2.13 Coated Wire Ion-Selective Electrodes

2.13.1 Construction of Perchlorate Electrodes

An electrode coating mixture was made by mixing approximately 0.7 g of Aliquat-ClO_4 solution (preparation of this solution is described in Section 2.2.1) with 6 ml of a 5 w/v % solution of poly(vinyl chloride) in tetrahydrofuran. Evaporation of solvent gives the optimal 70 weight % Aliquat-ClO_4 mixture. A wire of the desired type, approximately 1 mm in diameter, was soldered to a length of RG-58 coaxial cable. The wire was then dipped in the coating mixture several times to coat it uniformly and allowed to dry overnight. The sensitive tip was immersed in a 0.1 M $NaClO_4$ solution for various lengths of time before measurements were made. Prior to use, the exposed portion of the wire was wrapped tightly with Parafilm (American Can Co.).

2.13.2 Measurement Procedure

Two solutions of $NaClO_4$, 10^{-2} and 10^{-4} M, were prepared for electrode testing. Prior to measurement, the electrode was soaked for 15 min in water. The electrode tip was then immersed in one of the standard solutions and the potential of the test cell was recorded when equilibrium was established, as evidenced by a stable reading ($\pm$ 0.2 mV). Electrodes were evaluated by measuring response as a logarithmic function of the perchlorate ion activity.

CHAPTER 3

RESULTS AND DISCUSSION

3.1 Quaternary Ammonium Salts, R_4N^+,X^-

Most of this study has been involved with the investigation of the conduction process in R_4N^+,X^-/polymer mixtures. The general experimental methods utilized are applicable, however, to other conductance systems, e.g., potassium-valinomycin, ion-exchange resins, etc. Also, the relationships developed in this section for characterizing the charge transport process are sufficiently broad to cover all systems described.

3.1.1 Electrothermal Analyses

The effect of changes in the nature of the quaternary ammonium salt and composition of the polymeric matrix on the electrical conductivity have been examined by means of a number of electrothermal analysis experiments.

The very first conductivity experiments were performed on a series of Aliquat salts in a number of polymer matrices: poly(styrene), poly(methyl methacrylate), poly(vinyl chloride), and epoxy resin in a 1:6 weight ratio. The most surprising feature of the electrical conductivity of these polymer dispersed salts was the unusually high positive temperature coefficients. From the results shown in Figures 3.1-3.4, the temperature dependence of conductivity is seen to be exponential, following the operational semiconductor expression:

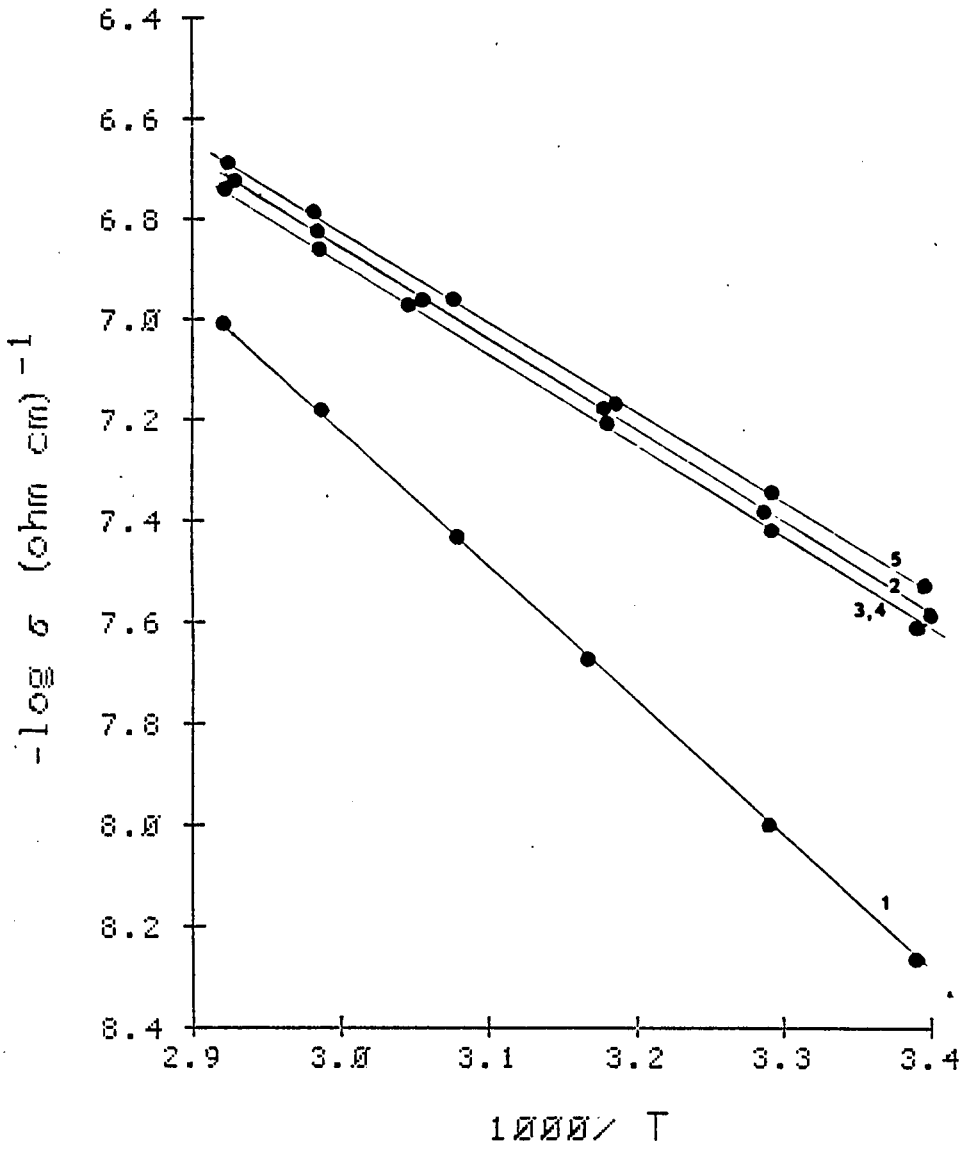

Figure 3.1 Temperature Dependence of Conductivity of Aliquat Salts in Poly(Methyl Methacrylate). -- 1. ClO_4^-. 2. NO_3^-. 3,4. OAc^-, CNS^-. 5. Cl^-.

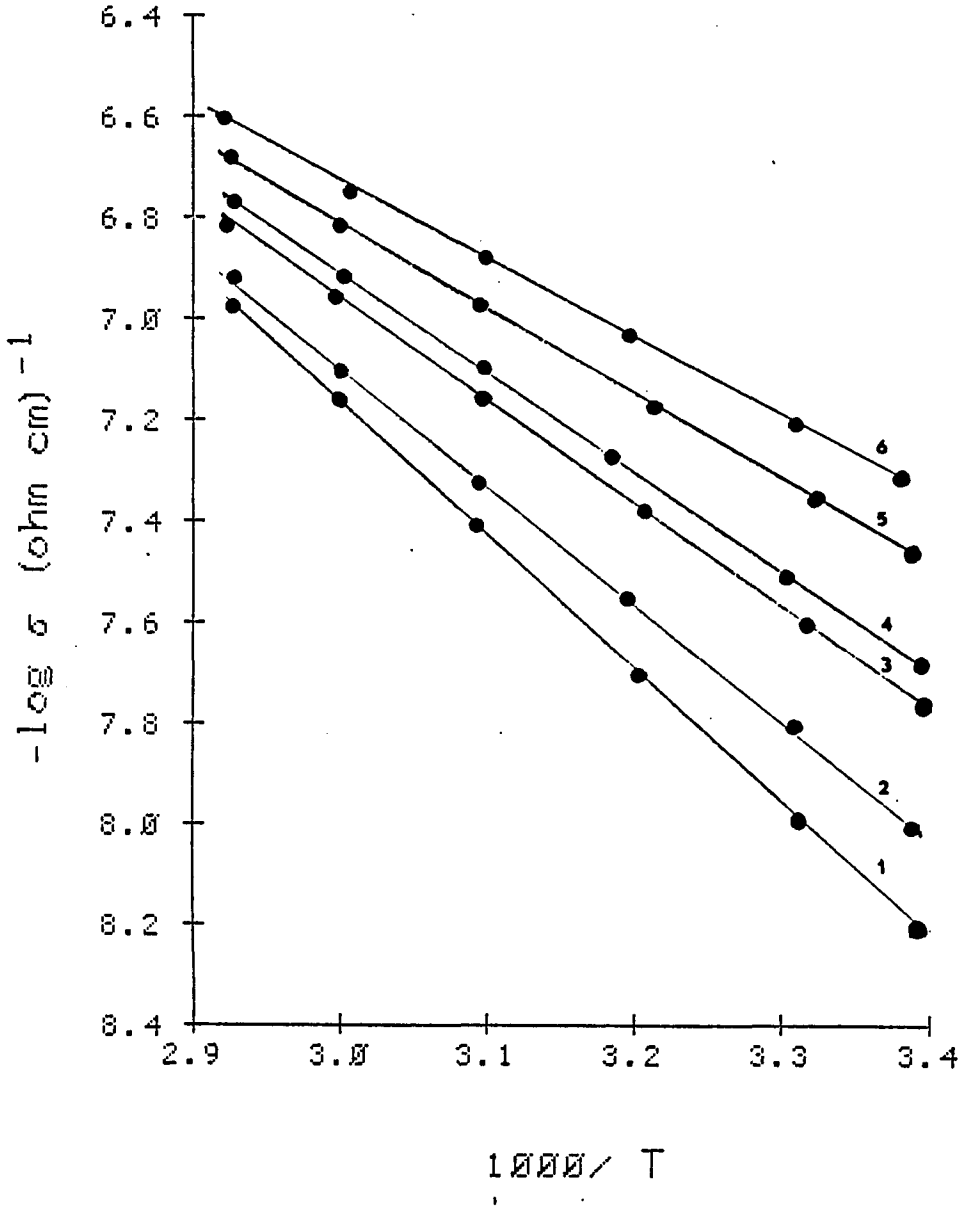

Figure 3.2 Temperature Dependence of Conductivity of Aliquat Salts in Poly(Styrene). -- 1. ClO_4^-. 2. NO_3^-. 3. Cl^-. 4. OAc^-. 5. SO_4^-. 6. CNS^-.

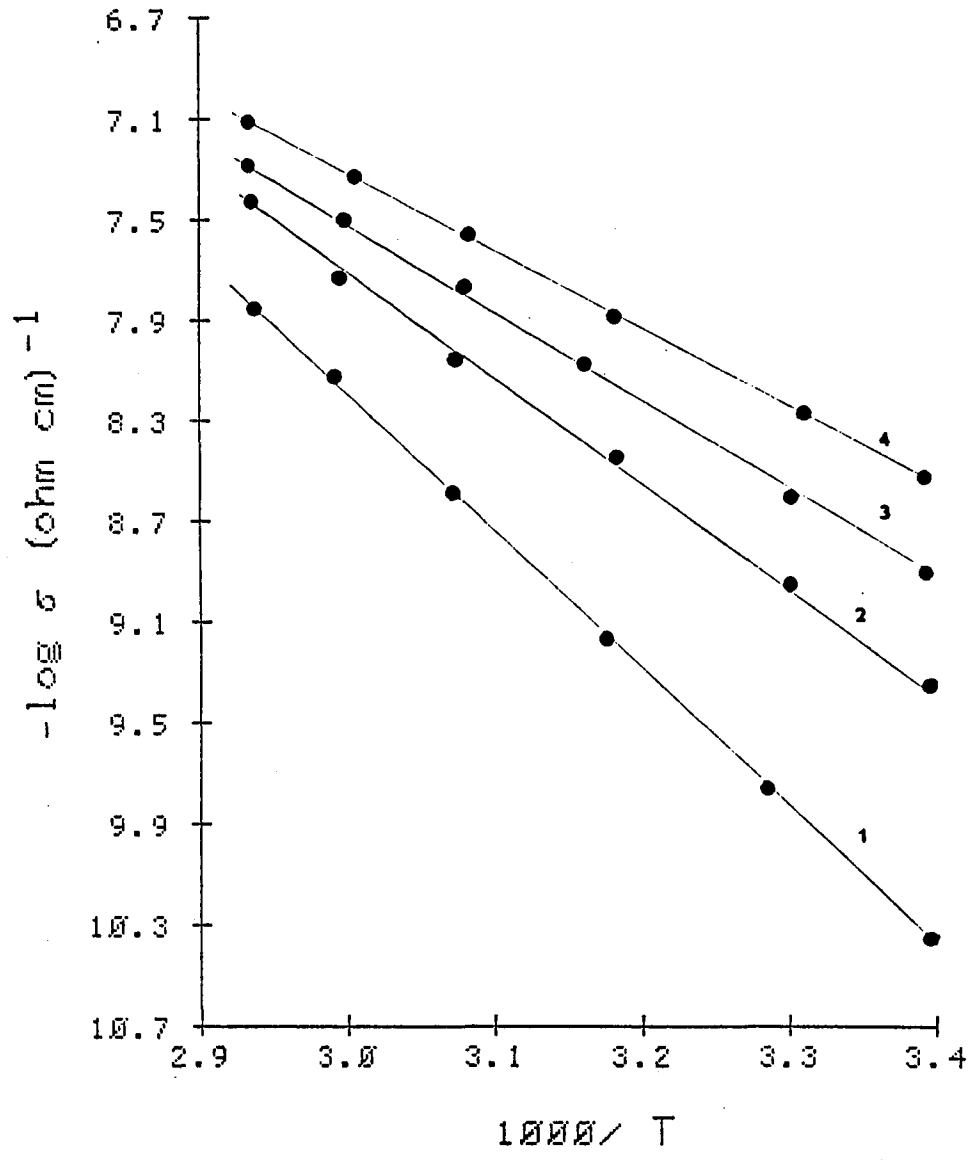

Figure 3.3 Temperature Dependence of Conductivity of Aliquat Salts in Poly(Vinyl Chloride). -- 1. ClO_4^-. 2. NO_3^-. 3. OAc^-. 4. Cl^-.

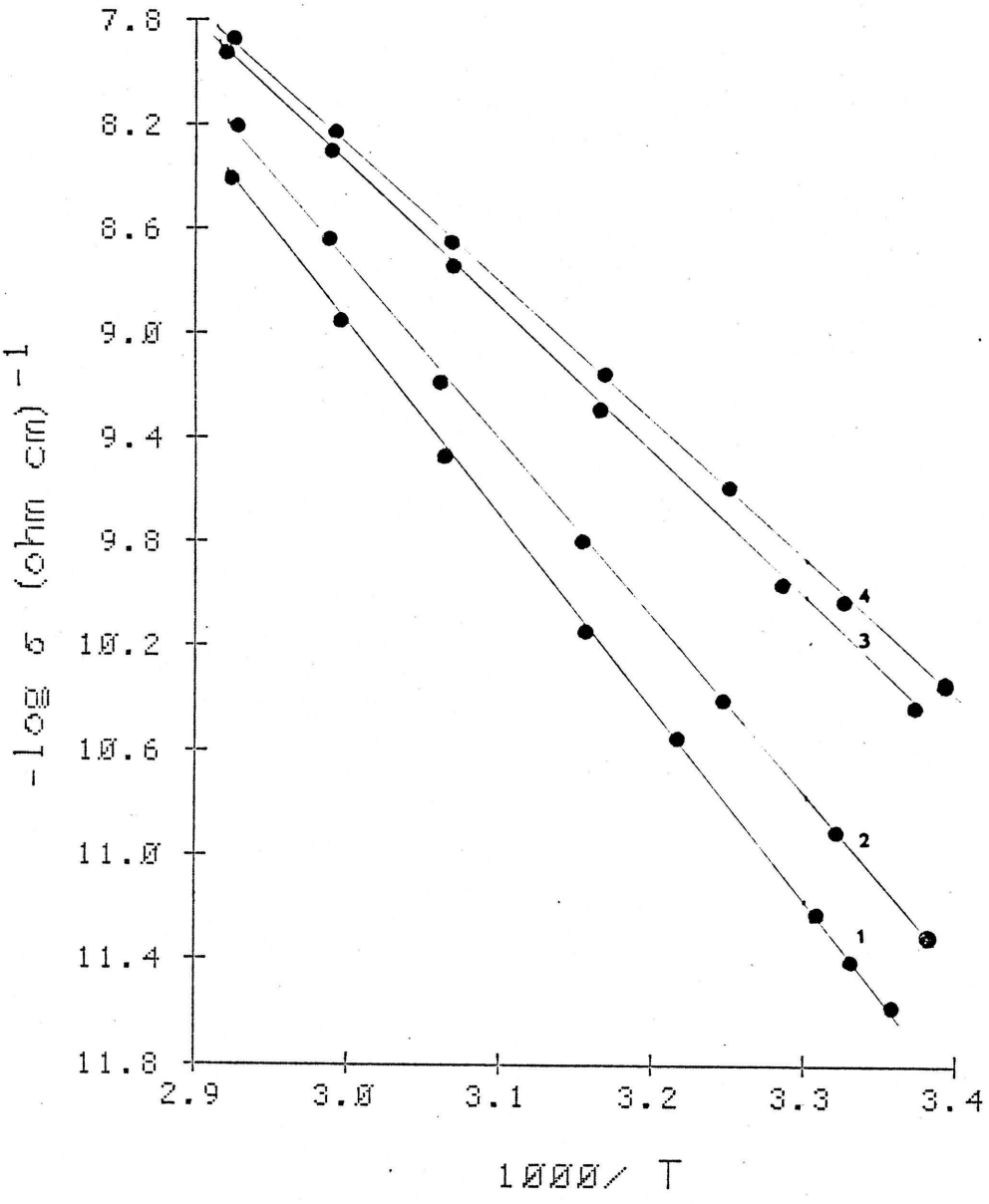

Figure 3.4 Temperature Dependence of Conductivity of Aliquat Salts in Epoxy. -- 1. ClO_4^-. 2. SO_4^-. 3. CNS^-. 4. Cl^-.

$$\sigma = \sigma_0 \exp(-E_a/2kT) \qquad (3.1)$$

where σ is the conductivity, σ_0 is the extrapolated conductivity at infinite temperature, E_a is the semiconductor activation energy, k is the Boltzmann constant (8.617×10^{-5} electron volts), and T is the absolute temperature. Thus, the temperature dependence of electrical conductivity is characterized experimentally by the two constants, E_a and σ_0.

As may be seen from Table 3.1, listing the values of E_a calculated for a series of Aliquat salts in various polymeric matrices using Equation (3.1), the activation energies vary from 0.6 to almost 3 electron volts (or 15-75 Kcal/mol). This is in sharp contrast to the behavior of cellulose acetate films impregnated with alkali metal salts which was characterized not only by low conductivity (~ 10^{-14} ohm-cm^{-1}) but also by low activation energies (< 1.0 eV) (91). Although the amount of material sorbed by the film is small (6 μmole/g), the conductivity parameters are still quite useful as a general comparison of a system with many similarities to the ones of this study. Polyaromatic and other organic semiconductors which have been observed to have E_a values similar to ours (92) show conductivities that are 10^{12} or more fold lower than those observed with Aliquat salt-polymer materials (see Figure 3.5).

Earlier surveys of the literature by Many, Harnik, and Gerlick (93) and Gutmann and Lyons (94) have demonstrated the universality of log σ vs. E_a behavior for a number of polynuclear hydrocarbon compounds, suggesting the general relationship:

$$\log \sigma \simeq \alpha E_a + \beta \qquad (3.2)$$

Table 3.1 Conductance Activation Energies for Aliquat Salt-Polymer Films.

Aliquat Salt	Poly(styrene)		Poly(methyl methacrylate)		Poly(vinyl chloride)		Epoxy	
	eV	Kcal	eV	Kcal	eV	Kcal	eV	Kcal
ClO_4^-	0.96	22.1	1.03	23.8	2.05	47.3	2.78	64.1
NO_3^-	0.88	20.3	0.66	15.2	1.53	35.3	-	-
SO_4^{2-}	0.60	13.8	-	-	-	-	2.56	59.0
OAc^-	0.70	16.1	0.67	15.5	1.33	30.7	-	-
CNS^-	0.50	11.5	0.67	15.5	-	-	2.13	49.1
Cl^-	0.74	17.1	0.64	14.8	1.10	25.4	2.08	48.0

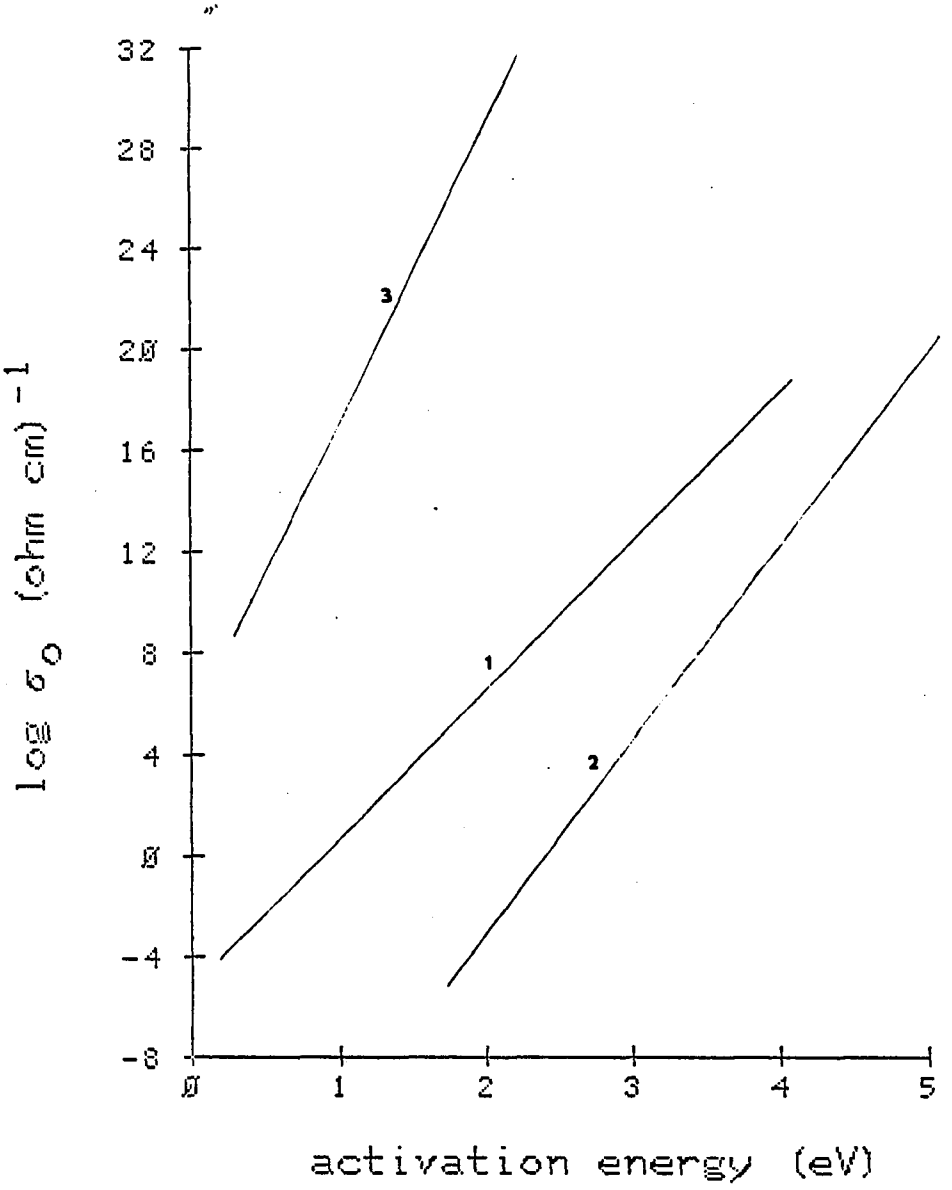

Figure 3.5 Conductivity-Activation Energy Relationships for Various Organic Systems. -- 1. Aromatics. 2. Proteins. 3. Aliquat-ClO_4.

where α and β are constants for the entire class of compounds. Eley (in 95) pointed out that a somewhat similar relationship has been known for some time in the inorganic semiconductor field where it is called the Meyer-Neldel rule (96). It should be noted that the Aliquat salts-polymer mixtures not only possess much higher β values but also much larger α terms than have been reported previously.

Another point of similarity in the behavior of these materials to that of organic semiconductors (92, 97) can be shown by making a second type of plot (Figure 3.6) of the Aliquat-ClO_4 data. It is evident from this figure in which the extrapolated lines representing the application of Equation (3.1) intersect, not at $T^{-1} = 0$ but rather at a "characteristic temperature," T_0, found here to be equal to 375°K. These results can be described by the three-constant equation:

$$\sigma = \sigma_0' \exp(-E_a/2kT_0) \exp(-E_a/2kT) \quad . \tag{3.3}$$

Equation (3.3), compared to the original semiconductor equation (Equation 3.1), yields the often observed (98) identity (see Figure 3.7):

$$\sigma = \sigma_0' \exp(-E_a/2kT_0) \tag{3.4}$$

Expressed logarithmically, Equation (3.4) becomes:

$$\log \sigma_0 = (2kT_0)^{-1} E_a + \log \sigma_0' \tag{3.5}$$

which is exactly the form of the Meyer-Neldel rule as expressed in Equation (3.2), with $(2kT_0)^{-1} = \alpha$ and $\log \sigma_0' = \beta$.

Characteristic temperature, T_0, values reported include T_0 = 350°K for aromatic compounds and 430°K for proteins (95). Rosenberg (98) calculated a value of 490°K for oxidized cholesterol.

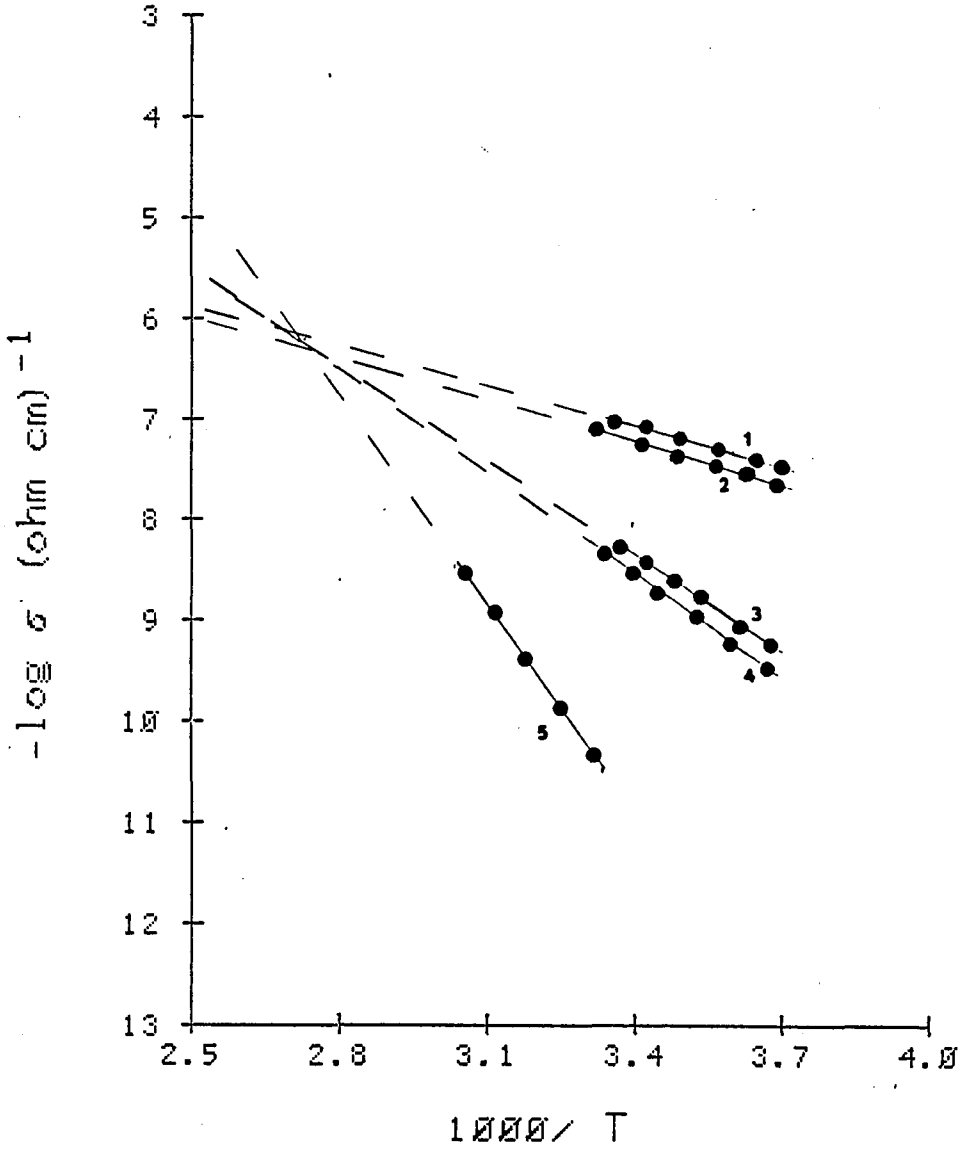

Figure 3.6 Temperature Dependence of Conductivity of 0.3 M Aliquat-ClO_4 in Various Polymeric Matrices. -- 1. Poly(ethylene). 2. Poly(styrene). 3. Poly(methyl methacrylate). 4. Nylon-66. 5. Epoxy.

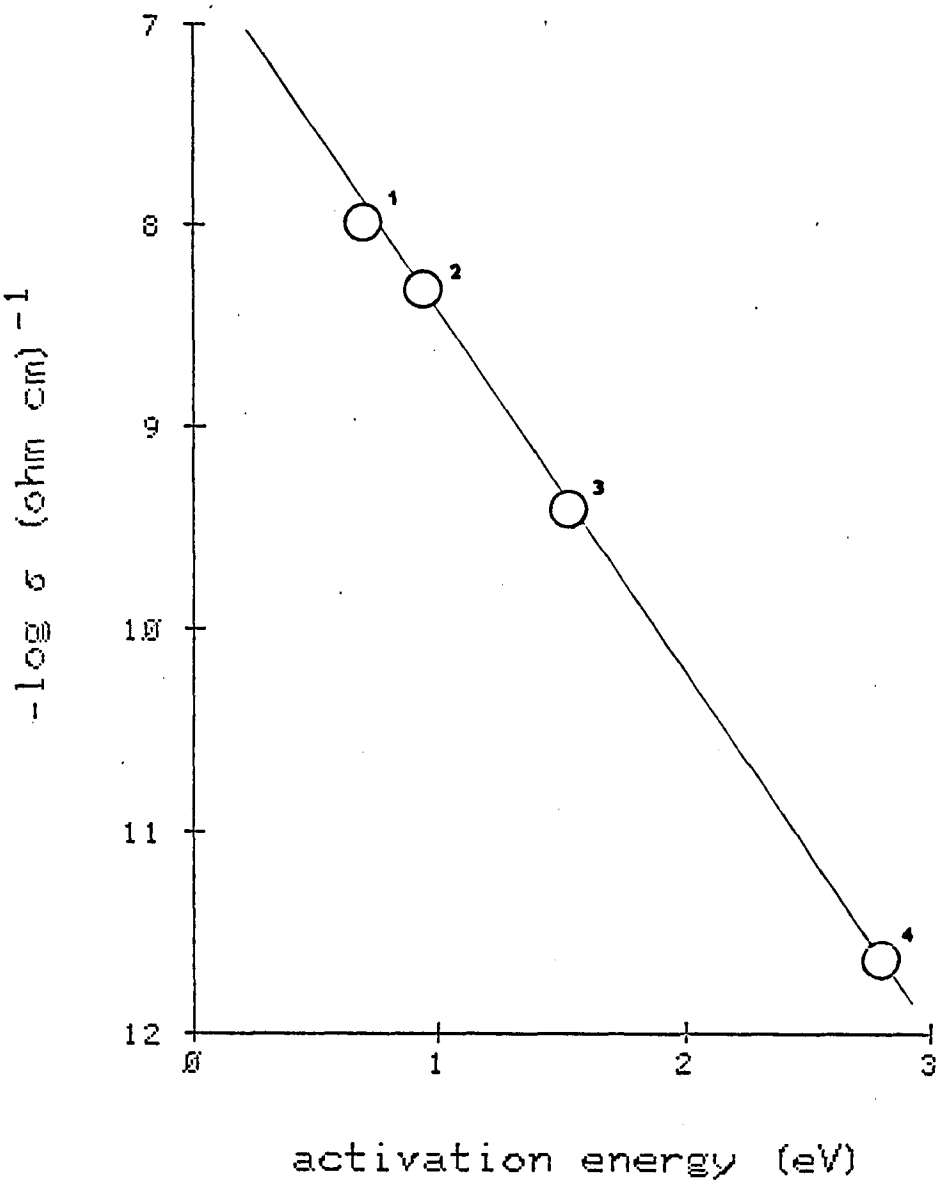

Figure 3.7 Conductivity-Activation Energy Relationship for Aliquat-ClO_4 in Various Polymeric Matrices. -- 1. Poly(ethylene). 2. Poly(styrene). 3. Poly(methyl methacrylate). 4. Epoxy.

Equations as shown above for the rate of transfer of charge-carrying particles within a solid or liquid matrix can be put into the more familiar form of activated complex theory (99):

$$k_f = (kT/h) \exp (\Delta S^{\neq}/R) \exp (-\Delta H^{\neq}/RT) \qquad (3.6)$$

where k_f is a rate constant, and $\Delta S^{\neq}$ and $\Delta H^{\neq}$ are entropy and enthalpy of activation, respectively. In addition, there are many examples in other areas, especially in heterogeneous catalysis (100) of so-called "compensation relations" of the form:

$$\Delta S^{\neq} = \alpha' \Delta H^{\neq} + \beta' \ . \qquad (3.7)$$

Hence, relationships such as Equation (3.5) exhibit compensation between energy and entropy of activation of the conduction, probably based on fundamental properties of potential energy curves and free volume.

As alluded to earlier, if the activation energy within a class of organic semiconductors is varied in any manner, the compensation relationship (Equations 3.3-3.5) can be experimentally verified. An interesting experiment demonstrating this is shown in Figure 3.8; differing amounts of water have been added to a R_4N^+,Cl^-/epoxy film causing the conductivity (and E_a) to change greatly. The proposed mechanism of this compensation behavior (Figure 3.9) will be discussed in subsequent sections.

The primary concern of these investigations has been to identify the charge carriers and quantitatively evaluate the parameters involved in their generation and mobility. The difficulty in determining the mechanism of conduction in organic materials is compounded by the similar behavior of both ionic particles and electrons when they are thermally

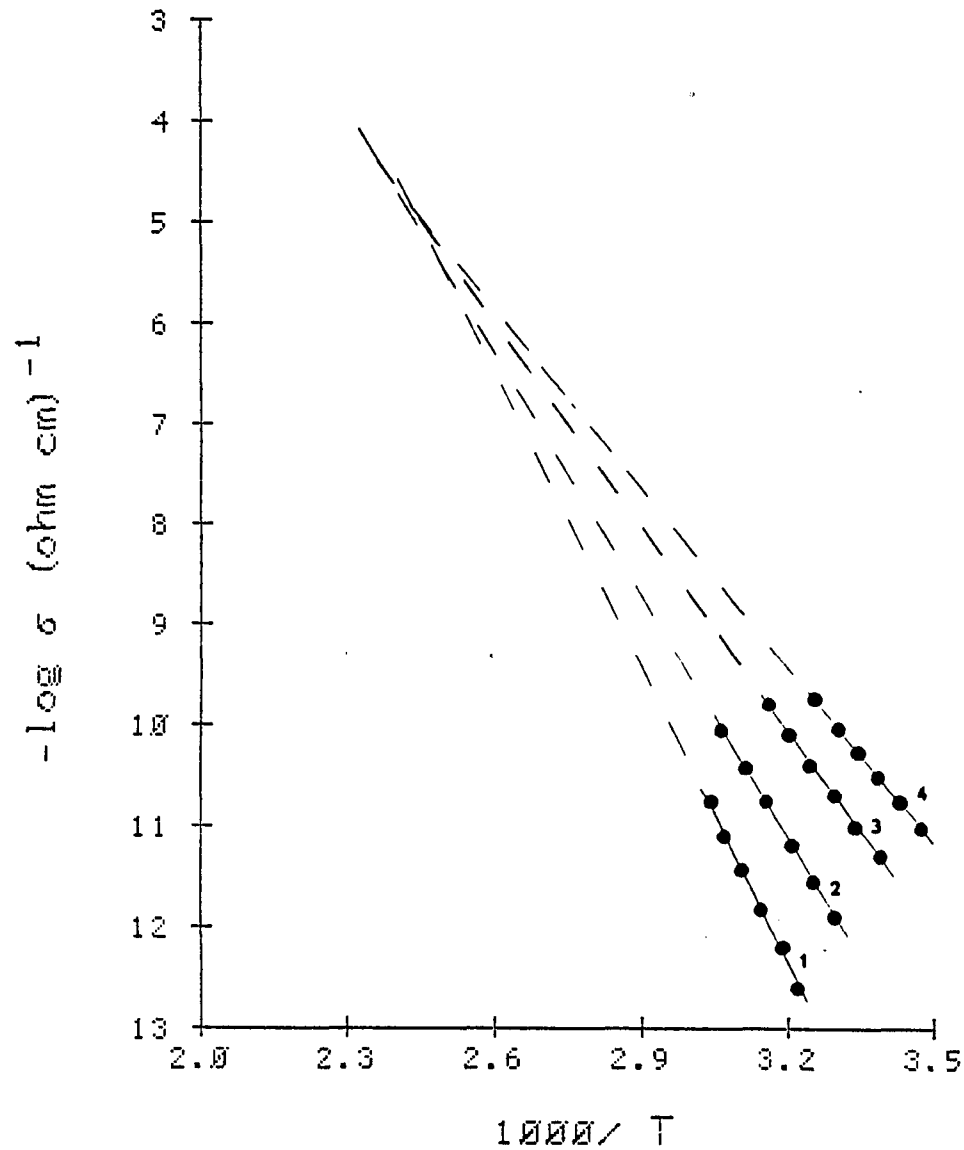

Figure 3.8 Temperature Dependence of Conductivity of 0.1 M Tetra-Pentylammonium Chloride in Epoxy Resin as a Function of Water Content (Wt %). -- 1. 0%. 2. 1.1%. 3. 1.8%. 4. 4.6%.

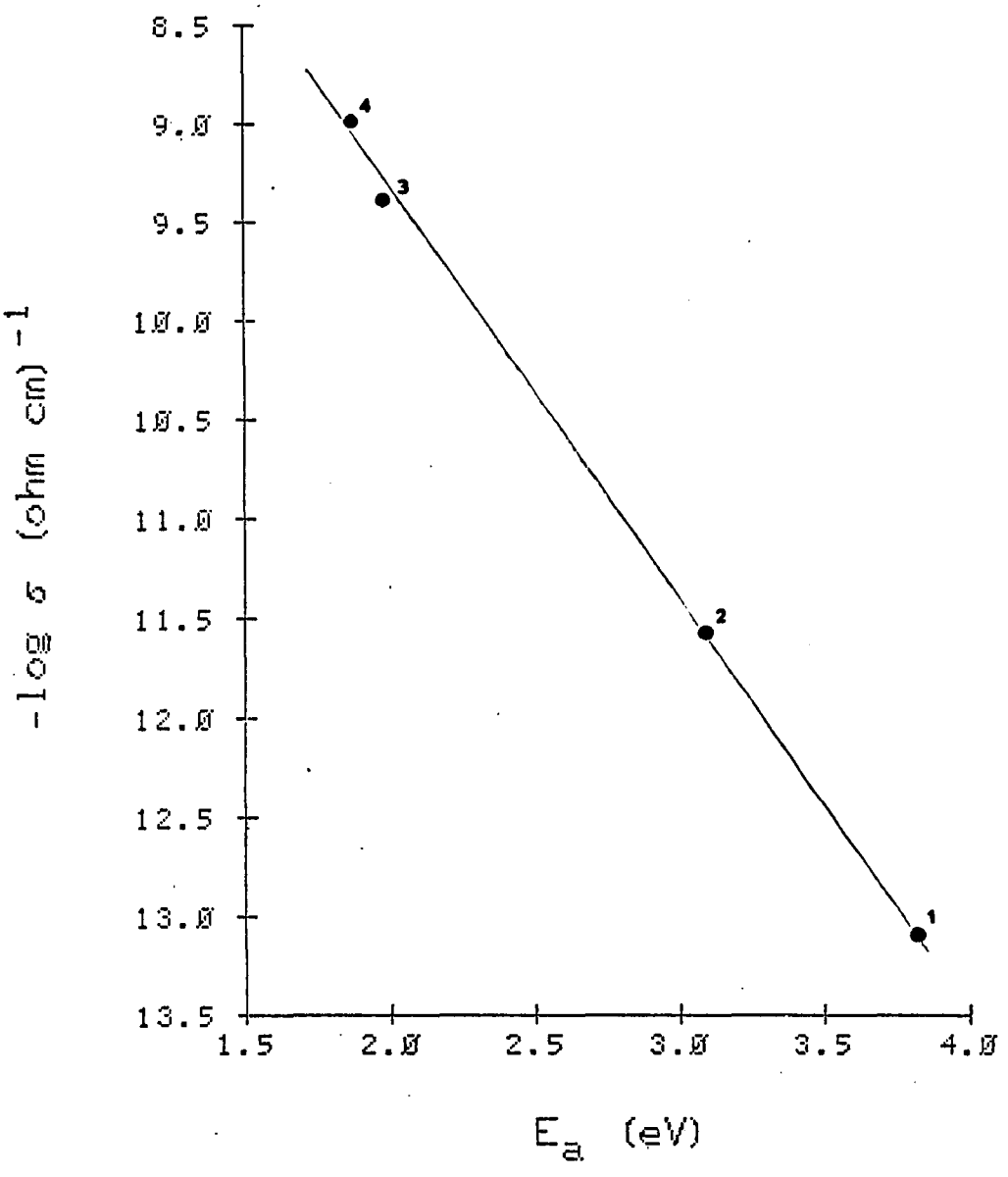

Figure 3.9 Conductivity-Activation Energy Relationship for Tetrapentyl-Ammonium Chloride in Epoxy Resin as a Function of Water Content (Wt %). -- 1. 0%. 2. 1.1%. 3. 1.8%. 4. 4.6%.

stimulated to promote electrical conduction. Regardless of the carrier types, a general description of the conductivity has the form:

$$\sigma = \sum_i q_i n_i(T)\mu_i(T) \qquad (3.8)$$

where q_i is the charge, n_i the number, and μ_i the mobility of the ith charge carrying species. The incorporation of the high concentrations of weakly dissociated ionic salts into a polymer matrix will tend to "swamp out" the effects of residual ionic or electronic carriers found as impurities. The reported concentration of ionogenic impurities in a variety of polymeric materials has shown that an upper limit of ca. 1% can be expected (101). More typically, however, a pure polymer will have much lower impurity levels (102). The result of doping with such a high concentration of ionic material is that at least part, if not all, of the observed conductivity will be ionic. For an ionic process, the observed conductivity relationship (Equation 3.1) can be expressed in combination with Equation (3.8), giving:

$$\sigma = qn_0 \exp(-E_c/2kT)\ \mu n_0 \exp(-E_\mu/kT) \qquad (3.9)$$

or, combining terms:

$$\sigma = \sigma_0 \exp[-(E_c + 2E_\mu)/2kT] \qquad (3.10)$$

where E_c and E_μ are the activation energy of carrier generation and mobility, respectively, and σ_0 contains the terms μ and n_0. Models to describe the observed electrical conductivity must, therefore, include parameters for both carrier generation and mobility.

Experimental studies described here and in subsequent sections have been formulated in an attempt to separate and individually characterize E_c and E_μ terms.

Turning to the aspect of carrier generation in the quaternary ammonium salt systems, the primary source for the generation of ionic charge carriers is the dissociation of R_4N^+ salts, e.g.:

$$\underset{n_0(1-\alpha)}{R_4N^+ \cdot Cl} \rightleftarrows \underset{n_0\alpha}{R_4N^+} + \underset{n_0\alpha}{Cl^-} \qquad (3.11)$$

for which an equilibrium expression $K = \alpha^2 n_0/1-\alpha$ can be written. For such cases, Barker and Sharbaugh (91) have developed a relationship of ionic conductivity and the equilibrium constant by using the equation:

$$\sigma = [(Kn_0)^{1/2} \exp (-U_0'/2\varepsilon'kT)](\mu_+ + \mu_-)e \qquad (3.12)$$

where ε' is the effective dielectric constant of the system, U_0' is the energy needed to separate the ions in the vacuum, μ is the ion mobility, and e is the electronic charge.

As indicated by Equation (3.12), the conductivity would be expected to vary with the square root of the concentration of the ion pair for 1:1 electrolyte impregnated polymers. Experimentally such relationships are known (103). Figure 3.10 shows the temperature dependence of conductivity as a function of Aliquat-ClO_4 concentration for an epoxy matrix. Inasmuch as the conduction varies by six orders of magnitude, while the concentration varies by only a factor of twelve, Equation (3.12) cannot adequately describe the observed behavior. Such apparently contradictory behavior can be more fully clarified by

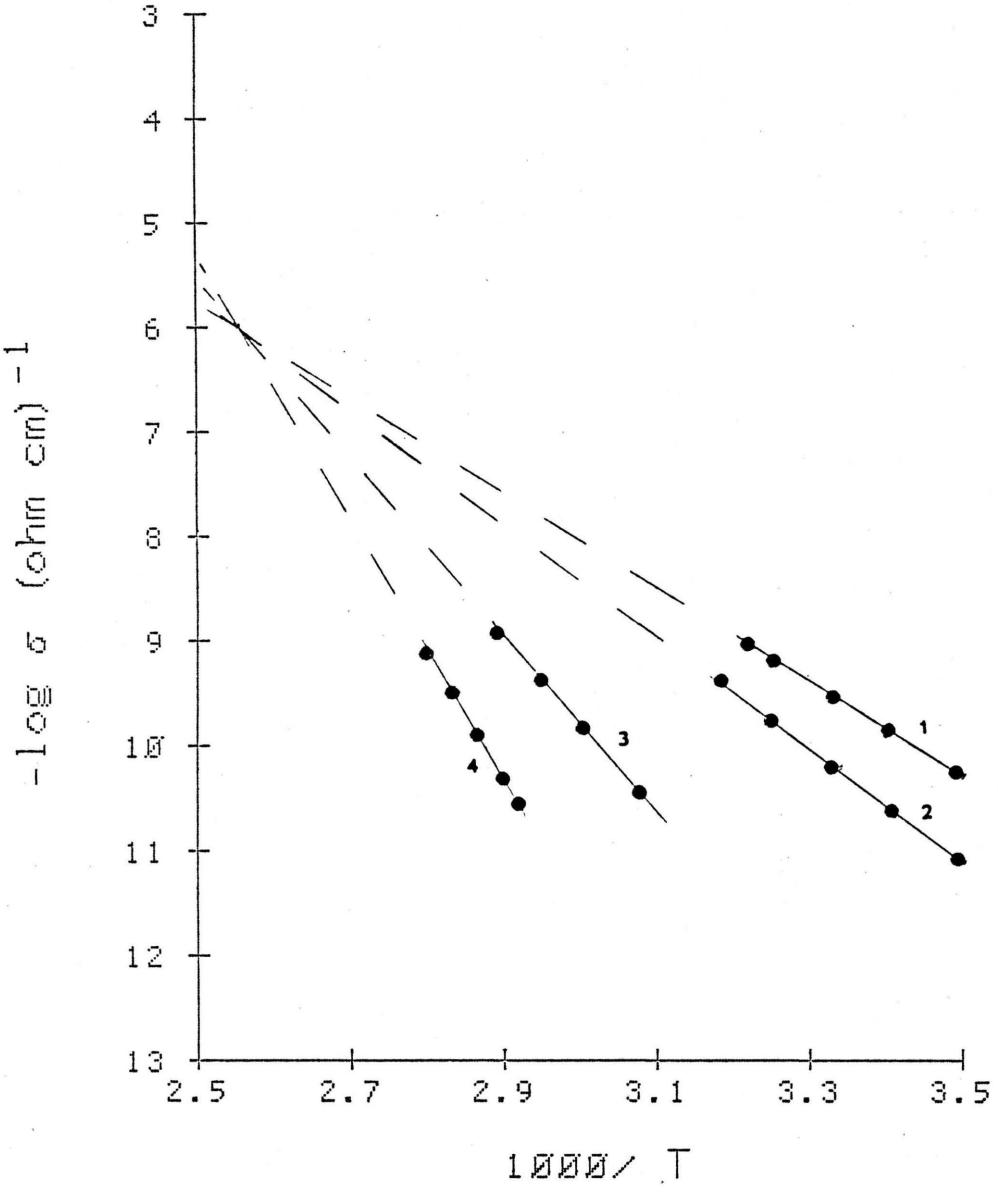

Figure 3.10 Temperature Dependence of Conductivity of Aliquat-ClO_4 in Epoxy Resin as a Function of Concentration. -- 1. 1.2 M. 2. 0.92 M. 3. 0.20 M. 4. 0.09 M.

referring to the data presented in Table 3.2 for Aliquat-Cl polymer mixtures. These data show, as King and Medley (104) have pointed out, that the addition of electrolytes to polymers in sufficient concentration increases the dielectric constant, which leads to greater dissociation. Moreover, ionic migration is facilitated by the plasticizing effect of the salt. Both phenomena thereby complicate the relationship between conductivity and the concentration of electroactive material.

Indeed, the conductivity-concentration data can be adequately described by properly considering the changes which occur in the dielectric constant (Section 3.1.4).

As seen from Equation (3.10), values of the activation energy can be described as comprising contributions from charge generation, i.e., dissociation of ion pairs, as well as from ion mobilities. From the Bjerrum theory, one can expect, in a series of ion pairs having the same cation, that the dissociation energy would decrease with increasing anionic radius. To this end, the original R_4N^+,X^- series of salts (Table 3.1) was expanded to include large, organic anions as shown in Table 3.3 (higher concentrations of electroactive material were used so exact correspondence is not possible).

This situation is even more complicated because of the formation of micellar aggregates. Light scattering and vapor pressure studies have suggested the existence of a 3-mer and a 25-mer for tetraheptylammonium nitrate and chloride in benzene solutions (105). Although ionic mobility depends on size, its temperature coefficient, and therefore E_μ, reflects the temperature variation of viscosity of the medium and is therefore

Table 3.2 Conductivity of Aliquat-Cl Polymer Films as a Function of Concentration.

Aliquat-Cl (wt %)	(M)[a]	ε' (1 KHz)	-log σ 25°C $(\Omega\ cm)^{-1}$	E_a (eV)
Epoxy Matrix				
11	(0.09)	3.5	12.4	2.27
25	(0.20)	4.6	10.2	1.79
50	(0.92)	7.0	7.6	1.44
67	(1.20)	8.0	7.0	1.00
PVC Matrix				
1	-	3.2	13.4	2.34
5	-	5.5	9.3	1.70
11	-	6.7	7.2	1.08
50	-	8.1	6.9	0.58

[a]Approximate concentration in final mixture.

Table 3.3 Conductivity Parameters for R_4N^+,X/Polymer Films.

	PVC[a]		Epoxy[b]	
Aliquat-336S Salt	E_a (eV)	-log σ 25°C $(\Omega\ cm)^{-1}$	E_a (eV)	-log σ 25°C $(\Omega\ cm)^{-1}$
Cl^-	0.58	6.9	1.79	10.2
SCN^-	0.60	7.4	-	-
NO_3^-	0.92	8.2	-	-
ClO_4^-	1.25	8.8	-	-
I^-	1.35	9.0	-	-
Benzoate	0.68	7.6	2.28	9.4
Acetate	0.76	8.0	-	-
Laurate	0.82	7.9	2.04	8.8
1-Amino-2-naphthol 4-sulfonate	1.55	9.5	-	-
p-Toluene sulfonate	1.06	9.6	2.36	9.8

[a] 0.2 g PVC + 0.2 g Aliquat salt.

[b] 0.3 g epoxy + 0.1 g Aliquat salt.

substantially independent of ionic radius (which is independent of temperature). This relationship may be confused by solvation, as in the case of the alkali metals where Li^+, nominally the smallest ion, is large by virtue of hydration. The results of Table 3.3, in particular the inorganic anions, would indicate that solvation of ions may be significant even in these low dielectric constant polymeric matrices.

One can crudely estimate, at least in principle, the relative effect of anion or cation size on the electrical conductivity by recalling (Equation 3.12) that the conductivity should show a square root dependence on the ion-pair equilibrium constant. Approximate calculations of the ion-pair formation constant, K, can be made by using the simplified form of the Born equation:

$$K = \exp\ (336/\varepsilon' r_{ij} RT) \qquad (3.13)$$

where ε' is the dielectric constant of the medium and r_{ij} the distance of closest approach of the ion-pair. The r_{ij} values are obtained by summing the cation radius, derived by extrapolation of Stokes' radii of alkylammonium cations (106), and the anion radius (107). The validity of Equation (3.13) can be proven from a sample calculation of the ion-pair formation constant of tetrapentylammonium nitrate in a low dielectric constant solvent (108); using r_{ij} = 7.28 Å and the dielectric constant of 2.90, the calculated log K = 11.5 compares quite favorably with the measured value of log K = 12.0. A further application of the Born equation to the electrical conductivity data in this investigation is demonstrated in Section 3.1.4.

While the expected relationship between the activation energy of conduction and the anion radius could not be clearly established, the effect of cation size (Table 3.4) seems more in keeping with earlier predictions.

Table 3.4 Effect of Cation Size on the Activation Energy of Conduction for R_4N^+,Cl^-/Epoxy Films.

Cation (0.2 M) R =	Activation Energy (eV)
C,C_9 (Aliquat 336S)	1.80
C_7	2.15
C_6	2.75
C_5	2.70
$C_{4,3,1}$	(see text)

Conductivity measurements for cations smaller than pentyl were not reliable due to the very high resistances encountered. However, the high resistance values themselves might imply that correspondingly higher E_a values would be found for these quaternary ammonium compounds.

3.1.2 Time and Voltage Dependence of Conductivity

As described previously (Section 2.3.5), a strong time dependence of conductivity was observed. Reports (109, 110) of similar time-related phenomena have shown that the asymptotic decrease of conduction can be

characterized by a RC (resistive-capacitance) -like time constant from less than a second to more than 20 min. The limiting (steady-state) current value has been termed the "leakage" current, whereas the time-dependent component of the current is called the "absorption" current (111). Steady-state current was closely approached (within 85-95%) after approximately 10 s in this investigation providing the rationale for the selection of the sampling time (Section 2.3.5).

Current-voltage characteristics of the filled polymer specimens are useful for distinguishing electrode from bulk conduction processes. One must always be suspicious of high activation energy values, i.e., those greater than 1 eV, as they often arise from electrode injection and are totally uncharacteristic of the bulk material. Measurements made on samples with the range of electrodes used showed that current is directly proportional to voltage up to ca. 300 V/cm for the Aliquat-salt/PVC samples and ca. 1.2 kV for epoxy based samples. Figure 3.11 is representative of the behavior observed for the Aliquat salts listed in Table 3.3. For either matrix, conductivity becomes non-ohmic at the higher, yet still relatively low, fields.

Initially, this non-ohmic behavior coupled with activation energies in excess of 1 electron volt (eV), strongly suggests Richardson-Schottky field assisted thermionic electrode emission (112, 113). Hole photoemission studies have indicated that Richardson-Schottky barriers for hole emission from metal electrodes of high work function are on the order of 1.1 to 1.5 eV (114). Similar barriers for electron emission

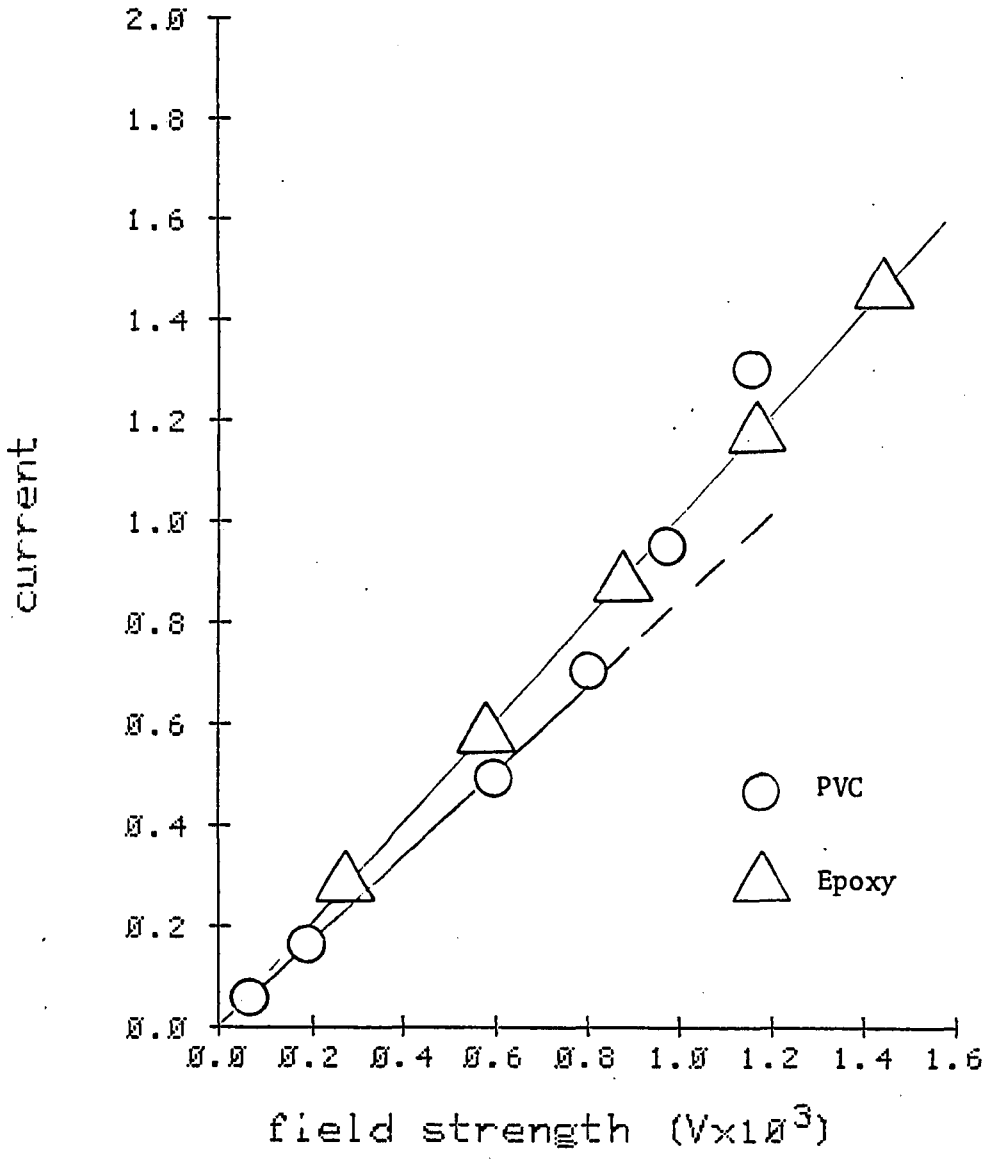

Figure 3.11 Current-Voltage Relationship of Aliquat 336S/Polymer Samples.

from the same metals are expected to be higher (greater than 2.5 eV) -- within the range of values of the epoxy samples.

The Richardson-Schottky equation is usually expressed in the form (113):

$$i = AT^2 \exp (S/kT) \exp (BV^{1/2}) \qquad (3.14)$$

where i is the current density, T the temperature, S is the Schottky (electrode) barrier, V the voltage, and A and B are constants. Analysis of the non-ohmic conductivity regions of the Aliquat salts by application of Equation (3.14) indicates that the expected log (i/V) versus $V^{-1/2}$ relationship does not exist. Therefore, the independence of activation energy with regard to the work function of the metallic electrode, and the absence of a Richardson-Schottky effect may be taken as adequate evidence against electrode injection of holes or electrons (115).

In the case of low-mobility material, a diffusion-limited Richardson-Schottky effect must be considered (116). Such an effect, called the bulk-limited Poole-Frenkel effect (117-119), can be experimentally described by an equation nearly identical to Equation (3.14). Hence, by similar reasoning, it can also be eliminated from consideration.

Amborski (120, 121) has developed a theoretical model which proposes an ionic conduction mechanism explaining non-ohmic conductance. This model assumes that the conductivity arises from the movement of ions in the polymer from their normal lattice to interstitial positions upon the application of an external field. The number, n, of interstitial ions can be calculated from:

$$\eta = N \exp(-E_a/2kT) \tag{3.15}$$

where N is the number of non-conducting ions.

For ionic movement, the ions must overcome the potential energy barrier separating interstitial positions. The probability that thermal energy will supply the energy necessary to accomplish this is:

$$Z = r' \exp(-U/kT) \tag{3.16}$$

where r' is the vibrational frequency of the interstitial ion and U is the height of the potential energy barrier. The barrier height is modified by the application of an external field, given by:

$$U \pm eVd/2 \tag{3.17}$$

where e is the charge of the ion and d the distance between equilibrium positions. The barrier height is decreased in the direction of the applied field (represented by a negative field quantity) and increased in the opposite direction. The net ionic migration rate can be described as the difference in the rate of migration in opposite directions, expressed as the difference of two exponential terms:

$$Z = \exp(-U/kT)[\exp(eVd/2kT) - \exp(eVd/2kT)] \; . \tag{3.18}$$

The current density, i, is equal to:

$$i = \eta ed\Delta Z \; . \tag{3.19}$$

In a simplified form for testing the experimental data, Equations (3.18) and (3.19) can be rewritten as:

$$i = a \sinh(bV) \tag{3.20}$$

where a and b are constants, i is the measured current, and V the voltage. As is demonstrated in Figure 3.12, the voltage dependence of

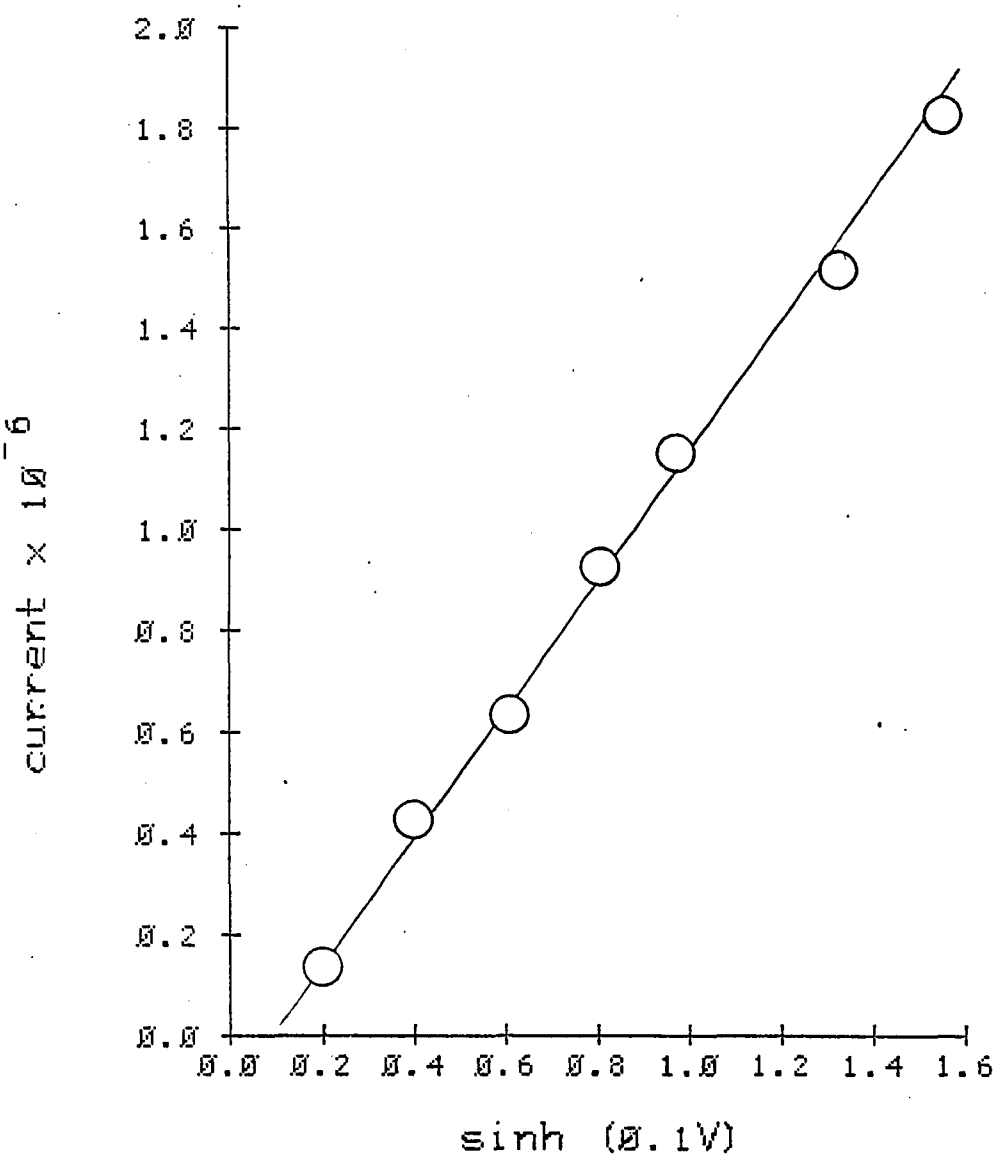

Figure 3.12 Hyperbolic Sine Relationship of Voltage to Current for Aliquat-336S in Poly(Vinyl Chloride).

Aliquat 336S in PVC (data from Figure 3.11) follows the relationship $i = 2 \sinh (0.1 V)$.

Similar hyperbolic sine relationships for the voltage dependence of conductivity in glasses has been observed (122). Experimental evidence clearly shows that conduction in these glasses is ionic, arising from the migration of sodium ions.

Time dependence of conductivity and non-ohmic behavior are often given as evidence supporting an ionic mechanism (101). Time-dependent phenomena of organic materials are usually described in terms of polarization, e.g., movement of polar groups within the moleculr, or "blocking" effects resulting from the accumulation of electrolysis products at the electrode. Further, one rarely observes non-ohmic behavior in electronic conduction systems unless extremely high field strengths are employed (typically greater than 30 kV/cm).

Our observation of persistent time-dependent properties and non-ohmic conductivity would, therefore, be supportive of an ionic process.

3.1.3 Electrolysis Study

Time-dependent conductivity, as described in the previous section, is attributable to polarization within the sample. Unfortunately, from a mechanistic viewpoint, sample polarization can occur either by electronic, dielectric polarization, or from ionic migration resulting in "electrode blocking" effects.

The transfer of weight after extended application of d.c. voltage can be used as a tool in distinguishing between the two conduction modes. If the conduction process is electronic, then no measurable weight

transfer is expected. On the other hand, conduction by ionic means involves the movement of species having discernible mass. The Tubandt method of analysis (86) is based on detection of weight differences after passing a known amount of electric charge through a sample. The amount of ionic conduction can be estimated by comparison of the experimental weight change to that calculated from Faraday's law. Weight changes less than those predicted from a purely ionic assumption indicate that part, or in the absence of any weight change all, of the observed conductivity is electronic.

Weight changes, ΔW, were calculated from the following ionic conductivity equation:

$$\Delta W = \frac{kMit}{N} \qquad (3.21)$$

where $k = 6.281 \times 10^{18}$ charges/A sec, i is the current, M is the atomic weight of the conducting ion, t is the duration, and N is Avogadro's number of atoms. Due to the time dependence of the current, the product i x t was usually replaced by the coulomb reading of the electrometer.

The results of the test are summarized in Table 3.5. Weight changes in the anode (electrode or electrode and outside section) were calculated by assuming ionic conductivity by Cl^- and its subsequent reaction with the copper-foil electrode. As mentioned above, ionic conductivity should result in a change of weight.

Table 3.5 Weight Change after Electrolysis.

	Weight Change Observed in			Calculated for Anode (g)
	Sample (g)	Cathode (g)	Anode (g)	
Method I				
1.22×10^{-4} A for 14 hrs	-0.00221	+0.00294	+0.00208	(+0.0019)
Method II				
2.5×10^{-5} A for 28 hrs	+0.00008	+0.00244	+0.00092	(+0.00076)

Epoxy samples through which 1-5 coulombs were passed exhibited visible electrode deposits. When copper electrodes were used, the anode was pitted and a green-blue material, evidently a Cu(II) salt, was deposited on the surface; the cathode was covered by a thin layer of a colorless oil. The fact that such deposits were not observed when epoxy alone was used eliminates the possibility of significant contribution of polymer electrodegradation products.

Analysis of cathode reactions and material deposition was not attempted due to uncertainty concerning the nature of the ionic process. Air was not excluded during these experiments making reactions with oxygen or water (vapor) probable. Such reactions are of particular importance for quaternary ammonium cations which are highly deliquescent and form hydroxides readily.

The results presented in Table 3.5 support an ionic conduction mechanism. With both sample arrangements, the experimentally measured

anode deposition products were slightly greater than that calculated for 100% ionic behavior. Although no attempt was made to estimate the degree of ionic/electronic conduction, it is clear that much, if not all, of the observed conductivity proceeds through an ionic mechanism.

3.1.4 Dielectric Constant

Dielectric constant, ε', as predicted by the dissociation hypothesis (Equation 3.12) and the Born equation (Equation 3.13) would be expected to exert a very strong influence on the observed electrical conductivity. Both these equations involve inverse first-order dependence on ε' of the log σ as might be expected from the recognition that the process of a movement of charge is charge separation.

The large change in dielectric constant that occurs with changes in quaternary ammonium salt concentration was used to determine the influence of dielectric constant on conductivity. Of course, changing ε' by simply altering the salt concentration neglects the parameters n_0 and μ in Equation (3.12). Nevertheless, as predicted by the dissociation hypothesis, a linear dependence of log σ of $1/\varepsilon'$ with a high degree of correlation was observed (Figure 3.13). Interestingly, this relationship seems nearly independent of the polymer matrix. The slope of the line in Figure 3.13, 0.35, can be compared to those observed in similar studies of alkali-metal salts in hydrated cellulose (slope = 0.6) or to the slope of such a plot for a large number of organic solvents (slope = 0.2) (91).

Although the purpose of the above comparison was to demonstrate the influence of dielectric constant on the electrical conductivity, inclusion of the n_0 parameter in the overall conductivity expression

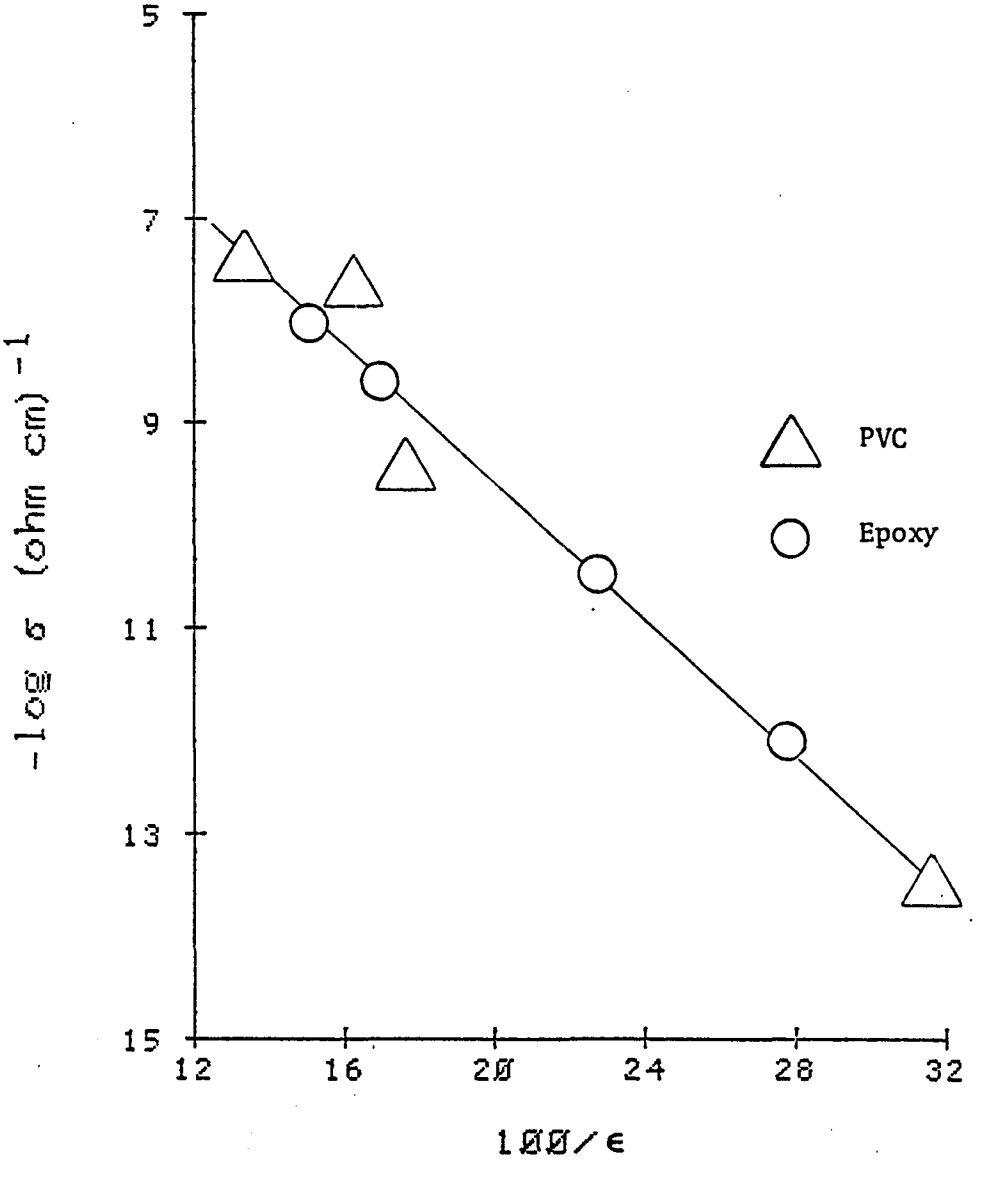

Figure 3.13 Conductivity-Dielectric Relationship for Various Aliquat 336S/Polymer Samples

(log σ - 1/2 log n_0 vs. $1/\varepsilon'$; Figure 3.14) further verifies the dissociation hypothesis (Equation 3.12).

The previously described lack of a conductivity dependence on the square root of concentration (Section 3.1.1) can now be explained by considering the variation of the dielectric constant in these mixtures. A more valid comparison would involve using the $(Kn_0)^{1/2}$ product where K is calculated from the Born equation (Equation 3.13) using the measured dielectric constant values (see Figure 3.15). With this approach a most interesting comparison can be made to the system, tetrabutylammonium thiocyanate/poly(styrene), studied by Dannhauser (in 123). The reported log σ value of 16.4 for a dielectric constant of 2.67 agrees extremely well (cf. Figure 3.15) with the systems studied here.

Additionally, the empirical similarity of the semiconductor equation (Equation 3.1) to the dissociation equation (Equation 3.12) suggests that the activation energy of conduction should vary with the dielectric constant. The expected reciprocal relationship, Figure 3.16, is demonstrable (correlation coefficient = 0.97) for the epoxy data. Included in this figure are data for hydrated DNA (98). Surprisingly, the PVC activation energy data do not fit an inverse relationship (r = 0.93), but are better expressed (r = 0.99) as a linear relationship with respect to the dielectric constant (Figure 3.17). The reason for this behavior is not clear, but it might reflect the influence of the mobility terms excluded from the relationship.

A final effect mentioned earlier (Figure 3.8) is the increased conductivity which results when water is added to the polymeric mixture.

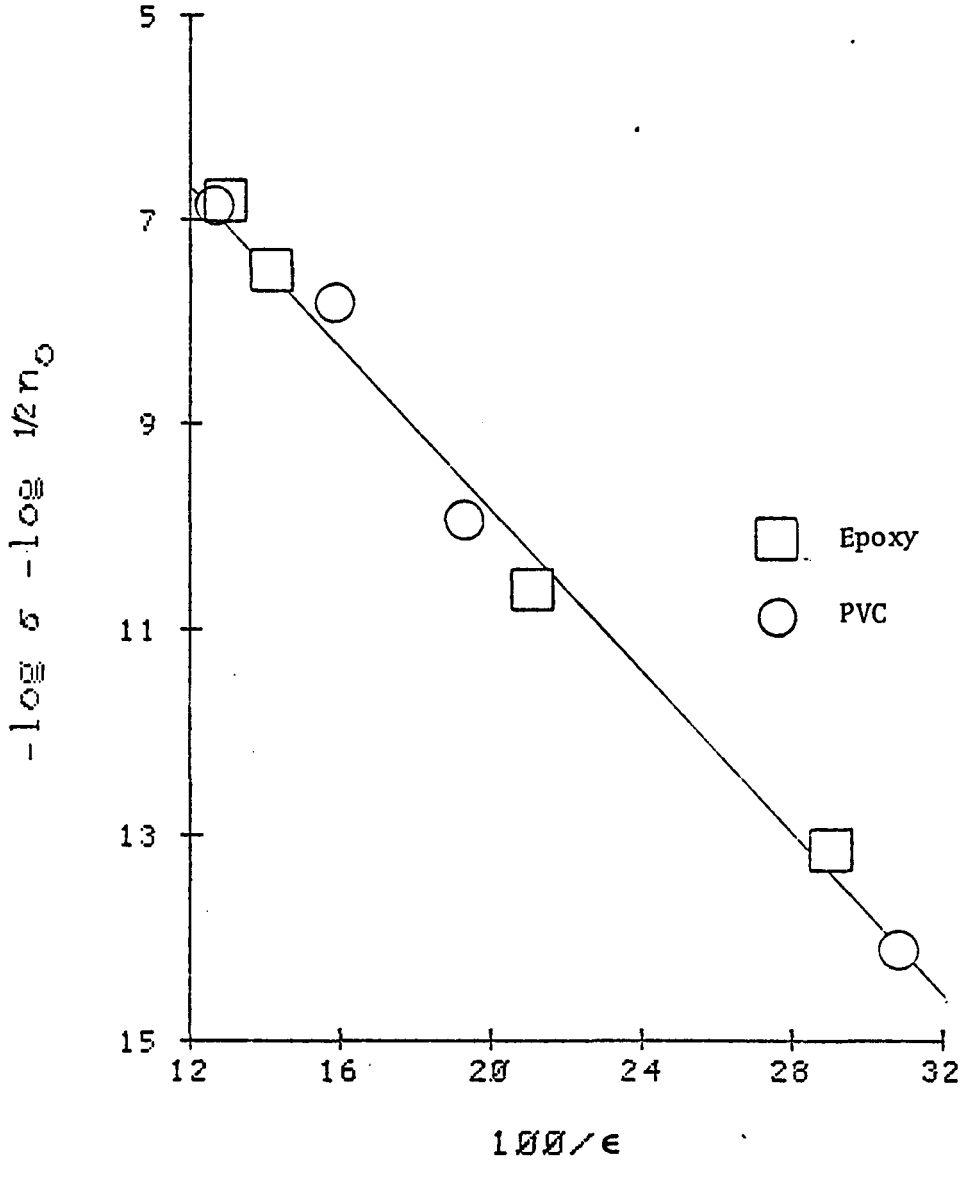

Figure 3.14 Conductivity-Dielectric Relationship for Various Aliquat 336S/Polymer Samples, Concentration Corrected.

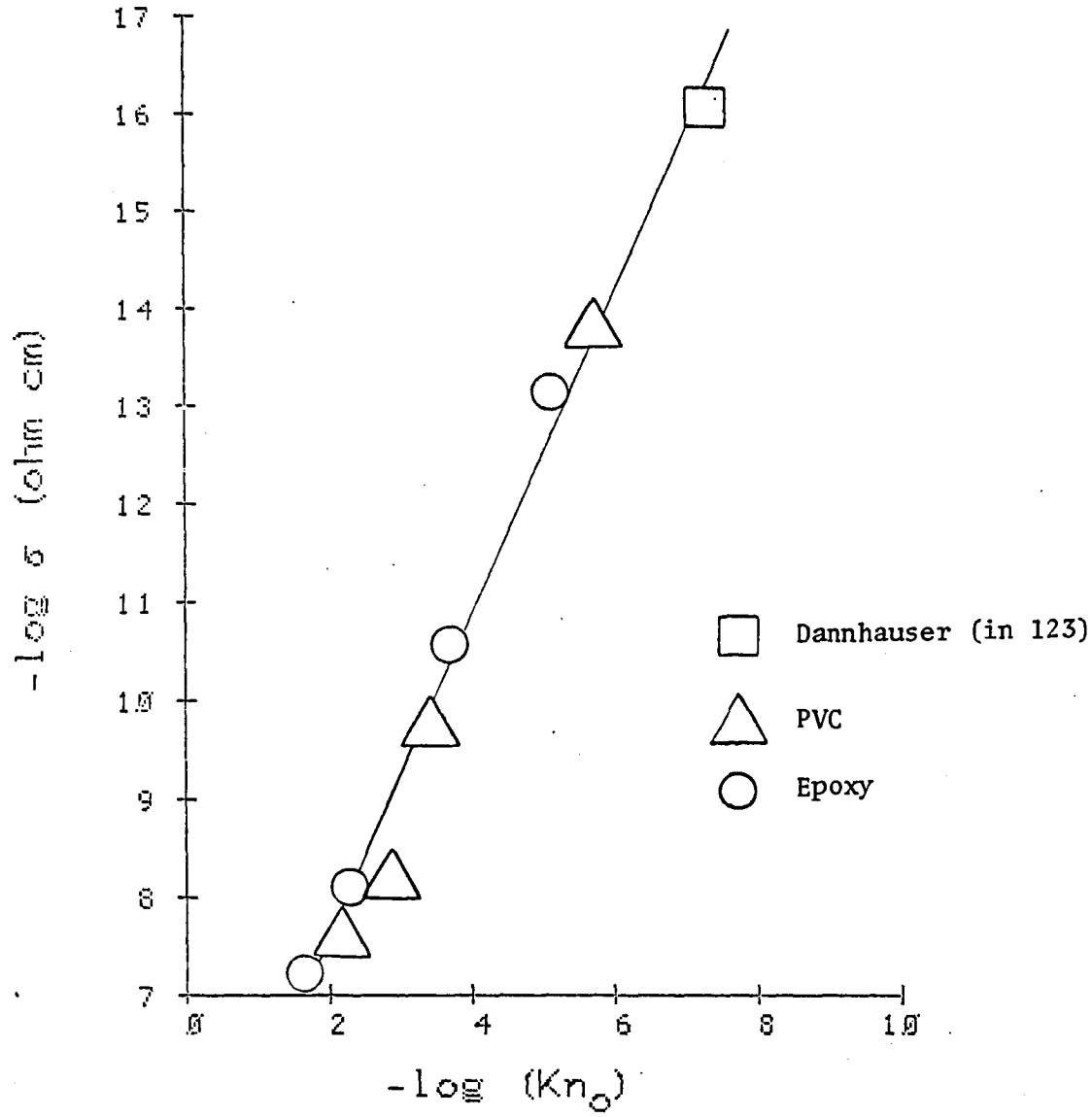

Figure 3.15 Conductivity of Various Quaternary Ammonium Salt/Polymer Mixtures as a Function of Square-Root of Concentration. -- PVC and epoxy data are for Aliquat 336S.

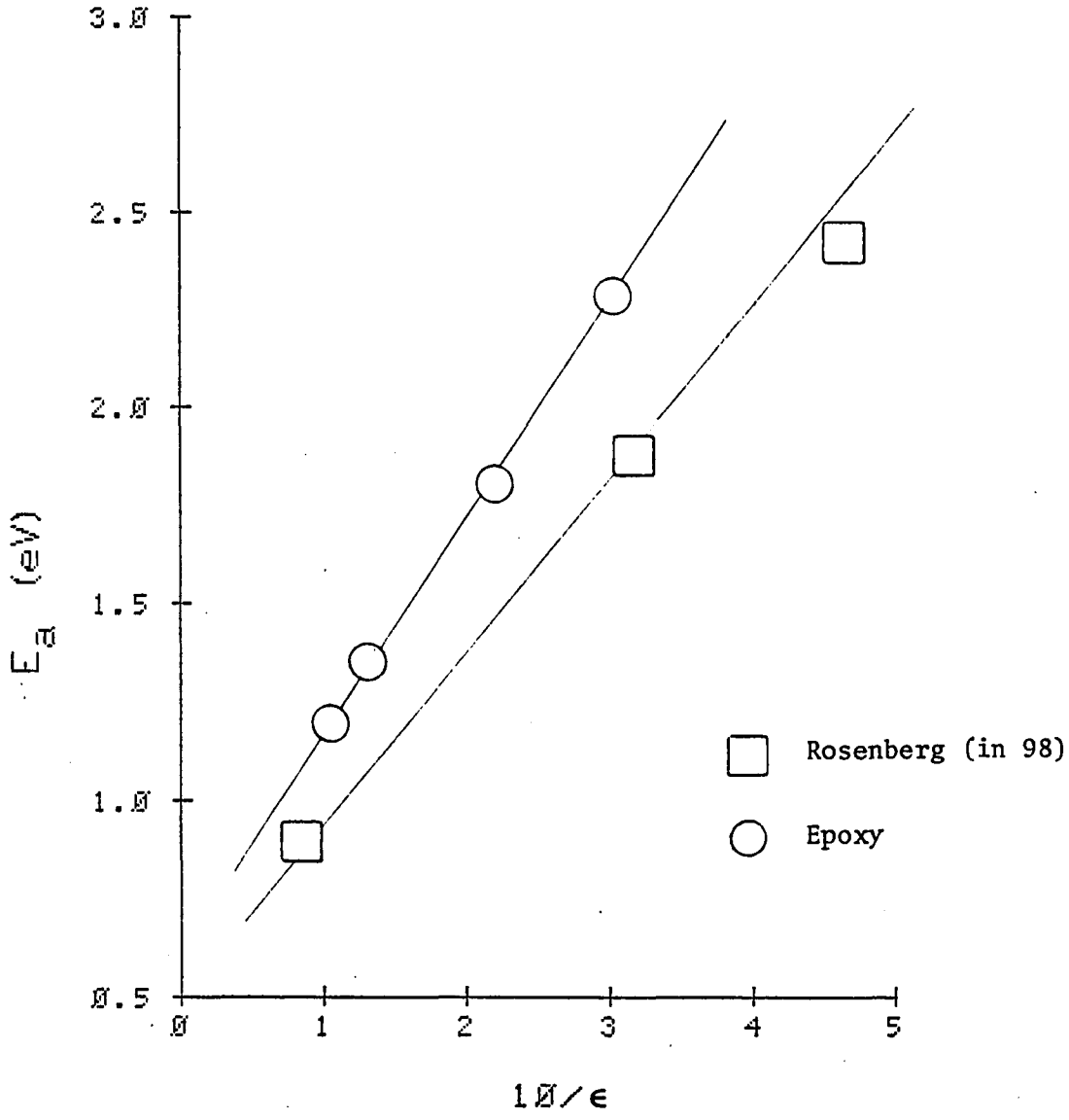

Figure 3.16 Activation Energy-Dielectric Constant Relationship for Aliquat 336S in Epoxy Resin. -- Data of Rosenberg for hydrated DNA are shown for comparison.

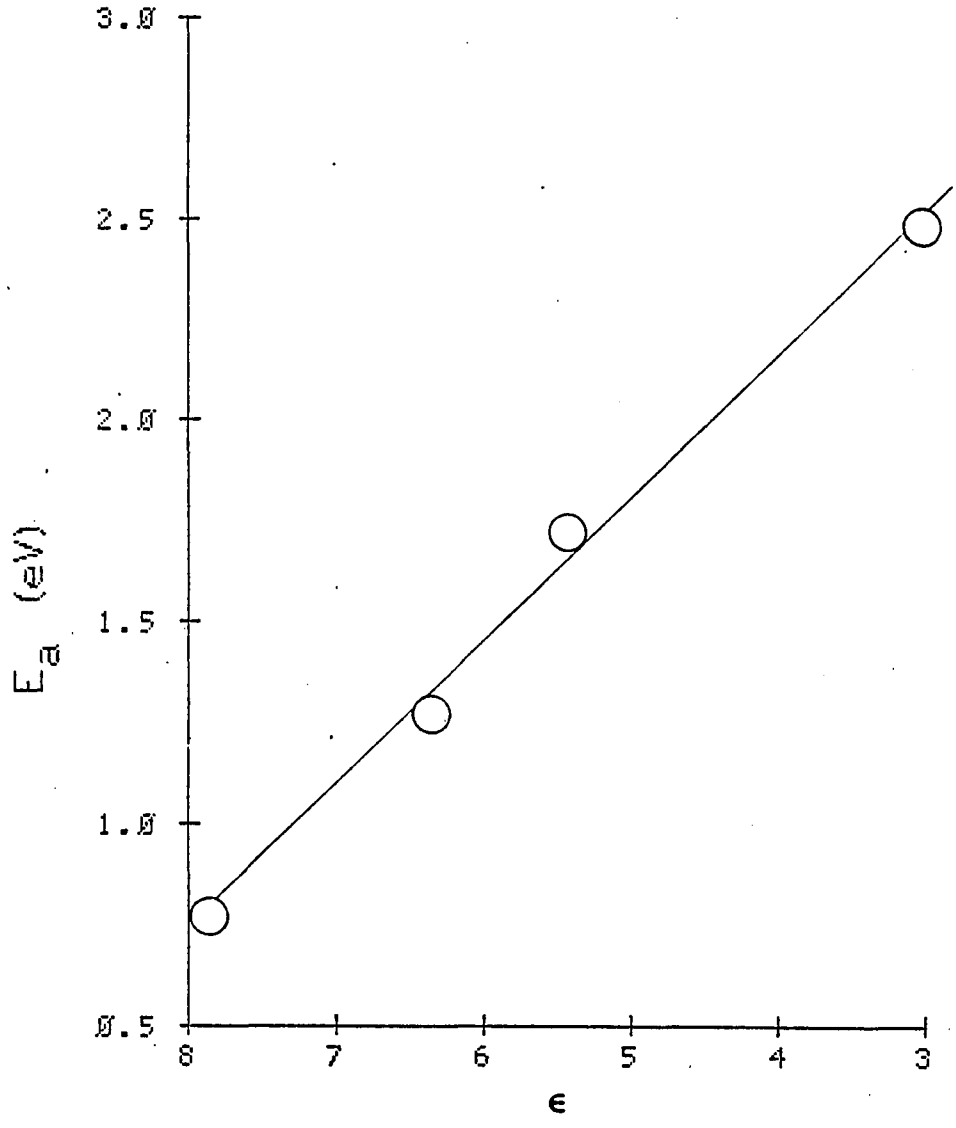

Figure 3.17 Activation Energy-Dielectric Constant Relationship for Aliquat 336S in PVC.

Numerous reports (124-126) have shown that the dielectric constant of many materials is greatly influenced by the sorption of water. An abrupt change in the dielectric properties often occurs at a coverage associated with primary adsorption sites determined from the Brunauer-Emmett-Teller (BET) monolayer. Prior to completion of monolayer coverage, a more gradual increase in dielectric constant as a function of water sorption is observed. Depending of course on the molecule, BET monolayer coverage generally begins at a water content of approximately 8-15% by weight of dry material. Although dielectric constant measurements were not made on the samples to which water had been added, the effect of an apparent increase in dielectric constant can be seen. It is also interesting to notice that the compensation temperature of ca. 400°K compares well to characteristic temperatures obtained by variation of other parameters. The low water content of these samples (less than 1 BET monolayer) assures the absence of conductivity arising from the water itself. Despite the possible contribution of protonic conductivity from the water to the overall electrical conductivity, the increased electrolytic dissociation of the Aliquat salt most likely is responsible for the increased electrical conductivity.

3.1.5 High Pressure Conductivity

The effect of high pressure on the electrical conductivity of a semiconductor can be used to distinguish ionic from electronic conduction. It has been observed that electronic semiconductors, i.e., metal oxides (127), glasses (128), and certain organic materials (129), show increased electrical conductivity as the pressure on the sample is increased,

whereas Sasabe, Yada, and others (in 111) demonstrated that ionic semiconductors show decreased conductivity with increased pressure. Were carriers to move by ionic diffusion, which requires the cooperative action of molecules to form (geometric) holes, loss of free volume due to increased pressure would diminish carrier mobility. Additionally, the production of ionic charge carriers from a dissociation process would also be diminish if, as it is expected, the free volume of the ion pair is smaller than the total free volume of the respective ions. On the other hand, if mobility and carrier concentration increase as pressure is applied, one would expect this to result from the increased tunnelling and hopping available to mobile electrons as pressure decreased the average intermolecular distances (129).

From a high pressure study, one can determine, without prior knowledge of the conduction mechanism, the rather definitive parameter of activation volume for conduction, $\Delta V^{\neq}$, through application of the following quasi-thermodynamic expressions:

$$\Delta V^{\neq} = \left(\frac{\partial \Delta G^{\neq}}{\partial P} \right)_T = - RT \left(\frac{\partial \ln \sigma}{\partial P} \right)_T \qquad (3.22)$$

with the assumption that the sample geometry remains relatively invariant throughout the pressure range utilized in this study.

The free energy of activation, $\Delta G^{\neq}$, has been used in place of E_a (or $\Delta H^{\neq}$) with the assumption that the activation entropy, $\Delta S^{\neq}$, remains constant (undoubtedly true since the temperature is held constant).

One might expect activation volumes involved in ionic (other than protonic) conduction processes to be reasonably large since they would be related to either a molar volume or an ion pair consisting of partners of

about equal size, or at least to the volume of the smaller of two ions as a limiting case (128). Activation volumes involving either protonic or electronic species, on the other hand, might be expected to be small. Proven cases involving electronic conduction have actually exhibited negative activation volumes (129). Such values have been attributed to the increase in the degree of orbital overlap between adjacent molecules that can occur with even moderate pressure increases.

The pressure dependence of conductivity for Aliquat 336S in PVC and epoxy matrices is shown in Figure 3.18 for a typical set of experiments. Activation volumes were computed from the slope of the line (cf. Equation 3.22). Table 3.6 summarizes calculated $\Delta V^{\neq}$ values for a study (the PVC data are shown in Figure 3.19 as representative of typical behavior) in which the concentration of electroactive material was varied. Results for both polymeric matrices clearly show increased $\Delta V^{\neq}$ values as the concentration of electroactive material was increased. Aliquat 336S and similar surfactants are good plasticizers for many polymers (130), including PVC and epoxy; higher concentrations may, therefore, lead to increased plasticization and increased pore size (131) allowing larger cations to diffuse more readily. Hence, the activation volumes may be weighted more in favor of the larger cation, resulting in the larger volumes observed. A similar effect may be seen in a study where cation size was varied (Figure 3.20 and Table 3.7). In this study, activation volumes increased as the cation size decreased, perhaps reflecting the greater contribution that the smaller, more mobile cation makes to the observed conductivity.

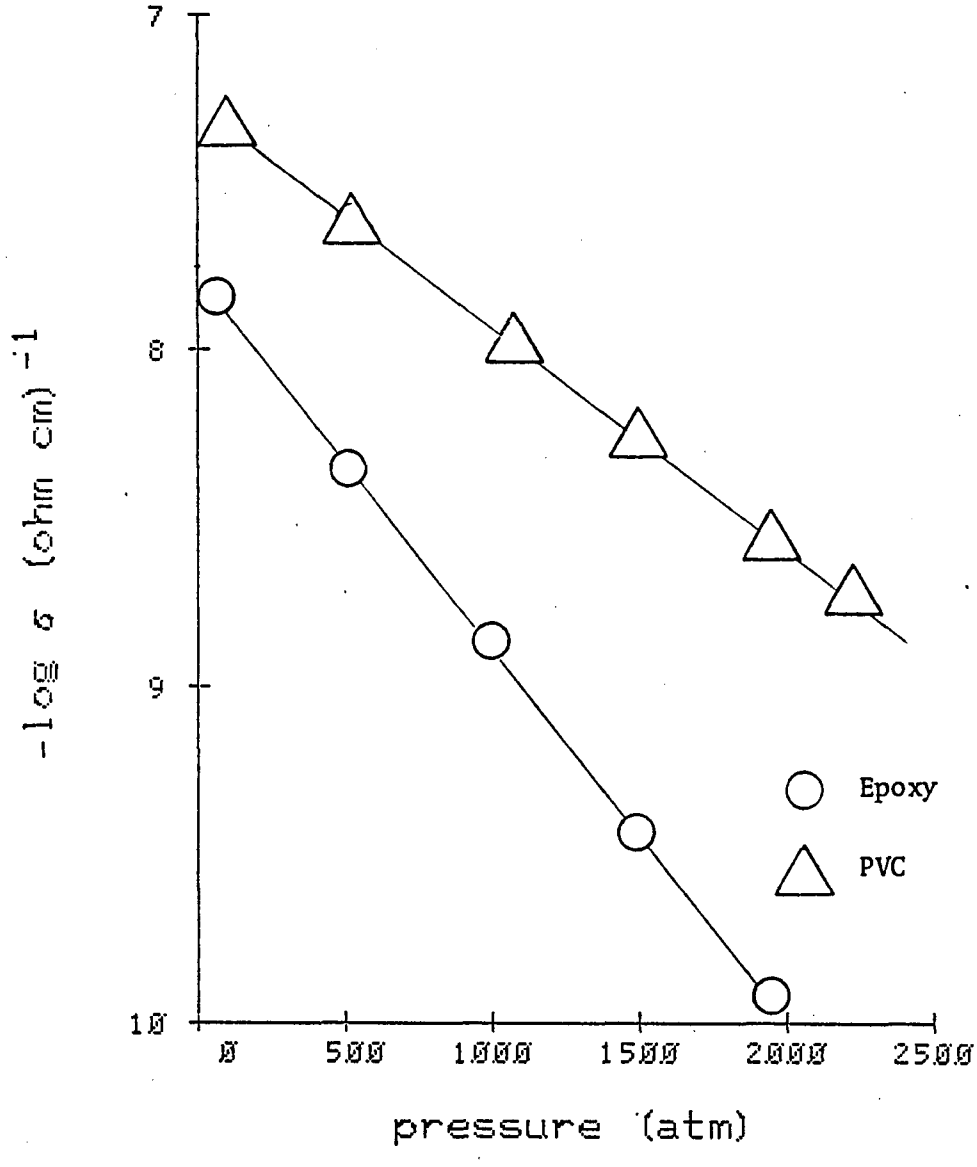

Figure 3.18 Pressure Dependence of Conductivity of Aliquat 336S/Polymer Samples (50 Wt %).

Table 3.6 Effect of Aliquat Concentration on Activation Volumes for Conduction in Epoxy and PVC.

Polymer	Polymer:Aliquat Weight Ratio	$\Delta V^{\neq}$ (cm^3/mol)
Epoxy	1:0.3	39
	1:1	56
	1:2.5	62
PVC	3:1	37
	8:1	34
	20:1	32

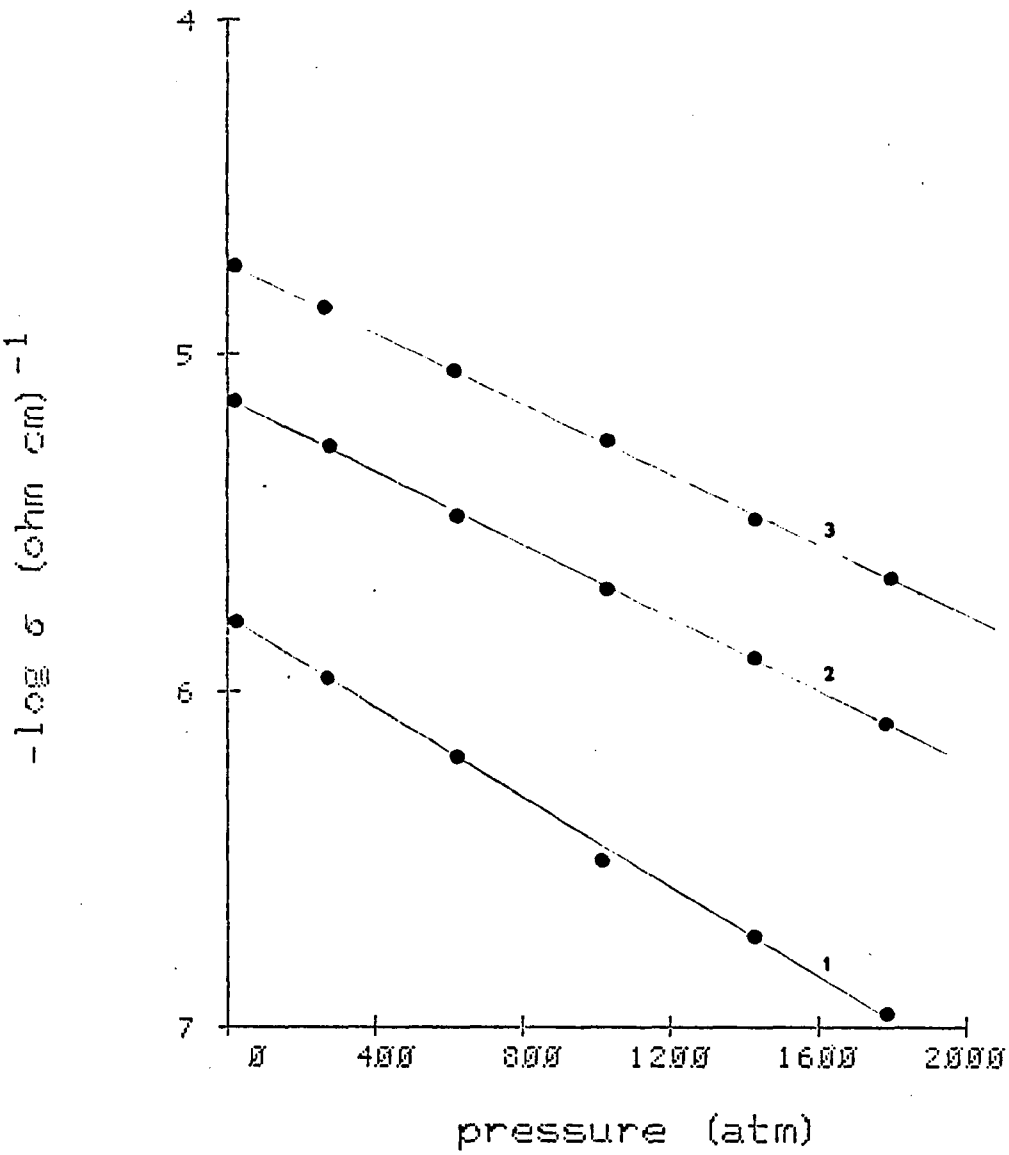

Figure 3.19 Pressure Dependence of Conductivity of Aliquat 336S in PVC as a Function of Concentration (Wt %). -- 1. 25%. 2. 12%. 3. 5%.

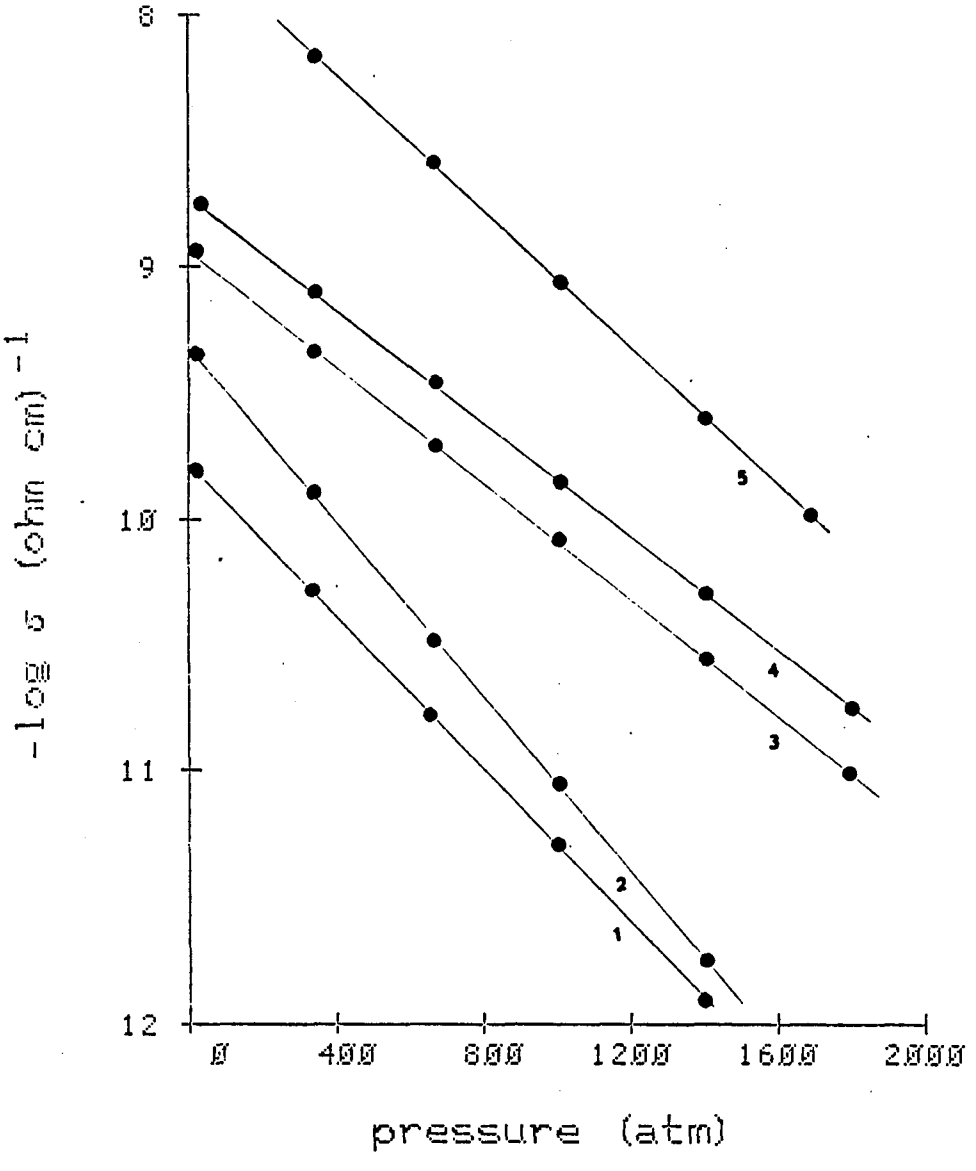

Figure 3.20 Pressure Dependence of Conductivity of Various R_4N^+,Cl^-/PVC Mixtures. -- 1. Butyl. 2. Pentyl. 3. Hexyl. 4. Methyltricaprylyl. 5. Heptyl.

Table 3.7 Activation Volume for Conduction in R_4N^+,Cl^-/Epoxy as a Function of Cation Size.

R =	$\Delta V^{\neq}$ (cm^3/mol)
Butyl	93
Pentyl	87
Hexyl	68
Methyltricaprylyl	65
Heptyl	63

While it is difficult to assign an exact molecular correspondence to these values of $\Delta V^{\neq}$, they are inconsistent in sign with electronic conduction, and in magnitude with protonic conduction. A more detailed interpretation of activation volumes for conduction is presented in Section 3.2.

A compensation-like (see Equation 3.7) relationship existing between activation energy and activation volume can be elucidated through a comparison of the E_a values for the variation in concentration and cation size to the $\Delta V^{\neq}$ values listed in Tables 3.2 and 3.4. Nachtrieb and Lawson (132) have pointed out that similar proportionalities between $\Delta V^{\neq}$ and $\Delta H^{\neq}$ exist for a variety of diffusional processes. Keyes (133) has presented a modified form of this relationship:

$$\Delta V^{\neq} = k\beta\Delta H^{\neq} \qquad (3.23)$$

where β denotes the isothermal compressibility of the substance, k is a constant which is approximately equal to 4 for a range of different substances. Theoretical models which consider lattice distortion parameters also predict a value of four.

Using a value of $\beta = 0.4$, an average compressibility factor for a number of polymers (134, 135), a comparison can be made to the data reported by Keyes (133). For clarity, a representative set of data for PVC and epoxy mixtures is compared in Figure 3.21 although the remainder of the data would also fit the proposed relationship. The universality of this relationship (Equation 3.23) is apparently realized in that a highly diverse range of systems is compared, e.g., ion mobility in AgBr,

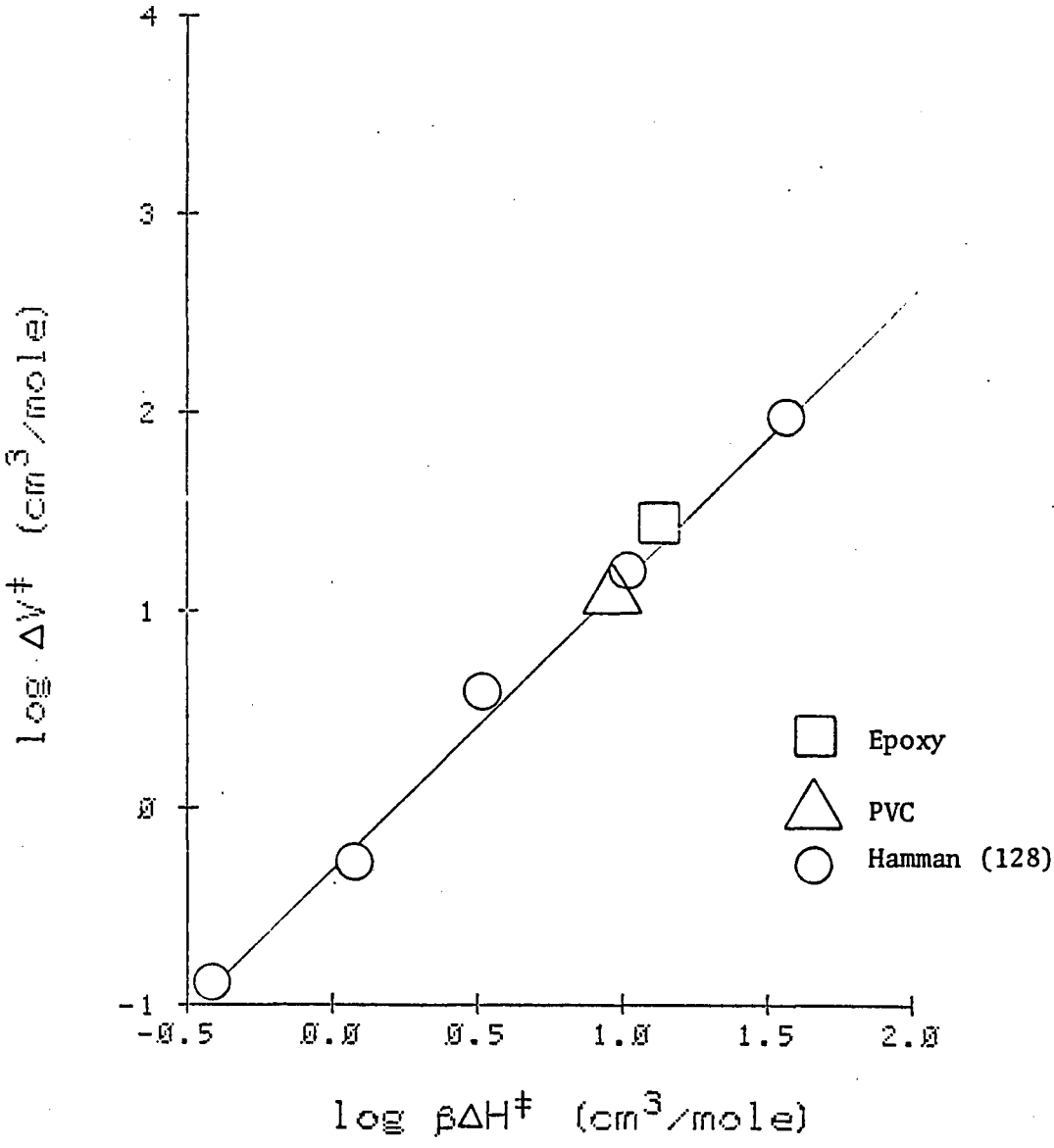

Figure 3.21 Activation Volume-Energy Relationship for Diffusional Processes under Pressure. -- The PVC and epoxy data are for Aliquat 336S.

self-diffusion of P, Pb, and liquid Hg and Ga, and the data from this study.

3.1.6 Plasticizers (and Organic Vapors)

The relative contribution of the energy required for ion mobility to the observed activation energy can, in principle, be estimated through changes in the sample viscosity. Hence, viscosity changes, at first glance, seem to offer an ideal method for further evaluating Equations (3.9) and (3.12). In theory, if the remaining, non-mobility parameters in these equations are held constant then observed changes in the activation energy as a function of viscosity would be solely due to changes in E_μ, the activation energy for mobility.

Ionic conductivity can be correlated to mobility by using the Nernst-Einstein-Townsend (NET) relation for the diffusion of ionic species:

$$\frac{\sigma}{D} = \frac{Nq^2}{kT} \tag{3.24}$$

where D is the diffusion coefficient and the remaining terms have their usual meaning. Combining the NET equation with the Stokes-Einstein equation:

$$6\pi\eta K_G r_i D = kT \tag{3.25}$$

gives an equation known as Walden's rule:

$$\eta\mu = q/6\pi K_G r_i \simeq \text{constant} \tag{3.26}$$

where η is the sample viscosity, r_i the particle radius, and K_G a geometric factor (equal to one for spheres). Therefore, according to

Walden's rule, the following proportionality between d.c. conductivity and viscosity should be observed:

$$\sigma \propto 1/\eta \qquad (3.27)$$

An attempt was made to gauge qualitatively the effect of σ on the samples by using dioctyl phthalate, DOP, as plasticizer. Surprisingly, these data could be described by the same linear relationship (Figure 3.13) applicable to the epoxy and unplasticized PVC samples. Thus, the influence of viscosity and, by implication, ionic mobility upon the conductivity would appear to be minimal. It should be noted, however, that in our measurements (Table 3.8), as with those reported in literature (136), the ε' increase is invariably accompanied by a viscosity decrease, so that dependence on the latter may be masked.

Table 3.8 Effect of Plasticizer on Conductivity of Aliquat 336S/PVC Films.

Dioctyl Phthalate* (wt %)	ε' (1 kHz)	-log σ 25°C $(\Omega\ cm)^{-1}$	E_a (eV)
0.0	5.5	9.3	1.70
4.8	6.0	8.9	1.30
13.0	6.2	8.8	1.16
16.7	6.6	7.9	1.15

*All samples contain 0.01 g Aliquat-Cl + 0.19 g PVC.

Furthermore, as demonstrated clearly by Kallweit (137) for DOP plasticized poly(vinyl chloride), Walden's rule often fails to adequately

predict the conductivity-viscosity behavior in high polymers. Although a number of possible explanations can be offered to describe this apparent failure, the most likely is simply that the viscosity, η, obtained by retardation experiments (best termed the "macroviscosity"), may not be a good approximation of the "microviscosity," or local viscosity, η', called for by Stoke's law. It has been suggested (123) that only in the case of liquids is η an adequate approximation of η'.

One can attempt to extend the viscosity reduction even further by simply eliminating the polymer matrix completely by replacing it with a liquid of identical dielectric constant. Table 3.9 summarizes the conductivity and E_a values measured for quaternary ammonium salts in low dielectric media. Comparison data for other R_4N^+,X^- systems of Dannhauser and Price (123) and Janz (108) are included in the table. As the other systems verify, a rather dramatic decrease of E_a, on the order of 1 eV or more, is associated with electrical conduction processes in liquid matrices. Because the dielectric constant was not determined after the addition of Aliquat-ClO_4 to the solvent, and since it is probably higher than the solvent alone, more quantitative estimates of the changes in E_a are not possible.

It is difficult at first to resolve these results in view of prior results. The previously developed relation between activation energy and dielectric constant (see Figure 3.16) shows that $E_a \approx 0$ when $1/\varepsilon' \rightarrow 0$, suggesting that $E_c \geq E_\mu$. However, the frequently observed failure of Walden's rule for high polymers (138) makes an accurate evaluation of viscosity effects (and E_μ) very difficult.

Table 3.9 Conductivity Parameters for Quaternary Ammonium Salts in Various Matrices.

R_4N^+ Salt	Matrix	ε'	E_a (eV)	Log R 25° (ohm)
Aliquat-ClO_4 (0.2 M)	Benzene	2.3[d]	0.36	5.0
	Chloroform	4.8[d]	0.13	4.0
	Epoxy	4.6	1.80	10.2
$(Butyl)_4SCN$[a] ($3.6x10^{-4}$ M)	Poly(styrene)	2.7	3.00	16.4
	P-xylene	2.2	0.51	13.2
$(Butyl)_4I$[b]	Anisole	4.3[d]	0.25	--
	N-butanol	11.4[d]	0.44	--
$(Pentyl)_4NO_3$[c]	Dioxane	--	0.70	--

[a]Reference (123).

[b]Reference (108).

[c]Reference (92).

[d]Dielectric constant of matrix before salt added.

Dannhauser (in 123) has shown that particles diffusing through polymeric matrices experience a microviscosity of ca. 1 poise (P) rather than the 10^7 calculated from retardation viscosity experiments. If this is indeed the case, one might expect from viscosity behavior alone that the ratio of electrical conductivity in liquids to that of polymers would be equal to the reciprocal liquid viscosity. In other words, Walden's rule would be applicable if η' is taken as 1 P. The measured viscosity for the liquids listed in Table 3.9 are ca. $5x10^{-3}$ P (139), which gives a Walden's rule predicted conductivity of approximately 200 times that of the polymer mixtures. Figure 3.10 shows that this conductivity increase corresponds to a change in activation energy of approximately 1.3 eV. Here again, the activation energy for mobility appears to be on the order of 1 eV.

One possible resolution of the apparent conflict in the magnitude of E_c compared to E_μ (and why E_a does not equal $E_c + 2E_\mu$) may be in the manner in which the dielectric experiments were conducted. Variations in dielectric constant were introduced by adding substances which themselves are plasticizers or viscosity reducing agents. Significantly, the change induced in dielectric constant is linear (Figure 3.22) with respect to the weight percent of additive (Aliquat 336S). It is known (130) that the viscosity of polymer/plasticizer mixtures generally varies in a linear manner with the weight percent of the plasticizer added. Obviously, then, both $1/\varepsilon'$ and $1/\eta$ would give nearly identical relationships as a function of additive concentration, either R_4N^+,X^- or plasticizer. Unfortunately, few viscosity measurements of the polymers

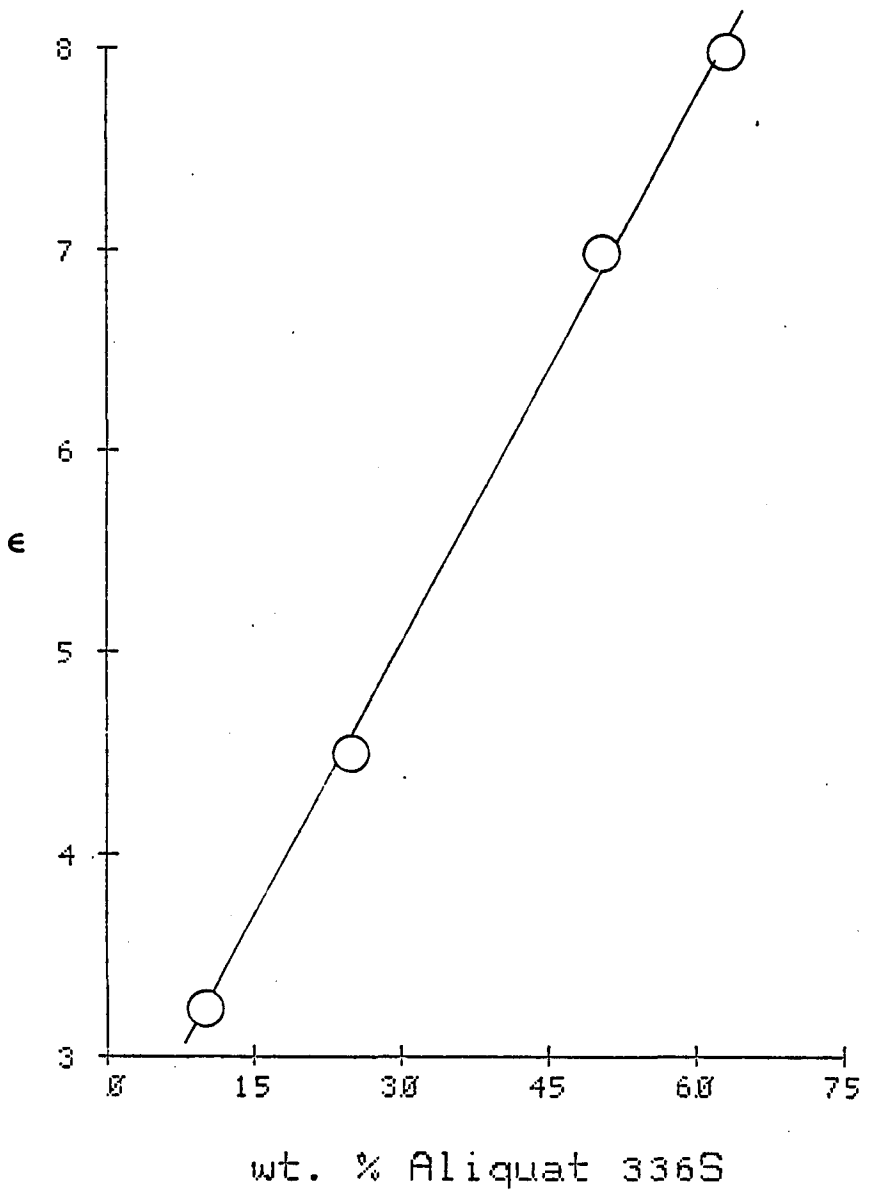

Figure 3.22 Dielectric Constant as a Function of Aliquat 336S Concentration in PVC.

used in this study have been reported. However, the extrapolated results from one such study (130) indicate that the viscosity should change 6-10 fold for the concentration range investigated in this study, i.e., 11-67 wt % Aliquat 336S in epoxy. Of course, it is difficult to assign a numerical change to the observed conductivity caused by the reduction in viscosity, particularly due to the uncertainty of Walden's rule behavior in high polymers.

An interesting plasticizer effect is caused by the penetration of solvating, organic vapors into an Aliquat 336S/PVC bead (Figure 3.23). The decrease in resistance after exposure to the solvent vapors is thought (131) to be caused by an increase in segmental motions, resulting from plasticization, making mass transfer easier and more rapid. Within a group of solvents, one can judge their conductivity effectiveness (and thereby their penetrability) through a comparison of solubility parameters to that of poly(vinyl chloride), $\delta = 9.5$. Chloroform ($\delta = 9.3$) would be predicted (140) to have greater PVC compatibility than either toluene ($\delta = 8.9$) or acetone ($\delta = 10.0$). Aliquat 336S, with its calculated solubility parameter of 9.7 (141), should not greatly affect the intrinsic solubility parameter of PVC. Figure 3.23 shows that, as predicted, chloroform exerts the greatest conductivity effect.

3.1.7 Polymer-Free Quaternary Ammonium Salts

Since the dissociation of the quaternary ammonium salts (Equation 3.11) most likely provides charge carriers for the electric current, a study of the polymer-free, crystalline material was undertaken.

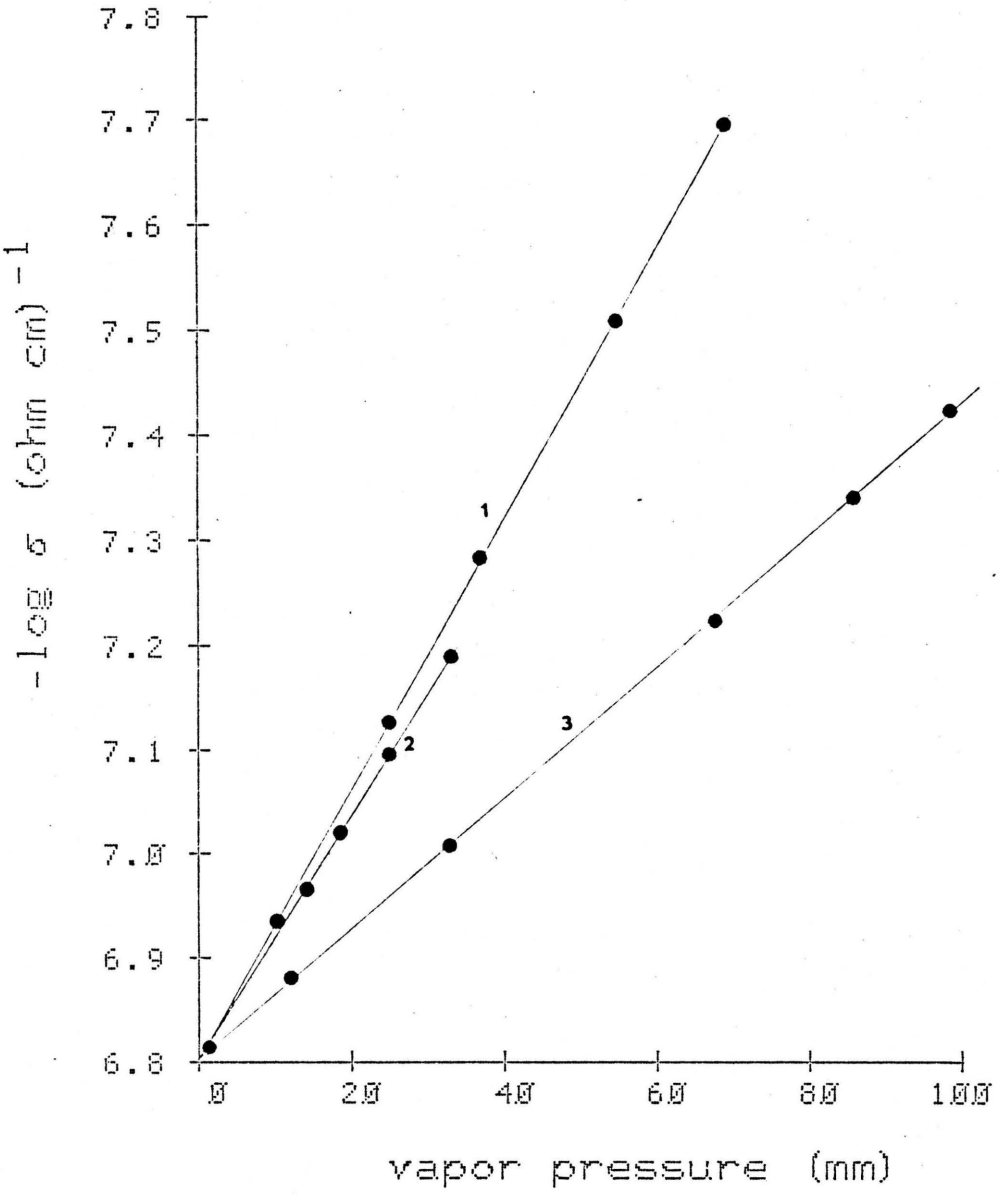

Figure 3.23 Effect of Organic Solvent Vapors on the Conductivity of Aliquat 336S/PVC. -- 1. Chloroform. 2. Toluene. 3. Acetone.

Unfortunately, the range of quaternary ammonium salts amenable to such a study was quite limited. The higher molecular weight salts were of uncertain purity and most were liquids at room temperature. Furthermore, nearly all of the R_4N^+,X^- compounds are hygroscopic to some degree, the higher molecular weight ones very much so. Results reported here were, therefore, restricted to methyl and pentyl chloride analogs.

Initial experiments were made using tetramethylammonium chloride as a means of evaluating the conductivity system through comparison to values reported in the literature. Table 3.10 shows that these experimental results compare favorably with those reported (142-144). Results for the other salts also fit well with those observed in other studies.

Activation energy values of these materials were taken as E_a rather than $E_a/2$ of Equation (3.1) for compatibility with calculation procedures customarily used in this field.

Measurements made on solid tablets of tetrapentylammonium chloride showed a two-slope conductivity behavior (Figure 3.24). Further studies showed that similar behavior could be obtained for tetramethylammonium chloride by extending the conductivity measurements to temperatures below approximately 70°. Owen and others (144) have reported a similar finding for ammonium perchlorate and attributed the two-slope behavior as indicative of ionic conduction. The low temperature slope, the so-called "extrinsic" region, was interpreted as being proportional to the activation energy for migration, E_μ', of point defects. In this region, charge carriers are initially present due to defects; therefore, one does not observe any thermodynamic (thermally promoted) generation of

Table 3.10 Conductance Activation Energy Values for R_4N^+,X^- Tablets.

R_4N Salt	Activation Energy (eV)	
	High Temperature	Low Temperature
NH_4I[a]	1.23	--
NH_4ClO_4[b]	1.10	0.65
NH_4Cl[a]	0.87	--
NH_4Cl	0.83	--
$(Methyl)_4I$[a]	1.13	--
$(Methyl)_4Cl$	1.13	0.38
$(Pentyl)_4Cl$	1.40	0.35
$(Hexyl)_4Cl$[c]	1.37	0.31

[a]Reference (143).

[b]Reference (144).

[c]Preliminary results.

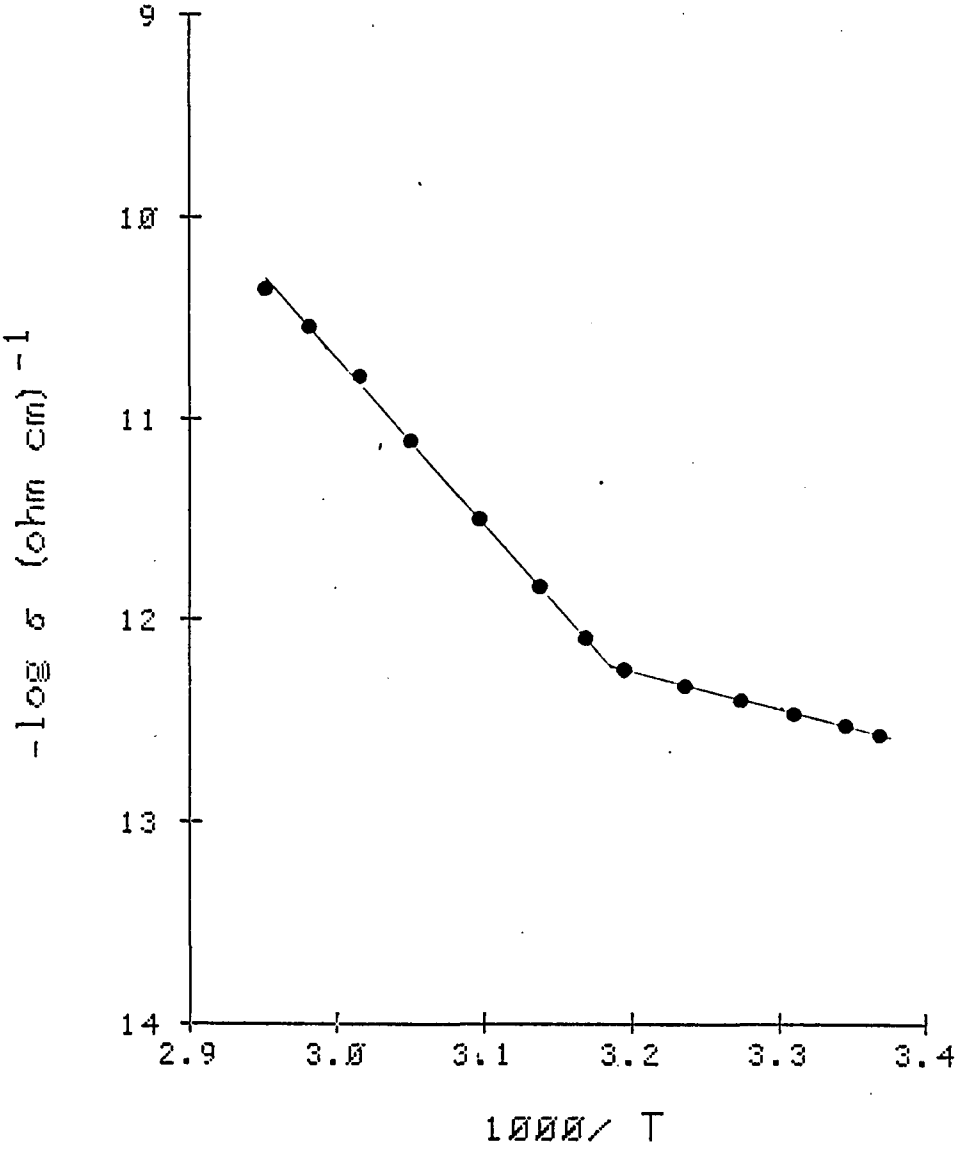

Figure 3.24 Temperature Dependence of Conductivity for Tetrapentylammonium Chloride.

these carriers. In the higher temperature or "intrinsic" region, the slope was suggested to be proportional to $1/2E_c' + E_\mu'$ where E_c' is the activation energy of point defect formation, i.e., the energy required to produce interstitial ions.

Following this approach, one would assign the low temperature activation energy of 0.35 eV to E_μ' and the high temperature value of 1.40 to $1/2E_c' + E_\mu'$. E_c' is, therefore, equal to 2.10 eV.

Comparison of these results to the polymer mixtures would be tenuous; nevertheless, some interesting comparisons can be made. The dielectric constant of the solid tablets was not measured, but it can be estimated by extrapolating the 100 MHz data from a study of hydrated quaternary ammonium halides (145) to zero hydration number. With the estimated dielectric constant value of approximately 5, an $E_a/2$ value can be obtained from Figure 3.16. The corresponding value of 0.8 eV represents an intermediate value between the low and high temperature regions.

A direct comparison of epoxy samples to the polymer-free tablets could not be accomplished experimentally because high resistances encountered precluded measurements below ca. 40° (the low temperature region). However, as discussed above, the activation energy values overlap from both systems to a sufficient degree that the polymer-free data might provide rough estimates of the values expected for the polymer mixtures.

3.1.8 Thermistor Applications

At present, nearly all commercially available thermistors are fabricated from semiconducting metal oxides (146). These materials are

expensive as well as being susceptible to damage (the majority are sealed in fragile glass beads).

The previously measured, rather large, negative temperature coefficient possessed by quaternary ammonium compounds dispersed in polymeric mixtures suggests that they may be useful as sensitive temperature probes. Such materials would have great advantages in terms of ease and reliability of fabrication, and possibility of a relatively wide and continuous range of variation of properties. In addition, these thermal sensitive resistors could be fashioned in a great variety of geometries in order to meet the unique specifications that might be demanded in biological and environmental sensing situations.

A number of relationships exist in the thermistor field for describing the behavior and sensitivity of these devices:

$$R_{25} = R_T \exp\left[\beta\left(\frac{1}{T_1} - \frac{1}{T_2}\right)\right] \qquad (3.28)$$

where β is a term similar to E_a of Equation (3.1). A temperature coefficient of resistance, α, is defined as:

$$\alpha_{25} = \frac{1}{R_T} \cdot \frac{dR}{dT} \qquad (3.29)$$

where α_{25} is the percent change in resistance for a 1° change in temperature, centered at 25°. Commercial thermistor devices have α values which range from -3 to -5% with corresponding resistances of typically 10^6 ohms or less.

Table 3.11 lists the α values expected for the activation energy range 0.5-4.0 eV, covering the extremes found for the materials used in this study. As is evident in this table, α_{25} values are generally much

greater for the substances studied than those commonly present for commercial devices. The change in resistance for the 3-4 eV materials is particularly dramatic for 10° changes in temperature (362-1310%).

Table 3.11 Percent Change in Resistance for Various E_a Values.

E_a	ΔT (°C)			
(eV)	0.01°	0.1°	1.0°	10.0°
			(α_{25})	
0.5	0.03	0.32	3.3	37
1.0	0.06	0.65	6.6	88
2.0	0.13	1.30	13.7	254
3.0	0.19	1.90	21.3	566
4.0	0.26	2.60	29.4	1150

As would be expected for any ionic conducting device, long-term drifts of resistance (time-dependent polarization) would cause problems for detecting small resistance changes. However, in an automated polymeric thermistor device, long-term drift can be compensated by a "feed-back" operational amplifier loop with a relatively long time constant (say 20 min). In some cases, the long-term drift of resistance was reduced to ca. -1 %/h by the selection of an appropriate polymeric mixture (low concentrations of electroactive materials in epoxy), although the resistances encountered for these mixtures was so large (10^{12} ohm) as to make measurements difficult.

Short-term instability, however, posed much more serious limitations (see Table 3.12) on the use of these materials as temperature probes.

Table 3.12 Comparison of Polymeric Thermistors to Commercial Devices.

	α (%)	Stability (%)	Smallest ΔT Measurable (m°C)
Polymeric thermistor	15	± 0.5	60
Allied thermistor network	4	± 0.005	2

3.2 Ion-Exchange Resins

In this study of polymer membranes containing dissolved quaternary ammonium salts, the determination of the pressure dependency of the conductivity of the membrane gave strong evidence of an ionic conduction mechanism. It was felt that parallel studies of ion-exchange resin membranes could provide a useful, simplified model in interpreting our earlier data, inasmuch as only one ion of the pair is mobile and capable of carrying charge.

Furthermore, a number of important separation processes utilize an electric field as the driving force to achieve partition of solution components across a membrane. Electrodialysis is an example of such a barrier separation process in which the membrane is fabricated from an ion-exchange resin. In addition to the electric current a pressure

gradient can be concurrently applied, as is done in the technique of forced flow electrophoresis.

Studies of the electrical conductivity of ion exchange and other electro-conductive membranes which have been reported (147) generally have been restricted to verification of an Ohm's law relationship without identification of the current-carrying species.

Data gathered from high pressure-conductivity experiments, when plotted ($\ln\sigma$ vs. P), were linear with a negative slope and were used to calculate the values of $\Delta V^{\neq}$ shown in Table 3.13. Molar volumes, Vm, for the anions presented in this table were calculated using $Vm = 4/3\ N_0 \pi r^3$, where N_0 is Avogadro's number of atoms and r is the Pauling ionic radius (148).

Table 3.13 Activation Volume for Electrical Conduction for Various Forms of Dowex-1® Ion Exchange Resin.

Resin Form	$\Delta V^{\neq}$[a] (cm^3/mole)	r (Å)	Vm (cm^3/mole)
Cl^-	19	1.81	15.0
Br^-	22	1.95	18.7
NO_3^-	23	1.93[b]	18.1
I^-	30	2.16	25.4

[a] $\Delta V^{\neq}$ values have a r.s.d. of 10%.

[b] Represents the distance from center of N to end of O.

As the values listed in Table 3.13 show, good correlation exists between conduction activation volumes and the molar volume of the respective anion calculated from crystallographic data. One may, therefore, conclude that the charge is anionically transported through the bulk resin by the anion with the experimentally measured $\Delta V^{\neq}$ corresponding to a process in which compression retards ion migration by decreasing vibrational and oscillatory motions of polymer segments, resulting in an increased local viscosity. Since the cationic resin species is immobilized, it probably does not contribute to the observed conductivity.

In the previous study (Section 3.1.5) of poly(vinyl chloride) films doped with the quaternary ammonium salt, methyltricaprylylammonium chloride, pressure-conductivity measurements yielded corrected $\Delta V^{\neq}$ values of 34 ± 2 cm^3/mole. In contrast to the ion exchange materials, the cation in this system is not chemically bonded to the polymer and despite its relatively low mobility, should be expected to contribute to the electrical conduction process.

One could very roughly estimate the contribution such an additional charge carrier would make to the calculated activation volume by taking the summation of individual molar volumes multiplied by their respective, weighted transport numbers (assumed to be proportional to the reciprocal of the molar volume). As a limit of relative ion sizes (cation volume >> anion volume), such a calculation would give a value of twice that of the anion volume. While this approximation is admittedly rather crude, it nonetheless suggests the earlier results are reasonable in view of this present study.

The conduction process in both the poly(vinyl chloride)-quaternary ammonium salt system and the ion-exchange resins resembles that in liquids where activation volumes for self-diffusion are generally one molar volume or greater (149, 150). In solids and crystalline materials, it is usual to find $\Delta V^{\neq} < Vm$. A theory (133) based on defect formation in solids suggests that $\Delta V^{\neq} \simeq 1/2\ Vm$ would be reasonable.

3.3 Valinomycin Study

3.3.1 Time Dependence of Conductivity

A time-dependent current, similar to that found earlier for the quaternary ammonium salts, was observed for poly(vinyl chloride) mixtures containing valinomycin (Val) and dibutyl adipate (DBA). A representative time-current curve is shown in Figure 3.25 for 1 V applied field.

The time-dependent decrease in current, as discussed earlier, is caused by polarization within the sample, i.e., it is due to the relative displacement of positive and negative charges inside the material. The time dependence of polarization can be characterized by two diverse theories. The space-charge polarization (SCP) theory (151) proposes that a region of charge accumulation occurs at both electrodes resulting in electrode "blocking." Further extensions of the SCP theory (152-154) predict a failure of Ohm's law behavior and a voltage dependence of the time-current curve. An alternate, opposite theory, called the dielectric relation (DR) theory (109), views the polarization not as a space-charge effect, but instead as a time-dependent change in the macroscopic dielectric constant within the material. According to this theory, the

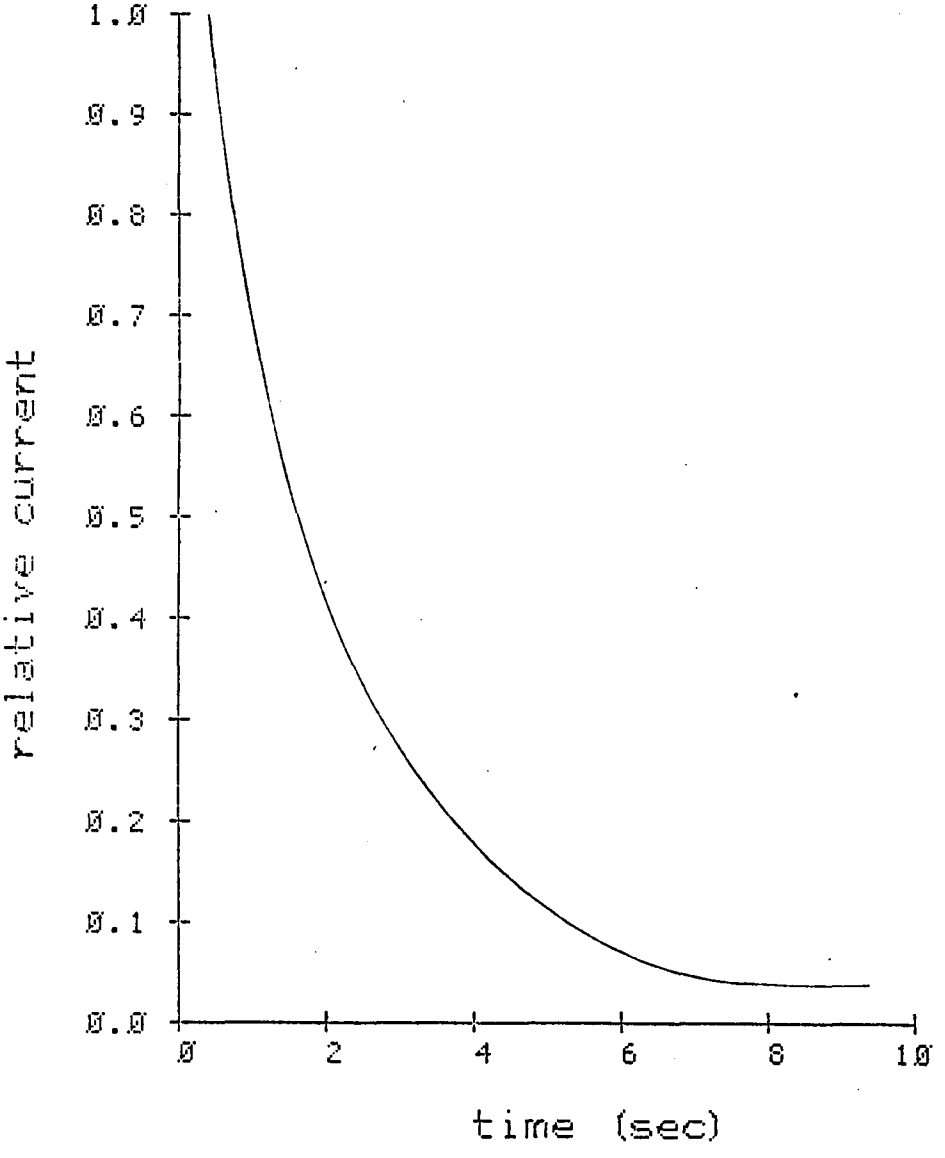

Figure 3.25 Time Dependence of Conductivity for K^+-Val.

time-dependent reorientation of permanent dipoles inside the material gives rise to the observed polarization. In contrast to SCP theory, Ohm's law behavior and voltage independence of the current-time curve should be observed.

Experimental results expressed as log-log plots of the time-dependent current as a function of the applied field are shown in Figure 3.26. These data, expressed in the form:

$$\sigma(t) = \alpha t^{-n} \qquad (3.30)$$

give values of n, showing a strong field effect ranging from 0.2 to 0.8. Commonly observed n values for supposedly ionic crystals (155) are less than 1.0, with most in the range 0.3-0.5.

The obvious deviation from Ohm's law and the strong dependence found for the time phenomena on the applied field strongly favor the space-charge polarization theory.

3.3.2 Electrothermal Analysis

Electrothermal analysis curves were prepared for valinomycin loaded with potassium ion (K^+-Val) as a function of the polymeric matrix as well as the plasticizer type and concentration. The K^+-Val concentration selected was the same as that usually employed in ion-selective electrode membranes (1.0 mg K^+-Val/5.0 mg polymer mixture).

The electrothermal analysis profiles for potassium-valinomycin/PVC samples plasticized with various concentrations of di(2-ethylhexyl) adipate (DOA) showed at least two distinct linear regions; a sample containing 30 weight % DOA represents a typical ETA profile (Figure 3.27).

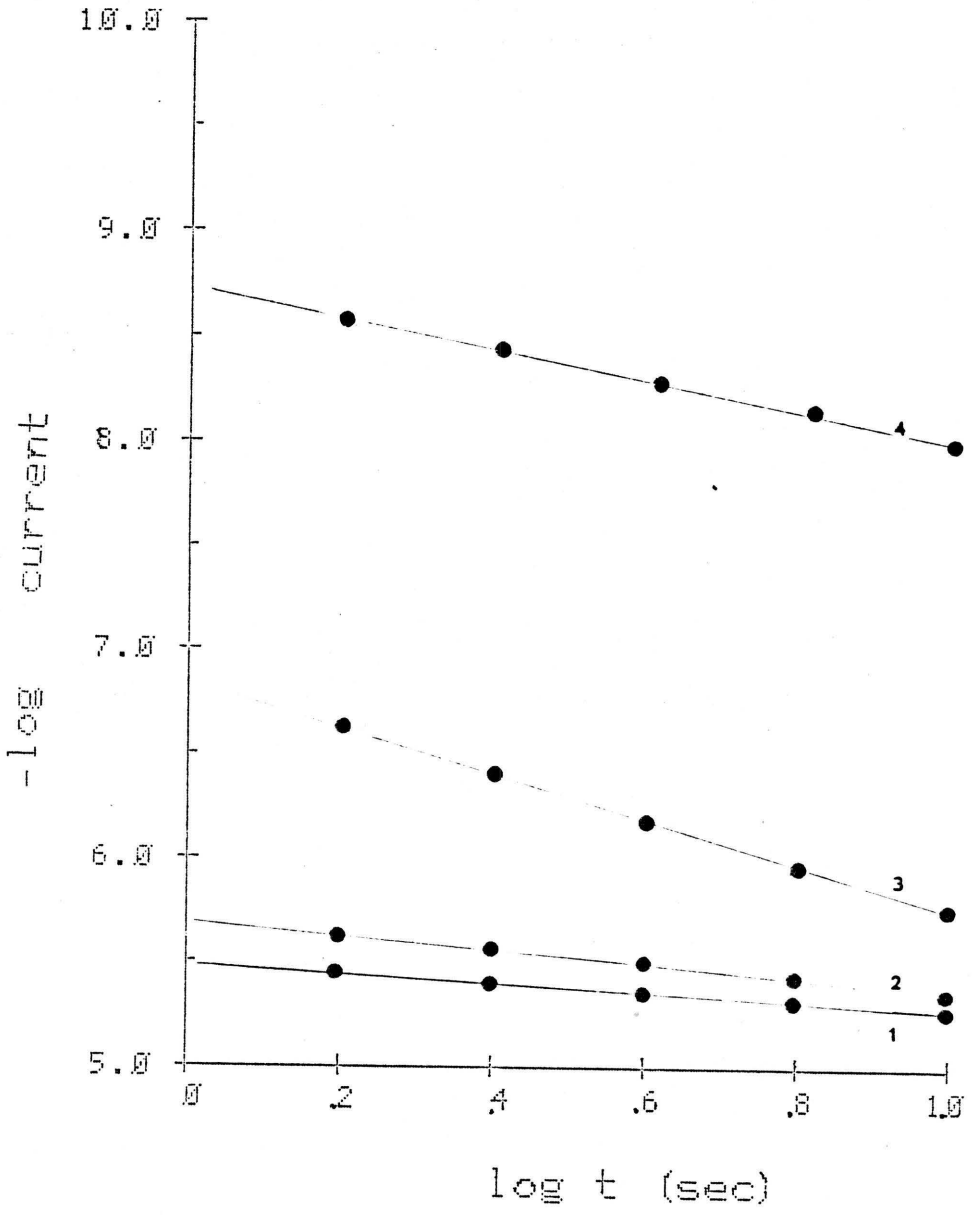

Figure 3.26 Conductivity-Time Relationship for Aliquat 336S as a Function of Applied Field (V). -- 1. 10.0. 2. 1.0. 3. 0.5. 4. 0.1.

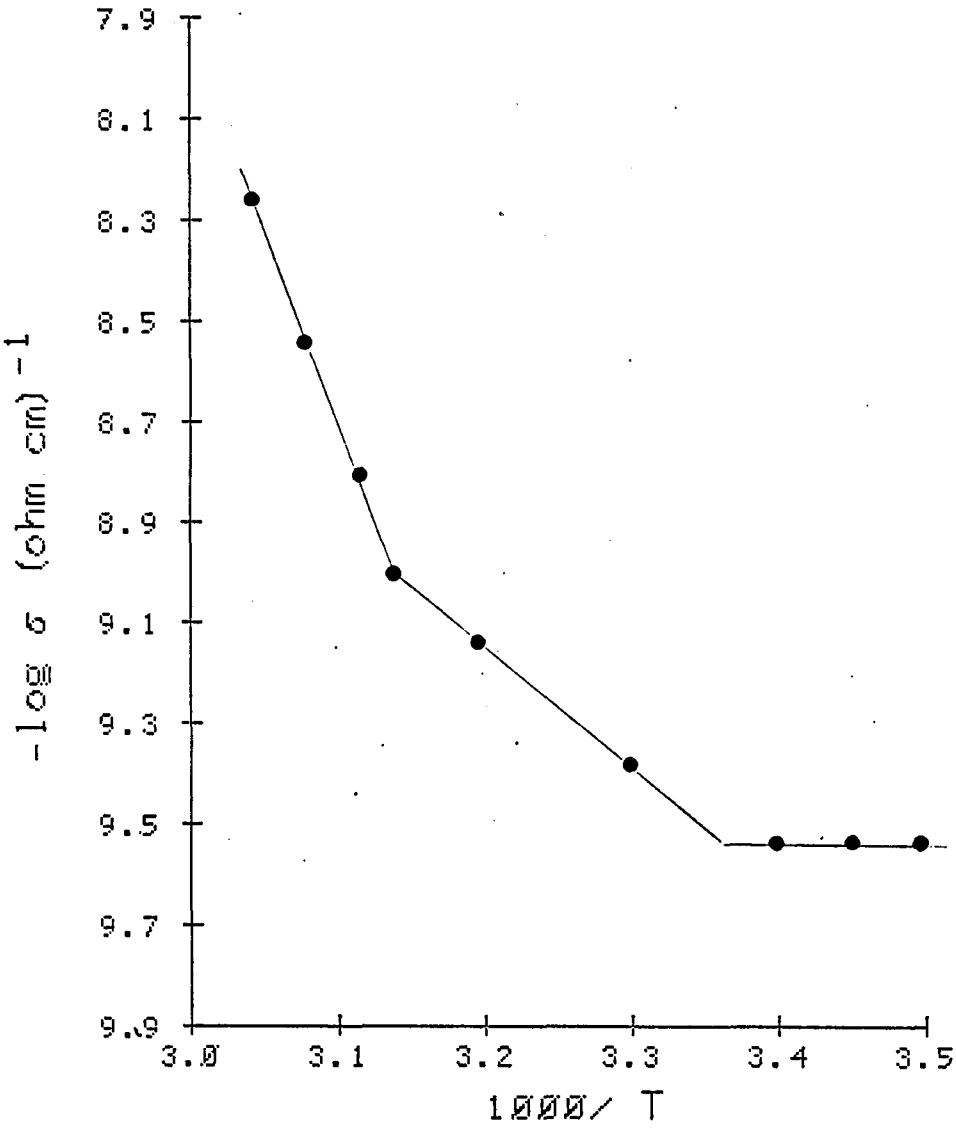

Figure 3.27 Temperature Dependence of Conductivity for Potassium-Valinomycin/PVC.

The lower temperature regions have a slope approximately equal to zero, while in the higher temperature regions the slope is much greater. Studies of similar behavior (111) have shown that the two-slope behavior is caused by a transition within the polymeric material. It is, therefore, possible to use dynamic electrothermal analysis profiles to detect second-order transitions such as the glass transition temperature, T_g. T_g values determined from the inflection point of the electrothermal line have been shown experimentally to be generally in good agreement with T_g's obtained from other methods (84).

The results for the DOA plasticized system are summarized in Table 3.14. Consistent with usual polymer behavior (130), the apparent T_g is decreased by increasingly higher concentrations of plasticizer. Indeed, a plot of volume % DOA versus T_g (Figure 3.28) demonstrates the linear relationship often observed for plasticized polymers.

Table 3.14 Effect of Di (2-Ethylhexyl) Adipate (DOA) on Electrical Conduction of K^+-Val/PVC.[a]

DOA		T_g	E_a (eV)	
Wt %	Volume %	(°C)	$< T_g$[b]	$> T_g$[c]
0	0	45	~ 0	2.3
30	23	26	~ 0	1.5
50	42	3	~ 0	1.3
70	63	-14	~ 0	3.4

[a] 1.0 mg K^+-Val/5.0 mg PVC.

[b] E_a for all samples was ca. 0 within experimental error.

[c] Region of largest slope.

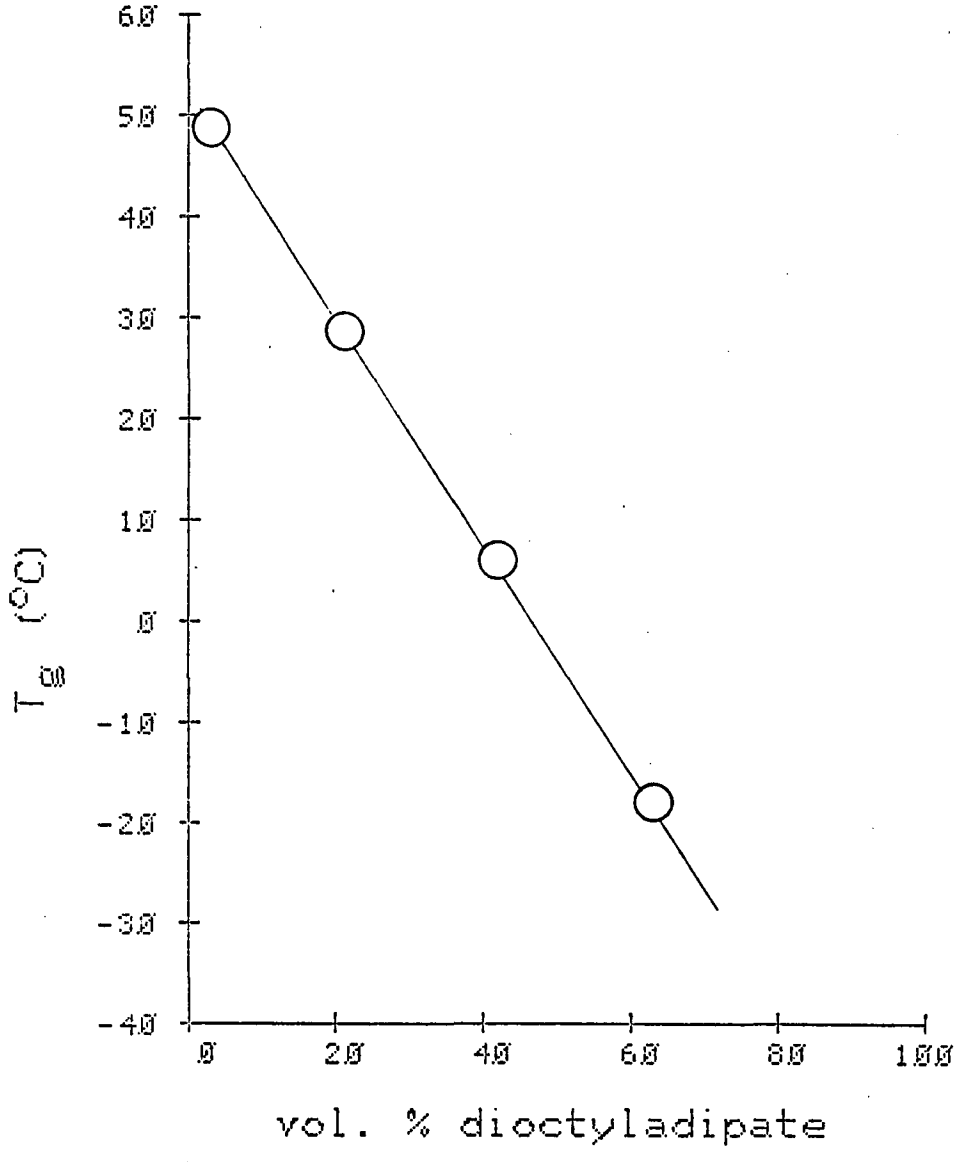

Figure 3.28 Glass Transition Temperature of Potassium-Valinomycin as a Function of Plasticizer Concentration.

Electrothermal analysis curves obtained for the other plasticized samples were similar to those reported for DOA in that regions of two differing slopes were observed. Using the inflection point as the glass transition temperature, a comparison of plasticizer effectiveness is summarized in Table 3.15. A more accurate comparison of these plasticizers could be made by calculating volume % values from the weight % values given, but assuming a linear relation between T_g and volume %, a maximum error of only ca. 3% results in the T_g.

Table 3.15 Comparison of T_g for K^+-Val/PVC[a] Mixtures Containing 70 Wt % Plasticizer.

Plasticizer	T_g (°C)
Bis(2-ethylhexyl) adipate	-10
Dibutyl sebacate	15
Dibutyl adipate	17
Dipentyl phthalate	28
Bis(2-ethylhexyl) phthalate	33

[a] 1.0 mg K^+-Val/5.0 mg PVC.

An anomalous, broad peak, centered around 5-15°C, was observed for a number of samples incorporating lower plasticizer concentrations (< 70%). Figure 3.29 shows the variation in electrothermal curves obtained for a variety of polymer-plasticizer combinations. Generally,

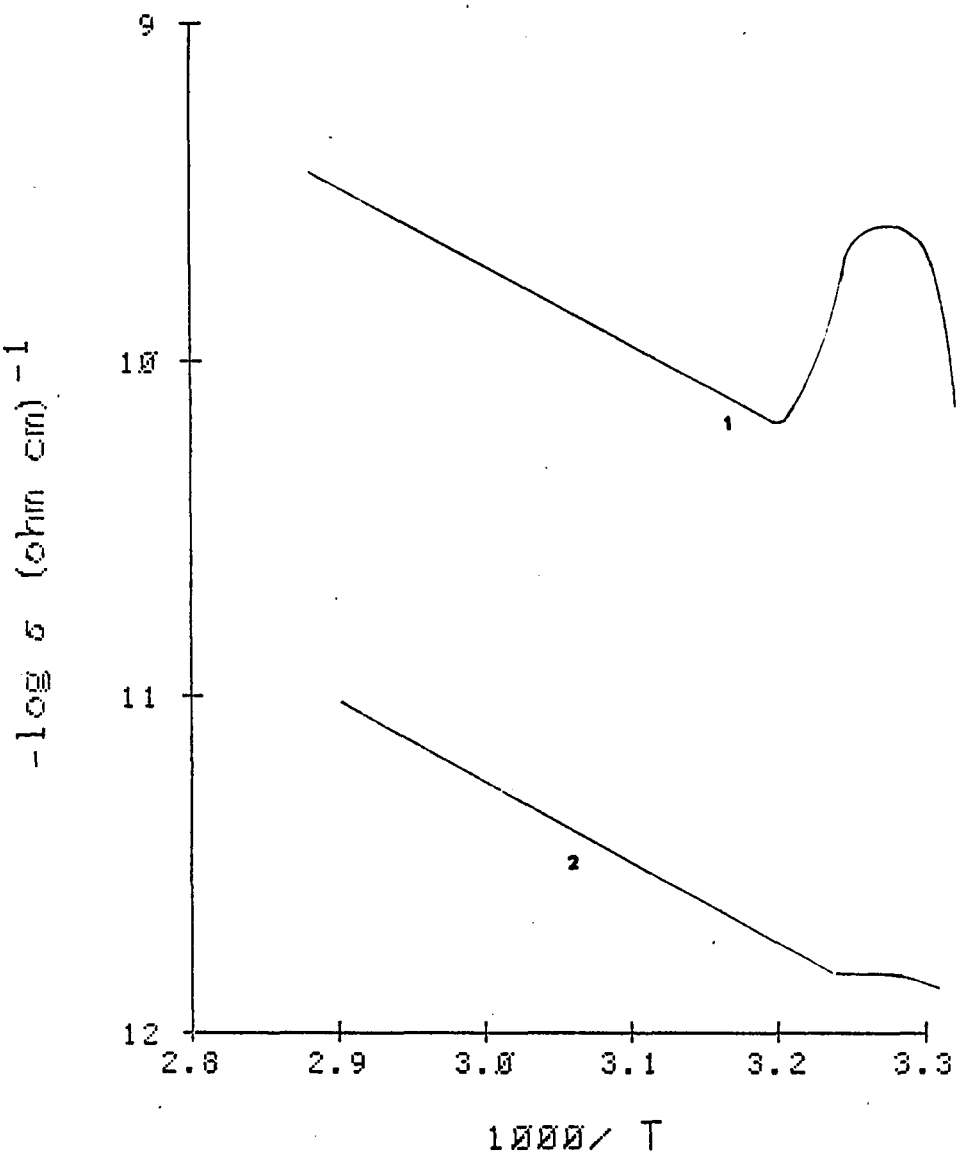

Figure 3.29 Anomalous Electrothermal Analysis Curves for Potassium-Valinomycin/Polymer Mixtures (30 Wt %). -- 1. Poly(styrene). 2. PVC.

the appearance of a low temperature, anomalous peak can be summarized as follows:

Polymer	Conditions for Anomalous Peak
PVC	$\leq$ 30% DOP
PS	$\leq$ 50% DOP
	$\leq$ 30% DOA
PMM	$\leq$ 50% DOA, DOP

As implied from the above table, such peaks also occurred for polymer mixtures containing no plasticizers, although to a much less extent for the PVC samples.

Anomalous peaks in electrothermal curves for a variety of polymers have been reported (156). Such peaks have been attributed to prior, low temperature polarization of the polymer sample with subsequent release of the trapped charge as the polymer was taken through the glass transition region.

The extremely large difference in activation energy, E_a, for the regions below and above the T_g is unusual. The value for the region above the T_g is quite similar to results reported for the quaternary ammonium salts. An important exception is the extremely unusual behavior of the 70% DOA sample, whose E_a of 3.4 eV is among the highest measured, yet it has a conductivity at 25° estimated to be $< 10^{-6}$ $(\text{ohm-cm})^{-1}$. The near zero value of activation energy at temperatures below the T_g may suggest a completely different mode of conductivity in this region. Such values are consistent with those generally found for electronically conducting, inorganic semiconductors (146).

3.3.3 Differential Scanning Calorimetry

As a means of confirming the ETA results, differential scanning "calorigrams" were prepared using samples exhibiting anomalous and normal (those with inflection points only) electrothermal curves (Figures 3.30 and 3.31). The usual glass transition regions observed in Figure 3.31 has been apparently replaced either by a considerably broadened transition, or by two transition regions. The temperatures which delineate the PS electrothermal peak (10°, 42°) coincide almost exactly with the inflections from the DSC (10°, 43°) scan. Table 3.16 summarizes these data.

Table 3.16 Comparison of Electrothermal and DSC Measurements.

Sample Composition	Electrothermal	DSC
PVC/30% DOA	Inflection 25°	24° T_g
PS/30% DOA	Peak 10°	Inflection 10°
	Inflection 42°	Inflection 43°

Therefore, it appears that some type of second-order transition is associated with the appearance of an anomalous peak.

3.3.4 Thermally Stimulated Discharge Currents

Persistent electrical polarization in polymer films is well known (156, 157) and has been shown to result from thermoelectric or thermomechanical (158-160) treatments. Dipolar electrets can be formed in

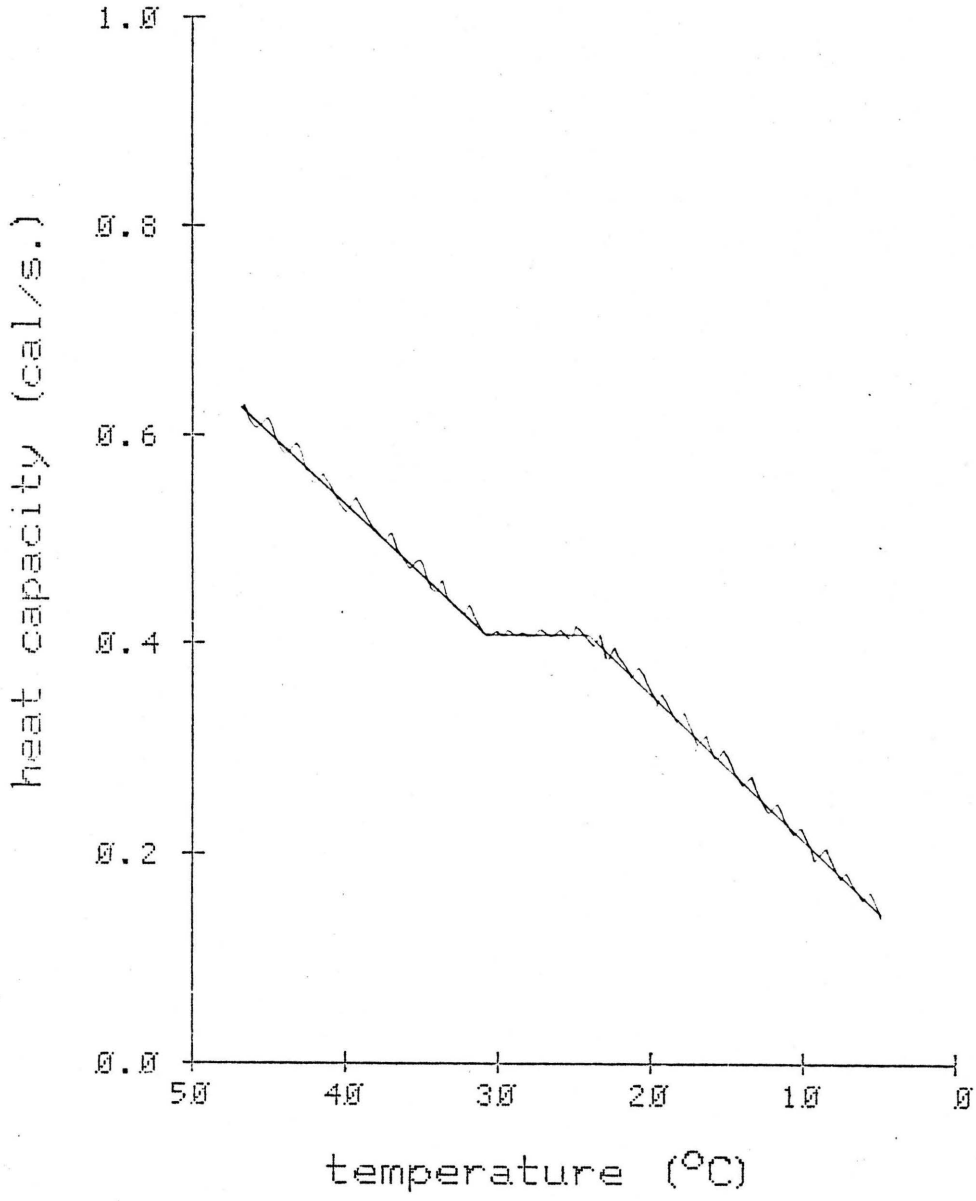

Figure 3.30 Differential Scanning Calorimetry of Potassium-Valinomycin/PVC/Dioctyl Adipate (30 Wt %).

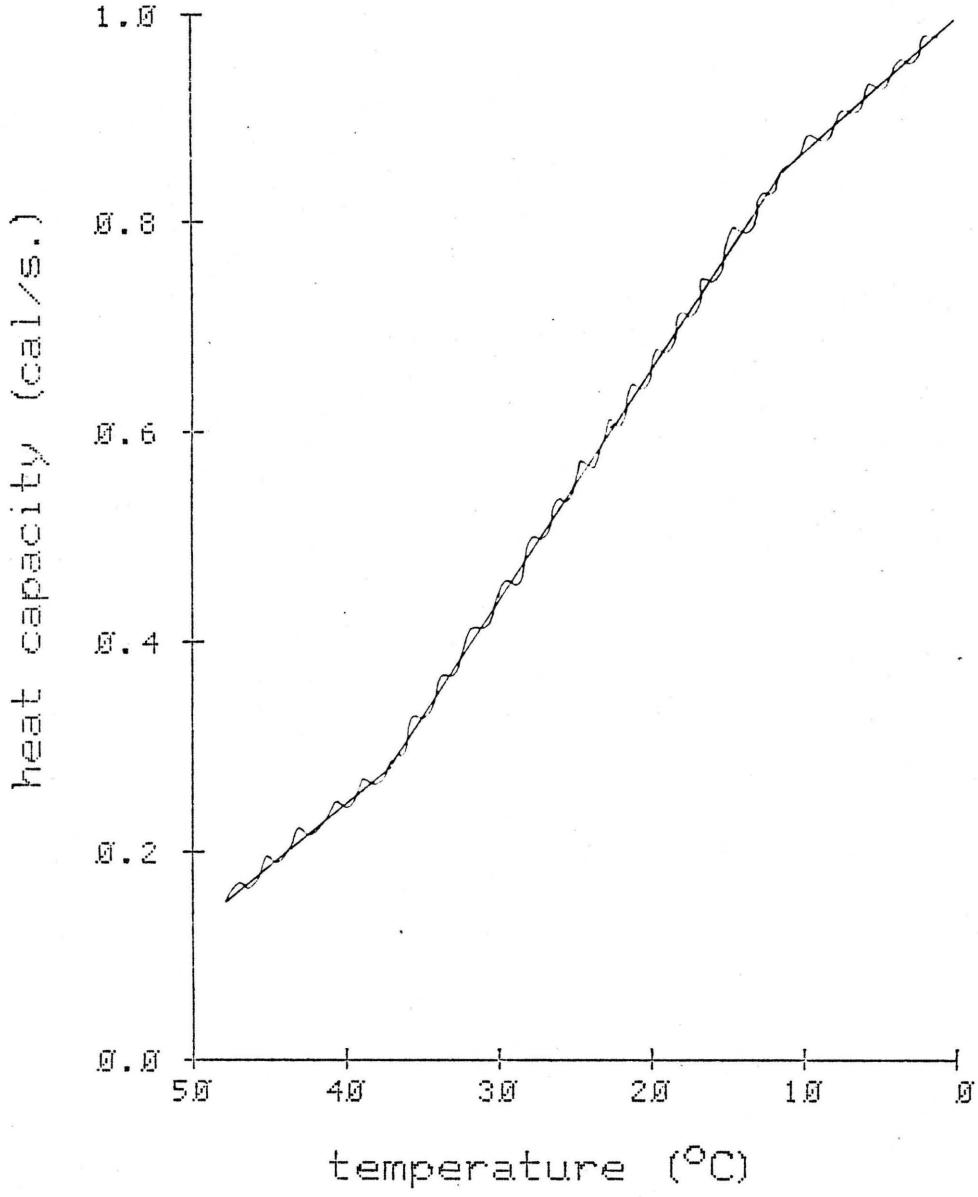

Figure 3.31 Differential Scanning Calorimetry of Potassium-Valinomycin/Poly(Styrene)/Dioctyl Adipate (30 Wt %).

polymeric materials by imparting a preferential orientation to dipolar groups with these polymers. This may be achieved by poling techniques which themselves cause the displacement of diffusible space charges by sufficient amounts to give rise to appreciable internal fields. Either of these two contributions to the persistent electrical polarization are expected to be very sensitive indicators of the physical microstructure within the polymeric matrix.

As a further test of the trapped charge or electret model proposed previously for potassium-valinomycin/PVC membranes, it should be possible to observe the release of such charges under conditions of zero applied voltage. As shown in Figure 3.32, a thermal discharge current peak is, indeed, observed which approximately coincides with the electrothermal peak.

The strength of the thermally stimulated discharge peak was observed to be dependent upon the initial poling conditions. Poling with high applied fields gave increasingly greater discharge signals. One may conclude then that the diffusion of the previously trapped ionic species apparently accounts for the thermally stimulated discharge observed in these samples.

3.3.5 High Pressure Conductivity

High pressure conductivity measurements were made in accordance with the technique discussed earlier. However, the very low concentration of electroactive material (1 mg in the polymeric mixture) gave concomitantly high resistances (ca. 10^9-10^{10} ohm), taxing the experimental conductivity measurement system. An exhaustive study of all the

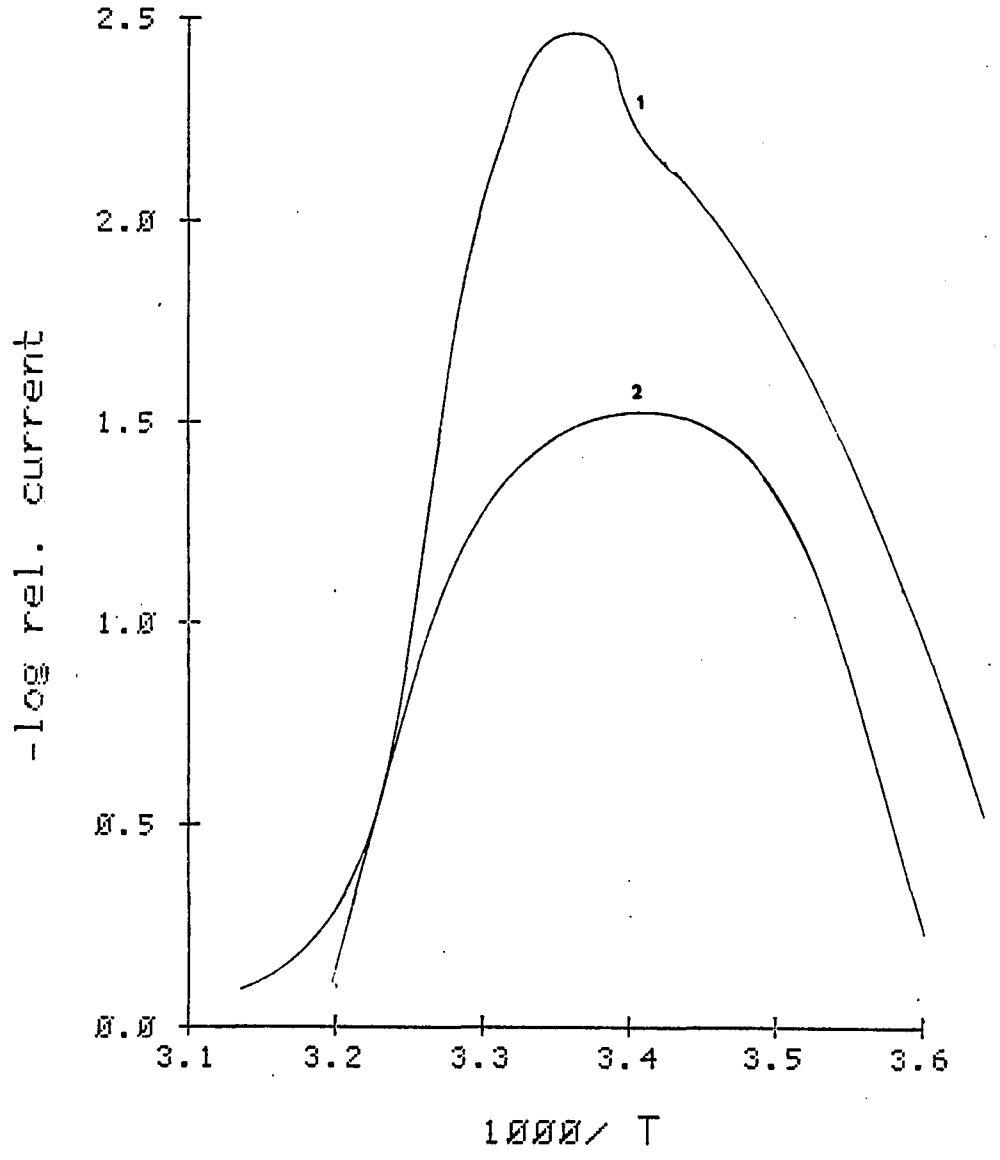

Figure 3.32 Comparison of Electrothermal Analysis Curve to Thermal Discharge Curve for Potassium-Valinomycin/Poly(Styrene). -- 1. Electrothermal analysis curve. 2. Thermal discharge curve.

parameters which might affect the electrical conductivity was not possible. The primary parameter studied was the effect of the T_g on the activation volume. High pressure conductivity measurements were made at approximately 25° with the T_g adjusted to the desired temperature by the addition of a plasticizer (dioctyl adipate). Table 3.17 summarizes the results for the valinomycin (both loaded and unloaded with potassium ion)/poly(vinyl chloride)/DOA samples.

Table 3.17 Activation Conduction Volumes for Various PVC-Valinomycin Mixtures.

PVC Sample	% DOA	T_g Expected (°C)	$\Delta V^{\neq}$ (cm^3/mole)	Log $R_{25}°$, 1atm (ohm)
Loaded[a]	40	0	39	8.2
Unloaded[b]	40		42	8.1
Loaded	30	8	54	9.3
Unloaded	30		47	8.8
Loaded	20	33	-	9.8
No VAL	40	-	44	10.0
No VAL	20		-	> 10.3
"Pure" PVC[c]	-	-	-	15.0
"Pure" PVC[d]	-		42	15.8

[a] K^+-Val.

[b] Val.

[c] PVC from this study.

[d] Reference (111).

A number of interesting features can be summarized from these results. Both the potassium loaded and the unloaded valinomycin-containing samples show similar conductivity behavior. Although the determined $\Delta V^{\neq}$ values appear not to be a function of valinomycin content, those samples which had valinomycin in them gave bulk conductivities which were 5- to 7-fold greater than plasticized PVC. One can, therefore, conclude that valinomycin participates in the conduction mechanism despite the fact that the experimentally determined $\Delta V^{\neq}$ is consistent with processes involving segmental motion in PVC (111) as the measured $\Delta V^{\neq}$ agrees closely with that reported for "pure" PVC, 42 cm^3/mole. A number of possible overall conduction mechanisms can be postulated with regard to the $\Delta V^{\neq}$ found.

A conduction process which might be termed "extrinsic," involving low molecular weight impurities, might account for the observed conductivity. Sources of these charge carriers may include compounds associated with the valinomycin molecule, either small organic or inorganic molecules.

By recalling that the measured $\Delta V^{\neq}$ is a weighted average of all the conducting species, the activation volume values of 40-50 cm^3/mole could very well represent an average of the chloride anion and the cationic valinomycin species.

Another possible "cooperative" conductivity mechanism is one in which valinomycin provides a source of charge carriers which are dependent upon segmental polymer motion for their mobility. Specifically, this could involve the production of proton or potassium ion

current-carriers from valinomycin which move along the polymer chain by a hopping or dissociation mechanism. Such a segmental motion-facilitated transport of protons has been suggested as the current-carrying mechanism in several polymeric materials (101).

This proposed process may also help to resolve the $\Delta V^{\neq}$ values found from electrothermal studies. The low temperature, low activation energy process may represent the diffusion of extrinsic charge carriers, while the higher temperature and higher activation energy process may be due to segmentally facilitated diffusion.

3.4 Other Systems

3.4.1 Calcium Di-N-Decyl Phosphate

Sample compositions used were similar to those employed in ion-selective electrode membranes, i.e., 70 wt % electroactive material in PVC. Electrothermal analysis gave the following results:

$$E_a = 0.58 \text{ eV}$$

$$\log \sigma_{25} = 7.6 \text{ (ohm-cm)}^{-1}$$

The magnitude of these parameters is similar to those obtained for the R_4N^+,X^-/PVC systems. This suggests that electrical conductivity is probably due to an ionic mechanism, namely, the diffusion of Ca^{++} ions. It has been suggested that conduction in this material may be protonic, although there is no evidence of this from our measurements. Additional high pressure conductivity measurements are necessary before a definitive carrier mechanism can be resolved.

3.4.2 Chelates

Oxinates of nickel, zinc, and copper and nickel dimethylgloxime were dispersed into a epoxy mixture (final concentration of complex was 0.02 M). Conductivity of the mixtures was approximately the same as that found for epoxy alone. These findings suggest that usable ion-selective electrodes could not be made from these mixtures unless, perhaps, a suitable ionic charge carrier was added to the polymeric mixture (24).

3.5 Application to Membrane Ion-Selective Electrodes

3.5.1 Use of Conductivity Data for Calculating Electrode Selectivity Parameters

A number of reports (24, 105) have shown that the ion-selective electrode selectivity constant, K_s, as defined by the Eisenman equation (50):

$$\Delta E = \frac{0.059}{n} \log \left(1 + K_s \frac{a_i}{a_A}^{n/z_i}\right) \qquad (3.31)$$

which relates the change in electrode potential, ΔE, arising from the addition of an interferant of activity a_i and charge z_i, to a solution of activity a_A to which the electrode responds, is a product of extraction and mobility terms. For a liquid ion-exchange material in which the counterion is associated with a poorly mobile site, the selectivity parameter, $P_{j/i}$, can be represented as:

$$P_{j/i} = \left(\frac{\mu_j^+ + \mu_s^-}{\mu_i^+ + \mu_s^-}\right) \frac{K_j^+}{K_i^+} \approx \frac{\mu_j^+}{\mu_i^+} \cdot \frac{K_j^+}{K_i^+} \qquad (3.32)$$

where $\mu_{i,j}^{+}$ and μ_{s}^{-} are the ionic mobilities of the counterior and site, respectively, and $K_{i,j}^{+}$ are the partition coefficients. Values of $K_{i,j}$ can be indirectly obtained from extraction data. Ionic mobilities are more difficult to determine, but Scibona (in 105) recently estimated them from bi-ionic membrane potentials. Electrical conductivity measurements can also be used to calculate mobility ratios. As characterized previously (Equation 3.12), the conductivity of salt-doped films has the proportionality:

$$(K\eta_0)^{1/2} \cdot (\mu_+ + \mu_-) \ . \tag{3.33}$$

For the system Aliquat 336S, R_4N^+, and NO_3^-,Cl^-, the observed conductivity is:

$$\sigma NO_3 \alpha (K_{NO_3^-}\eta_0)^{1/2} \cdot (\mu_{R_4N^+} + \mu_{NO_3^-}) \tag{3.34}$$

$$\sigma Cl \alpha (K_{Cl^-}\eta_0)^{1/2} \cdot (\mu_{R_4N^+} + \mu_{Cl^-}) \tag{3.35}$$

if

$$\eta_{0,NO_3^-} = \eta_{0,Cl^-}$$

and a poorly mobile site is assumed, i.e.,

$$\mu_{R_4N^+} < \mu_{NO_3^-,Cl}$$

(105), then,

$$\frac{\sigma_{NO_3^-}}{\sigma_{Cl^-}} = \left(\frac{K_{NO_3^-}}{K_{Cl^-}}\right)^{1/2} \cdot \left(\frac{\mu_{NO_3^-}}{\mu_{Cl^-}}\right) \ . \tag{3.36}$$

As was done previously, values for the ion-pair equilibrium constants can be estimated from the Born equation (Equation 3.13) using $r_{R_4N^+,Cl^-} = 8.24$ Å, $r_{R_4N^+,NO_3^-} = 8.43$ Å, and a dielectric constant of 8.1.

Using constants and values for Aliquat-X/PVC samples that have a composition similar to that used in electrode membranes (58 wt % Aliquat-Cl), one obtains: $K_{NO_3}/K_{Cl} = 0.82$ and $\sigma_{NO_3}/\sigma_{Cl} = 0.23$. Substituting these values into Equation (3.36), one can calculate $\mu_{NO_3^-}/\mu_{Cl^-} = 0.26$. Scibona (in 105) calculated the nearly identical value (0.25) for the mobility ratio of the tetraheptylammonium salts in benzene.

The mobility ratios obtained from conductivity data can be used as a multiplicative factor to correct the extraction selectivity coefficients so as to obtain true partition coefficients.

3.5.2 Effect of Conductor Material

Two prevalent theories (20) exist for characterizing the transfer of charge through "blocked interface" polymer membrane ion-selective electrodes.

In the "diffusion membrane" theory, charge transfer is required for the electric double layer potential to generate the potential difference in the membrane electrode. Hence, the movement of supposedly ionic species results in an accumulation of ions at the internal metal interface where they are either discharged or participate in reversible ion-exchange with some form of internal reference system generated in situ.

Contrasting this theory is the "capacitive coupling" mechanism suggested by Rechnitz (in 161) and others (20, 24). It is assumed in this theory that surface, interface charge is transferred to the internal element by a capacitive process.

An experimental arrangement to test the effect of the internal conductor material on the electrode E° value was carried out by preparing a dozen electrodes using copper and silver internal elements. E° values were calculated by using the Nernst equation:

$$E = E^\circ + \frac{RT}{nF} \ln a_{x-} \qquad (3.37)$$

and extrapolating to the E value when $a_{x-} = 10^0$ so that $E = E^\circ$.

The E° values calculated from these experiments are summarized in Table 3.18.

Table 3.18 Effect of Conductor Type on Electrode E°.[a]

Conductor	E° (mV)
Copper	- 73 ± 14
Silver	- 117 ± 7

[a]Saturated calomel reference.

While it is difficult to draw concrete conclusions from this limited study, the more than 40 mV difference in E° values between the two conductors does show a distinct dependence on conductor material.

However, these experiments suggest that a capacitive-coupling mechanism is unlikely.

3.6 Conclusion

The overall goal of these investigations was to relate conductivity measurements to electrode behavior. The high activation energy values from the electrothermal analyses strongly suggest an ionic process. The time dependency and the non-ohmic voltage behavior further confirm an ionic mechanism. The pressure dependence of the electrical conductivity, in view of the large activation volumes (30-93 cm^3/mole), proves that conduction in these materials is neither protonic nor electronic. Extended studies using plasticizers and polymer-free systems support a dissociation mechanism of conductivity in which the activation conduction energies for charge production and mobility are approximately equal (depending, of course, on the dielectric constant of the medium).

Hence, in the ion-selective electrode configuration of these polymeric mixtures, the electrical conductivity must be imparted by movement of ions. Therefore, electrical parameters are most useful for characterizing some aspects of electrode behavior, i.e., electrode selectivity coefficients. While further experimentation using other conductor types is necessary, the conductivity data show clearly that these electrodes function by ionic charge-coupling, most probably with an *in situ* generated reference system or by virtue of their low polarizability.

APPENDIX

LIST OF COMPUTER PROGRAMS

Listings of Nova 2 computer programs used for the automated electrothermal analysis and current-time procedures are included in this section.

Overall experimental control was handled by main FORTRAN programs (along with their data-processing subroutines).

FORTRAN-callable assembly language subroutines were used to access the hardware interface.

```
C ************************************
C *                                  *
C * CURRENT VS. TEMPERATURE ROUTINES *
C * FORTRAN CONTROL                  *
C * CALLS: CDATA                     *
C *        TIME                      *
C *                                  *
C ************************************
C
      EXTERNAL CDATA,TIME
      DIMENSION R(50),T(50),RC(50),TC(50),SAMPLE(30),NS(3)
      TYPE "SAMPLE NO.="
      READ (11,2) NS(1)
      TYPE "SAMPLE ID="
      READ (11,1) SAMPLE(1)
      ACCEPT "VOLTAGE=",V,"EXPONENT=",IX
      EX=10.**IX
C COLLECT DATA
      DO 10 I=1,50
      CALL CDATA (R(I),T(I))
      R(I)=-R(I)
      T(I)=T(I)/10.0
C SEE IF T=75DEG
      IF (T(I)-75) 9,30,30
C WAIT 2 MIN.
    9 CALL TIME(ITERM)
C SEE IF TERMINATE SWITCH SET (BIT 0=1)
      IF(ITERM) 30,10,10
   10 CONTINUE
   30 WRITE(10,4) NS(1),SAMPLE(1)
      TYPE "VOLTAGE=",V
      WRITE(10,5) IX
      DO 40 J=1,I
      R(J)=R(J)*0.001
      RC(J)=ALOG10(V/(R(J)*EX))
      TC(J)=1000./(T(J)+273.16)
   40 WRITE(10,6) T(J),R(J),TC(J),RC(J)
C  STORE ON DISK
      CALL DISKST(NS,TC,RC,I)
C CALL PLOTTING ROUTINE
      CALL PLOT(TC,RC,I)
C CALL LEAST SQUARES ROUTINE
      CALL LSQ(RC,TC,I)
    1 FORMAT(S30)
    2 FORMAT(S8)
    4 FORMAT("0","SAMPLE NO.",S8,2X,1S30)
    5 FORMAT("0",11X,"TEMPERATURE",5X,"A(10**",I3,
     1")",10X,"1000/T",5X,"LOG R")
    6 FORMAT(15X,F5.2,11X,F5.3,13X,F5.3,5X,F5.2)
      END
```

```
:       I=40
:       L=1
:       DO 77 N=1,40
:       IF (MOD(I,8)) 71,72,71
:    72 WRITE(10,1) YS(L),(K(I,J),J=1,66)
:       L=L+1
:       GO TO 70
:    71 WRITE(10,2) (K(I,J),J=1,66)
:    70 I=I-1
:    77 CONTINUE
:       WRITE(10,2) (K(41,J),J=1,66)
:       WRITE(10,3) (XS(I),I=2,7)
:       WRITE(10,4)
:     1 FORMAT(F6.2,"-",66S1)
:     2 FORMAT(7X,66S1)
:     3 FORMAT(9X,6(5X,F5.3))
:     4 FORMAT(38X,4H 1/T)
:       RETURN
:       END
```

```
      SUBROUTINE PLOT(X,Y,NPTS)
      DIMENSION K(45,72),X(50),Y(50),XS(50),YS(50)
      NPT=1H*
      NPLUS=1H+
      NXMRK=1H!
      NYMRK=1H-
      NBLK=1H
C BLANK ARRAY
      DO 10 I=1,45
      DO 10 J=1,72
   10 K(I,J)=NBLK
      XLARGE=X(1)
      XSMALL=X(1)
      YLARGE=Y(1)
      YSMALL=Y(1)
      DO 15 I=2,NPTS
      IF(XLARGE-X(I)) 16,17,17
   16 XLARGE=X(I)
      GO TO 19
   17 IF(XSMALL-X(I)) 19,19,18
   18 XSMALL=X(I)
   19 IF(YLARGE-Y(I)) 24,25,25
   24 YLARGE=Y(I)
      GO TO 15
   25 IF(YSMALL-Y(I)) 15,15,26
   26 YSMALL=Y(I)
   15 CONTINUE
C CALC. SCALING FACTORS
      XINC=66./(XSMALL-XLARGE)
      YINC=40./(YSMALL-YLARGE)
C PUT IN X,Y MARKS
      DO 30 I=1,67
      IF (MOD(I,10)) 30,22,30
   22 K(41,I)=NXMRK
   30 CONTINUE
C PUT IN BORDERS
      DO 50 I=1,40
      K(I,1)=NPLUS
   50 K(I,66)=NPLUS
      DO 60 I=1,67
      K(1,I)=NPLUS
   60 K(40,I)=NPLUS
C FILL ARRAY WITH POINTS
      DO 20 I=1,NPTS
      KAX=INT((X(I)-XLARGE)*XINC)*0.9
      KAY=INT((Y(I)-YLARGE)*YINC)*0.9
   20 K(KAY+3,KAX+3)=NPT
C CALC. SCALES
      DXS=(XSMALL-XLARGE)/0.9/5.6
      DYS=(YSMALL-YLARGE)/0.9/5.0
      YS(1)=YSMALL+0.25*DYS
      XS(1)=XLARGE-0.2*DXS
      R1=YS(1)
      R2=XS(1)
      DO 80 I=2,7
      R1=R1-DYS
      R2=R2+DXS
      YS(I)=R1
   80 XS(I)=R2
C PRINT ROUTINES
```

```
      I=40
      L=1
      DO 77 N=1,40
      IF (MOD(I,8)) 71,72,71
   72 WRITE(10,1) YS(L),(K(I,J),J=1,66)
      L=L+1
      GO TO 70
   71 WRITE(10,2) (K(I,J),J=1,66)
   70 I=I-1
   77 CONTINUE
      WRITE(10,2) (K(41,J),J=1,66)
      WRITE(10,3) (XS(I),I=2,7)
      WRITE(10,4)
    1 FORMAT(F6.2,"-",66A1)
    2 FORMAT(7X,66A1)
    3 FORMAT(9X,6(5X,F5.3))
    4 FORMAT(38X,4H 1/T)
      RETURN
      END
```

```
C ***********************************
C *                                 *
C * SUBROUTINE DISK WRITE           *
C * WILL DEFINE A USER FILE AND WRITE *
C * SEQUENTIALLY INTO IT, ALTERNATING *
C * BETWEEN TWO COLUMNS OF DATA     *
C *                                 *
C ***********************************
      SUBROUTINE DISKST (ID,DTEMP,DRES,NNUM)
      DIMENSION ID(3),DTEMP(50),DRES(50),DISKBUF(0:100)
      IBYTE=2*(4*NNUM)+4
      IE=0
      ISLOT=0
C  BUFFER PACKING
      DISKBUF(0)=NNUM
      DO 10 J=1,NNUM
      DISKBUF(2*J-1)=DTEMP(J)
   10 DISKBUF(2*J)=DRES(J)
C  DISK WRITE PROCEDURE
C
C  DEFINE A FILE, ID=FILE NAME
      CALL FDFFL (ID,IE)
C
C  GET A FILE SLOT, SLOT NO.=ISLOT
      CALL FGTFS (ISLOT,IE)
C
C  OPEN A FILE
      CALL FOPFL (ID,ISLOT,IE)
C
C  WRITE INTO FILE, DISKBUF=DATA BUFFER, IBYTE=NO. BYTES
      CALL FWTFL (ISLOT,DISKBUF,IBYTE,FE)
C
C  CLOSE FILE
      CALL FRSFL
```

```
      SUBROUTINE LSQ(RES,TEMP,NUM)
      DIMENSION RES(50),TEMP(50),M(50)
C ZERO ARRAY M
      DO 3 II=1,50
    3 M(II)=0
      INDEX=NUM
      N=1HN
      WRITE(10,1)
      READ(10,2) NY
      IF (NY .EQ. N) GO TO 5
      ACCEPT "HOW MANY?",NOS
      TYPE "WHICH POINTS?"
      DO 7 J=1,NOS
      ACCEPT "?",J
    7 M(J)=J
C READ IN DATA DELETING UNWANTED POINTS
      K=0
      J=0
      INDEX=NUM-NOS
      DO 10 L=1,INDEX
      J=J+1
      K=K+1
      IF (K .EQ. M(K)) J=J+1
      RES(K)=RES(J)
   10 TEMP(K)=TEMP(J)
    5 ACCEPT "SAMPLE DIAMETER=",D
      ACCEPT "SAMPLE THICKNESS=",T
      ACCEPT "LOG R AT 25DEG=",R,"<15>","<15>","<15>"
      S1=0.0
      S2=0.0
      S3=0.0
      S4=0.0
      S5=0.0
      DO 20 I=1,INDEX
      S1=S1+TEMP(I)
      S2=S2+RES(I)
      S3=S3+TEMP(I)**2
      S4=S4+RES(I)**2
   20 S5=S5+TEMP(I)*RES(I)
      X2=S1/INDEX
      Y2=S2/INDEX
      A1=((INDEX*S5)-(S1*S2))/((INDEX*S3)-(S1**2.0))
      E=A1*0.3968
      A2=Y2-A1*X2
      A3=A3S(((S4-(S2**2/INDEX))-(A1**2*(S3-S1**2/INDEX)))/((INDEX-2
     1)*(S3-S1**2/INDEX)))
      A3=SQRT(A3)
      A4=A3*SQRT(S3/INDEX)
      V=R-ALOG10(T*2.539)+ALOG10(3.142*(D/2*2.539)**2)
      TYPE "SLOPE=",A1,"   INTERCEPT=",A2
      TYPE "SIGMA=",A3,"      SIGMA=",A4,"<15>"
      TYPE "ACTIVATION ENERGY=",E
      TYPE "LOG VOLUME RESISTIVITY=",V
    1 FORMAT(" DELETE ANY POINTS?(Y OR N)",Z)
    2 FORMAT(1S1)
      RETURN
      END
```

```
                ; ****************************************
                ; *                                      *
                ; * DATA COLLECTION AND CONTROL SUBROUTINES *
                ; * SUBROUTINE:                          *
                ; *     CDATA  APPLIES VOLTAGE, READS AMPS, *
                ; *            TEMPERATURE AFTER 10 SEC  *
                ; *     TIME   PAUSES 2 MIN              *
                ; *                                      *
                ; ****************************************
                      .TITL  INPUT
                      .ENT  CDATA, TIME
                      .EXTU
                      .EXTN  .I, .BCDB
                      .NREL
00000'000002          2
00001'006005$ CDATA: JSR  @.CPYL        ;SUBROUTINE:CDATA
00002'060121          NIOS 21           ;SWITCH ON VOLTAGE RELAY
00003'014431  LOOP1: DSZ RLY1           ;10SEC VOLTAGE ON LOOP
00004'000402          JMP .+2
00005'000406          JMP OUT
00006'014427          DSZ RLY2
00007'000777          JMP .-1
00010'024426          LDA 1,DRLY
00011'044424          STA 1,RLY2
00012'000771          JMP LOOP1
00013'024423  OUT:   LDA 1,DRLY
00014'044420          STA 1,RLY1
00015'060321          NIOP 21           ;PLACE HOLD ON DVM'S
00016'064421          DIA 1,21          ;READ KEITHLEY(AMPS)
00017'004446          JSR CONV          ;CONVERT BCD TO BINARY
00020'000004$         FXFL1             ;CONVERT FIXED TO REAL, LOAD 0
00021'000102'         AC1
00022'000001$         FFST1             ;POP NS, PACK AND STORE IN
00023'100011          @11               ;FORTRAN ADDRESS
00024'065421          DIB 1,21          ;READ ORION (TEMP)
00025'004440          JSR CONV
00026'000004$         FXFL1
00027'000102'         AC1
00030'000001$         FFST1
00031'100012          @12
00032'060221          NIOC 21           ;REMOVE HOLD
00033'000003$         FRET              ;RETURN
00034'003404  RLY1:   3404
00035'003404  RLY2:   3404
00036'003404  DRLY:   3404
00037'000001          1                 ;RESERVE 1 TEMPORARY LOCATION
00040'006005$ TIME: JSR  @.CPYL         ;SUBROUTINE:TIME
00041'014422  LOOP2: DSZ WAIT1          ;2 MIN  WAIT LOOP
00042'000402          JMP .+2
00043'000406          JMP OUT1
00044'014420          DSZ WAIT2
00045'000777          JMP .-1
00046'024414          LDA 1,WAITS
00047'044415          STA 1,WAIT2
00050'000771          JMP LOOP2
00051'024411  OUT1: LDA 1,WAITS
00052'044411          STA 1,WAIT1
00053'074477          READS 3           ;READ SWITCH REGISTERS
00054'054426          STA 3,AC1         ;TRANSFER TO FORTRAN CALLING
00055'000004$         FXFL1             ;PROGRAM
```

```
00056'000102'           AC1
00057'000002$           FLFX1               ;BIT 15=1 CAUSES TERMINATION
00060'100011            @11
00061'000003$           FRET
00062'014000    WAITS:  14000
00063'014000    WAIT1:  14000
00064'014000    WAIT2:  14000
00065'054417    CONV:   STA 3,RET           ;BCD TO BINARY CONVERSION ROUT
00066'125112            MOVL# 1,1,SZC       ;TEST SIGN BIT
00067'000405            JMP MIN             ;IF NEGATIVE, JUMP TO SIGN ROU
00070'020413            LDA 0,MASK
00071'107400            AND 0,1             ;MASK THRU LOWER 13 BITS
00072'006413            JSR  @BCD           ;BCD TO BINARY
00073'000405            JMP .+5
00074'020407    MIN:    LDA 0,MASK          ;NEGATIVE NUMBER ROUTINE
00075'107400            AND 0,1
00076'006407            JSR  @BCD           ;MASK AS ABOVE
00077'124400            NEG 1,1             ;NEGATE RESULT
00100'044402            STA 1,AC1
00101'002403            JMP @RET            ;RETURN
00102'000000    AC1:    0
00103'017777    MASK:   17777
00104'000000    RET:    0
00105'177777    BCD:    .BCDB
                        .END
```

```
                ; ********************************************
                ; *                                          *
                ; * CURRENT VS. TIME SUBROUTINES             *
                ; * PROGRAM NOTE:  MOST OF THE CURRENT VS.   *
                ; *   TEMPERATURE ROUTINES HAVE BEEN RETAINED *
                ; *   BUT DEGENERATE INDEXES HAVE BEEN USED  *
                ; *   WHERE APPROPRIATE                      *
                ; *                                          *
                ; ********************************************

                      .TITL  INPUT
                      .ENT  CDATA, TIME
                      .EXTU
                      .EXTN  .I, .BCDB
                      .NREL
00000'000002          2
00001'006010$ CDATA: JSR  @.CPYL        ;SUBROUTINE:CDATA
00002'060121          NIOS 21           ;TURN ON VOLTAGE RELAY
00003'014430  LOOP1: DSZ RLY1           ;THIS TIMING LOOP NOT USED
00004'000402          JMP .+2           ;(SEE LOOP INDEXES)
00005'000406          JMP OUT
00006'014426          DSZ RLY2
00007'000777          JMP .-1
00010'024425          LDA 1,DRLY
00011'044423          STA 1,RLY2
00012'000771          JMP LOOP1
00013'024422  OUT:   LDA 1,DRLY
00014'044417          STA 1,RLY1
00015'060321          NIOP 21           ;PLACE HOLD ON DVM'S
00016'064421          DIA 1,21          ;READ KEITHLEY (AMPS)
00017'004445          JSR CONV          ;CONVERSION ROUTINE BCD TO BIN
00020'000006$         FXFLI             ;CONVERT FIXED TO REAL, LOAD 0
00021'000101'         AC1
00022'000002$         FFSTI             ;POP NS, PACK AND STORE IN
00023'100011          @11               ;FORTRAN ADDRESS
00024'065421          DIB 1,21          ;NOT USED
00025'004437          JSR CONV          ;NOT USED
00026'000005$         FXFL1             ;NOT USED
00027'000101'         AC1               ;NOT USED
00030'000001$         FFST1             ;NOT USED
00031'100012          @12               ;NOT USED
00032'000004$         FRET              ;RETURN
00033'000001  RLY1:   1
00034'000001  RLY2:   1                 ;DUMMY INDEXES
00035'000001  DRLY:   1
00036'000001          1
00037'006010$ TIME: JSR  @.CPYL         ;SUBROUTINE:TIME
00040'014433  LOOP2: DSZ WAIT1          ;1 SEC WAIT LOOP
00041'000402          JMP .+2
00042'000406          JMP OUT1
00043'014430          DSZ WAIT2
00044'000777          JMP .-1
00045'024414          LDA 1,WAITS
00046'044415          STA 1,WAIT2
00047'000771          JMP LOOP2
00050'024411  OUT1: LDA 1,WAITS
00051'044407$         STA 1,WAIT 1
00052'074477          READS 3           ;NOT USED
00053'054426          STA 3,AC1         ;NOT USED
00054'000006$         FXFLI             ;NOT USED
```

```
00055'000101'           AC1                 ;NOT USED
00056'000003$           FLFX1               ;NOT USED
00057'100011            @11                 ;NOT USED
00060'000004$           FRET                ;NOT USED
00061'000734    WAITS:  734
00062'000734    WAIT1:  734
00063'000734    WAIT2:  734
00064'054417    CONV:   STA 3,RET           ;BCD TO BINARY CONVERSION ROUT
00065'125112            MOVL# 1,1,SZC       ;TEST SIGN BIT
00066'000405            JMP MIN             ;NEGATIVE NO.
00067'020413            LDA 0,MASK
00070'107400            AND 0,1             ;MASK THRU LOWER 13 BITS
00071'006413            JSR  @BCD           ;BCD TO BINARY
00072'000405            JMP .+5
00073'020407    MIN:    LDA 0,MASK          ;NEGATIVE NUMBER ROUTINE
00074'107400            AND 0,1
00075'006407            JSR  @BCD           ;MASK AS ABOVE
00076'124400            NEG 1,1             ;NEGATE RESULT
00077'044402            STA 1,AC1
00100'002403            JMP @RET
00101'000000    AC1:    0
00102'017777    MASK:   17777
00103'000000    RET:    0
00104'177777    BCD:    .BCDB
                        .END
```

LIST OF REFERENCES

1. M. Cremer, Z. Biol., 47, 562 (1906).
2. F. Haber and Z. Klemensiewicz, Z. Phys. Chem., 67, 385 (1909).
3. H. J. C. Tendeloo, J. Biol. Chem., 113, 333 (1936).
4. M. R. Wyllie and H. W. Patnode, J. Phys. Chem., 54, 204 (1950).
5. J. S. Parsons, Anal. Chem., 30, 1262 (1958).
6. E. Pungor, K. Toth, and J. Havas, Hung. Sci. Inst., 3, 2 (1965).
7. E. Pungor, J. Havas, and K. Toth, Acta Chim. Hung., 41, 239 (1964).
8. E. Pungor, J. Havas, and K. Toth, Z. Chem., 5, 9 (1965).
9. A. Shatkay, Anal. Chem., 39, 1056 (1967).
10. R. W. Cattrall and H. Freiser, Anal. Chem., 43, 1905 (1971).
11. H. James, G. Carmack, and H. Freiser, Anal. Chem., 44, 856 (1972).
12. E. Hopirtean, C. Liteanu, and E. Stefaniga, Rev. Roum. Chim., 19, 1651 (1974).
13. E. Hopirtean and E. Stefaniga, Rev. Roum. Chim., 20, 863 (1975).
14. G. J. Moody, R. B. Oke, and J. D. R. Thomas, Analyst, 95, 910 (1970).
15. J. W. Ross, Science, 156, 1378 (1967).
16. R. A. Durst, Ed., "Ion-Selective Electrodes," National Bureau of Standards Special Publication No. 314, U. S. Gov. Print. Off., Washington, D. C., 1969.
17. J. Koryta, "Ion-Selective Electrodes," Cambridge Monographs in Physical Chemistry, No. 2, Cambridge University Press, Cambridge, Massachusetts, 1975.
18. G. J. Moody and J. D. R. Thomas, "Selective Ion-Sensitive Electrodes," Merrow, Watford, 1970.

19. E. Pungor, Ed., "Ion-Selective Electrodes," symposium held at Mátrafüred, Hungary, 23-25 October, 1972, Akademial Kiadó, Budapest, 1973.

20. R. P. Buck, Anal. Chem., 46, 28R (1974); 48, 23R (1976).

21. W. Simon, H. R. Wuhrmann, M. Vasak, L. A. R. Pioda, R. Dohner, and Z. Stefnac, Angew. Chem., 9, 445 (1970).

22. R. P. Buck, Anal. Chem., 44, 270R (1972).

23. E. Pungor and K. Toth, Analyst, 95, 625 (1970).

24. A. K. Covington, CRC Crit. Rev. Anal. Chem., 3, 355 (1974).

25. B. Lengyel and E. Blum, Trans. Faraday Soc., 30, 461 (1969).

26. G. S. Bagdasarova, A. A. Belyustin, and A. M. Pisarevskii, Sov. Electrochem., 4, 1194 (1968).

27. C. T. Baker and I. Trachtenburg, J. Electrochem. Soc., 118, 571 (1971).

28. R. G. Bates, G. Eisenman, G. Mattock, and S. M. Friedman, in "The Glass Electrode," Interscience, New York, 1962.

29. G. Eisenman, Ed., "The Glass Electrode," Marcel Dekker, New York, 1967.

30. J. Koryta, Anal. Chim. Acta, 61, 329 (1972).

31. R. A. Durst and J. K. Taylor, Anal. Chem., 39, 1483 (1967).

32. A. Sher, R. Solomon, and K. Lee, Phys. Rev., 144, 593 (1966).

33. J. Ruzicka and C. G. Lamn, Anal. Chim. Acta, 53, 206 (1971).

34. J. Ruzicka and C. G. Lamn, Anal. Chim. Acta, 54, 1 (1971).

35. H. Hirata and K. Higashiyama, Anal. Chim. Acta, 51, 209 (1970).

36. U. Fiedler and J. Ruzicka, Anal. Chim. Acta, 67, 179 (1973).

37. E. Pungor and K. Toth, Pure and Appl. Chem., 47, 291 (1969).

38. M. Mascini and A. Liberti, Anal. Chim. Acta, 47, 339 (1969).

39. H. Hirata and K. Date, Talanta, 17, 883 (1970).

40. E. Pungor and K. Toth, Pure and Appl. Chem., 34, 105 (1973).

41. O. D. Bonner and D. C. Lumney, J. Phys. Chem., 70, 1140 (1966).

42. C. J. Coetzee and H. Freiser, Anal. Chem., 40, 2071 (1968).

43. H. James, G. Carmack, and H. Freiser, Anal. Chem., 44, 853 (1972).

44. J. W. Ross, Jr., U. S. Patent 3, 483, 112 09 Dec. 1969.

45. A. Jyo, M. Yonemitsu, and N. Ishibashi, Bull. Chem. Soc. Japan, 46, 3734 (1973).

46. G. Eisenman, in "Ion-Selective Electrodes," R. A. Durst, Ed., National Bureau of Standards Special Publication No. 314, U. S. Gov. Print. Off., Washington, D. C., 1969, p. 1.

47. C. J. Pedersen and H. K. Frensdorff, Angew. Chem., 11, 16 (1972).

48. S. Mesaric and E. M. F. Dahmen, Anal. Chim. Acta, 64, 431 (1973).

49. A. Ansaldi and S. I. Epstein, Anal. Chem., 45, 595 (1973).

50. E. H. Hansen, J. Ruzicka, and C. H. Lamn, Anal. Chim. Acta, 59, 403 (1972).

51. J. Ruzicka, E. H. Hansen, and J. Chr. Tjell, Anal. Chim. Acta, 62, 15 (1972).

52. I. M. Kolthoff and H. L. Sanders, J. Am. Chem. Soc., 59, 416 (1937).

53. M. R. Thompson, J. Res. Nat. Bur. Stand., 9, 833 (1932).

54. H. Bender and D. J. Bye, U. S. Patent, 2, 117, 596; 17 May (1938).

55. L. W. Niedrach and W. H. Stoddard, Jr., Ger. Offen. 2, 220, 841 (Nov. 1972).

56. G. J. Moody, R. B. Oke, and J. D. R. Thomas, Lab. Pract., 18, 941 (1969).

57. J. Bagg, Proceedings of Royal Australian Chemical Institute, 38 91 (1971).

58. G. J. Hills, in "Reference Electrodes," D. J. G. Ives and G. J. Janz, Eds., Academic Press, New York, 1961, p. 411.

59. J. W. Ross, in "Ion-Selective Electrodes," R. A. Durst, Ed., National Bureau of Standards Special Publication No. 314, U. S. Gov. Print. Off., Washington, D. C., 1969, p. 57.

60. E. Pungor, Anal. Chem., 39(13), 29A (1967).

61. N. Lakshminarayanaiah, "Membrane Electrodes," Academic Press, New York, 1976.

62. G. D. Carmack and H. Freiser, Anal. Chem., 45, 1975 (1973); 47, 2249 (1975).

63. J. D. R. Thomas, Proc. Soc. Anal. Chem., 11, 340 (1974).

64. H. K. Wipf and W. Simon, Biochem. Res. Comm., 34, 707 (1969).

65. D. H. Haynes, A. Kowalsky, and B. C. Pressman, J. Biol. Chem., 244, 502 (1969).

66. O. Ryba, E. Knizakova, and J. Petranek, Collection Czechoslov. Chem. Commun., 38, 497 (1973).

67. K. Toth, E. Pungor, and W. Simon, Anal. Chim. Acta, 64, 477 (1973).

68. M. Sharp and G. Johansson, Anal. Chim. Acta, 54, 13 (1971).

69. M. Sharp and G. Johansson, Anal. Chim. Acta, 53, 130 (1970).

70. D. S. Acker and W. R. Hertler, J. Amer. Chem. Soc., 84 3370 (1962).

71. G. Haugaard, J. Phys. Chem., 45, 148 (1941).

72. R. A. Durst and J. W. Ross, Anal. Chem., 40, 1343 (1968).

73. A. Wikby and G. Johansson, J. Electroanal. Chem., 23, 23 (1969).

74. A. Wikby, J. Electroanal. Chem., 33, 145 (1971).

75. M. J. D. Brand and G. A. Rechnitz, Anal. Chem., 42, 478 (1970).

76. K. C. Frisch and A. Patsis, "Electrical Properties of Polymers," Technomic, New York, 1972.

77. R. B. Hall, Thin Solid Films, 8, 263 (1971).

78. D. A. Seanor, J. Polym. Sci., Part C, 17, 195 (1967).

79. D. A. Seanor, in "1967 Annual Report, Conference on Electrical Insulation and Dielectric Phenomena," NHS-NRC Pub. 1578, Washington, D. C., 1967, p. 9.

80. American Society for Testing and Materials, Philadelphia, Pa., Method D 257-61.

81. XDOS Operating Manual, Xebec Systems, Inc., 1974.

82. FORTRAN IV, Data General Corp., 1974.

83. FORTRAN IV Run-Time Library, Data General Corp., 1974.

84. E. M. Barrall and J. F. Johnson, in "Techniques and Methods of Polymer Evaluation," P. E. Slade and L. T. Jenkins, Eds., Marcel Dekker, New York, 1970, p. 1.

85. N. A. Lange, "Handbook of Chemistry," McGraw-Hill, New York, 1967, p. 1320.

86. C. Tubandt and S. Eggert, Z. Anorg. Chem., 110, 196 (1920).

87. M. S. Mizzoni, J. Electrochem. Soc., 120, 1592 (1973).

88. F. E. Karasz, "Dielectric Constant of Polymers," Plenum, New York, 1972.

89. American Society for Testing and Materials, Philadelphia, Pa., Method D-1673-61.

90. L. G. Johnson and J. Chomicz, Insulation (London), 14, 61 (1968).

91. R. E. Barker and A. H. Sharbaugh, J. Polymer Sci., Part C, 10, 139 (1965).

92. D. D. Eley, J. Polymer Sci., C17, 73 (1967).

93. A. Many, E. Harnik, and D. Gerlich, J. Chem. Phys., 23, 1733 (1955).

94. F. Gutmann and L. E. Lyons, "Organic Semiconductors," John Wiley & Sons, Inc., New York, 1967, pp. 428-435.

95. D. D. Eley and R. B. Leslie, Nature, 197, 898 (1963).

96. W. Meyer and H. Neldel, Z. Tech. Physik, 18, 588 (1937).

97. B. Rosenberg, B. B. Bhowmik, H. C. Harder, and E. Postow, J. Chem. Phys., 49, 4108 (1968).

98. B. Rosenberg and M. R. Powell, Bioenerg., 1, 493 (1970).

99. S. Glasstone, K. J. Laidler, and H. Eyring, "The Theory of Rate Processes," McGraw-Hill, New York, 1941.

100. E. Cremer, Advan. Catalysis, 7, 75 (1955).

101. A. E. Binks and A. J. Sharples, J. Polymer Sci., Part A-2, 6, 407 (1968).

102. H. Sasabe, K. Sawamura, S. Saito, and K. Yada, Polymer J., 2, 518 (1970).

103. F. Sandrolini, S. Pietra, and D. Manarisi, Chim. Ind. (Milan), 53, 755 (1971).

104. G. King and J. A. Medley, J. Colloid Sci., 8, 148 (1958).

105. P. R. Danesi, M. Magini, and G. Scibona, "Progress in Coordination Chemistry," Elsevier, Amsterdam, 1968, paper J-19.

106. R. A. Robinson and R. H. Stokes, "Electrolyte Solutions," Butterworths, Washington, D. C., and New York, New York, 1959, p. 125.

107. P. R. Danesi, F. Salvemini, G. Scibona, and B. Scuppa, J. Phys. Chem., 75, 554 (1971).

108. G. J. Janz, "A Survey of Non-Aqueous Conductance Data," Rensselaer Polytechnic Institute, 1962.

109. P. H. Sutter and A. S. Nowick, J. Appl. Phys., 34, 734 (1963).

110. J. R. MacDonald, Phys. Rev., 92, 4 (1953).

111. S. Saito, H. Sasabe, T. Nakajima, and K. Yada, J. Polym. Sci., Part A-2, 6, 1297 (1968).

112. D. M. Taylor and T. J. Lewis, J. Phys. D(Appl. Phys.), 4, 1346 (1971).

113. P. J. Reucroft, S. K. Ghosh, and D. Keever, J. Polymer Sci., 10, 2305 (1972).

114. A. I. Lakatos and J. Mort, Phys. Rev. Letters, 21, 1444 (1968).

115. A. K. Jonscher, Thin Solid Films, 1, 213 (1967).

116. J. Frenkel, Phys. Rev., 54, 657 (1938).

117. R. M. Hill, Phil. Mag., 23, 59 (1971).

118. J. H. Sharp, J. Phys. Chem., 71, 2587 (1967).

119. A. Szymanksi and M. M. Labes, J. Chem. Phys., 50, 3568 (1969).

120. L. E. Amborski, J. Polym. Sci., 62, 331 (1962).

121. L. E. Amborski, J. Chem. Phys., 32, 237 (1960).

122. B. Karlberg, J. Electroanal. Chem. Interfacial Electrochem., 45, 127 (1973).

123. W. Dannhauser and J. R. Price, 1967 Annual Report, Conference on Electrical Insulation and Dielectric Phenomena, NHS-NRC Pub. 1578, Washington, D. C., 1967, p. 32.

124. L. J. Kaufman and F. A. Bettelheim, J. Polymer Sci., Part A-2, 9, 917 (1971).

125. A. J. Curtis, J. Res. Nat. Bur. Stand., 65A, 185 (1961).

126. J. E. Algie, Kolloid-Z., 223, 13 (1968).

127. W. H. Bentley and R. B. Aust, J. Chem. Phys., 41, 1856 (1964).

128. S. D. Hamann, Aust. J. Chem., 18, 1 (1965).

129. P. K. Datta, J. Sci. Ind. Res., 30, 222 (1971).

130. I. Mellan, "The Behavior of Plasticizers," Pergamon Press, New York, 1961.

131. C. A. Kumins, J. Polym. Sci., Part C, 10, 1 (1965).

132. N. H. Nachtrieb and A. W. Lawson, J. Chem. Phys., 23, 1193 (1955).

133. R. W. Keyes, J. Chem. Phys., 29, 467 (1958).

134. Y. Ishida, J. Polym. Sci., 7, 1835 (1969).

135. K. H. Hellewege, W. Knappe, and P. Lehmann, Kolloid-Z. Z.-Polym., 183, 110 (1962).

136. J. M. Davies, R. F. Miller, and W. F. Busse, J. Am. Chem. Soc., 63, 361 (1941).

137. J. H. Kallweit, J. Polymer Sci., 4, 337 (1966).

138. R. E. Barker, in 1967 Annual Report, Conference on Electrical Insulation and Dielectric Phenomena, NHS-NRC Pub. 1578, Washington, D. C., 1967, p. 1.

139. N. A. Lange, "Handbook of Chemistry," McGraw-Hill, New York, 1967, p. 1223.

140. J. A. Brydson, "Plastics Materials," Van Nostrand, New York, 1970.

141. P. A. Small, J. Appl. Chem., 3, 71 (1953).

142. H. Wise, J. Phys. Chem., 71, 2843 (1967).

143. T. M. Herrington and L. A. K. Staveley, Phys. Chem. Solids, 25, 921 (1964).

144. G. P. Owen, J. M. Thomas, and J. O. Williams, J. C. S. Dalton, 2365 (1973).

145. G. T. Koide and E. L. Carstensen, J. Phys. Chem., 76, 1999 (1972).

146. N. B. Hannay, "Semiconductors," Reinhold, New York, 1959.

147. F. Helfferich, "Ion Exchange," McGraw-Hill, New York, 1962.

148. N. A. Lange, "Handbook of Chemistry," McGraw-Hill, New York, 1967, p. 122.

149. J. Naghizadeh and S. A. Rice, J. Chem. Phys., 36, 2710 (1962).

150. A. F. M. Barton, B. Cleaver, and G. J. Hills, Trans. Faraday Soc., 64, 208 (1968).

151. A. Joffe, "The Physics of Crystals," McGraw-Hill, New York, 1962.

152. J. R. Macdonald, J. Chem. Phys., 23, 2308 (1955).

153. J. R. Macdonald, J. Chem. Phys., 23, 275 (1955).

154. A. Von Hippel, E. P. Gross, J. G. Jelatis, and M. Geller, Phys. Rev., 91, 568 (1953).

155. A. Smekal, Phys. Z., 36, 742 (1935).

156. H. V. Boenig, "Structure and Properties of Polymers," John Wiley, New York, 1973.

157. J. van Turnhout, "Thermally Stimulated Discharge of Polymer Electrets," Elsevier Scientific, New York, 1975.

158. S. I. Stupp and S. H. Carr, J. Appl. Phys., 46, 4120 (1975).

159. W. J. Burland and J. L. Parsons, J. Polymer Sci., 22, 249 (1956).

160. N. Grassie and J. N. Hay, J. Polymer Sci., 56, 189 (1962).

161. M. S. D. Brand and G. A. Rechnitz, Anal. Chem., 41, 1185 (1969).